HYDROGEOLOGY AND LAND SUBSIDENCE, EDWARDS AIR FORCE BASE, ANTELOPE VALLEY, CALIFORNIA, JANUARY 1989-DECEMBER 1991

By C.J. Londquist, D.L. Rewis, D.L. Galloway, and W.F. McCaffrey

---

U.S. GEOLOGICAL SURVEY

Water-Resources Investigations Report 93-4114

Prepared in cooperation with the

U.S. DEPARTMENT OF THE AIR FORCE

Sacramento, California
1993

U.S. DEPARTMENT OF THE INTERIOR
BRUCE BABBITT, *Secretary*

U.S. GEOLOGICAL SURVEY
Dallas L. Peck, *Director*

For sale by the
U.S. Geological Survey
Earth Science Information Center
Open-File Reports Section
Box 25286, MS 517
Denver Federal Center
Denver, CO 80225

For additional information write to:
District Chief
U.S. Geological Survey
Federal Building, Room W-2233
2800 Cottage Way
Sacramento, CA 95825

CONTENTS

FIGURES

TABLES

CONVERSION FACTORS, VERTICAL DATUM, AND WELL-NUMBERING SYSTEM

Conversion Factors

Multiply	By	To obtain
acre-foot (acre-ft)	1,233	cubic meter
acre-foot per year (acre-ft/yr)	0.001233	cubic hectometer per year
acre-foot per square mile (acre-ft/mi^2)	476	cubic meter per square kilometer
foot (ft)	0.3048	meter
foot per day (ft/d)	0.3048	meter per day
foot per second (ft/s)	0.3048	meter per second
foot per year (ft/yr)	0.3048	meter per year
foot square per day (ft^2/d)	0.0929	meter squared per day
inch (in.)	25.4	millimeter
mile (mi)	1.609	kilometer
mile per hour (mi/h)	1.609	kilometer per hour
square mile (mi^2)	2.590	square kilometer

Temperature is given in degrees Fahrenheit (°F), which can be converted to degrees Celsius (°C) by the following equation:

$$°F=1.8(°C)+32.$$

Vertical Datum

Sea level: In this report, "sea level" refers to the National Geodetic Vertical Datum of 1929--a geodetic datum derived from a general adjustment of the first-order level nets of the United States and Canada, formerly called Sea Level Datum of 1929.

Well-Numbering System

Wells are identified and numbered according to their location in the rectangular system for the subdivision of public lands. Identification consists of the township number, north or south; the range number, east or west; and the section number. Each section is divided into sixteen 40-acre tracts lettered consecutively (except I and O), beginning with "A" in the northeast corner of the section and progressing in a sinusoidal manner to "R" in the southeast corner. Within the 40-acre tract, wells are sequentially numbered in the order they are inventoried. The final letter refers to the base line and meridian. In California, there are three base lines and meridians; Humboldt (H), Mount Diablo (M), and San Bernardino (S). All wells in the study area are referenced to the San Bernardino base line and meridian (S). Well numbers consist of 15 characters and follow the format 009N010W34R002S. In this report, well numbers are abbreviated and written 9N/10W-34R2. Wells in the same township and range are referred to only by their section designation, 34R2. The following diagram shows how the number for well 9N/10W-34R2 is derived.

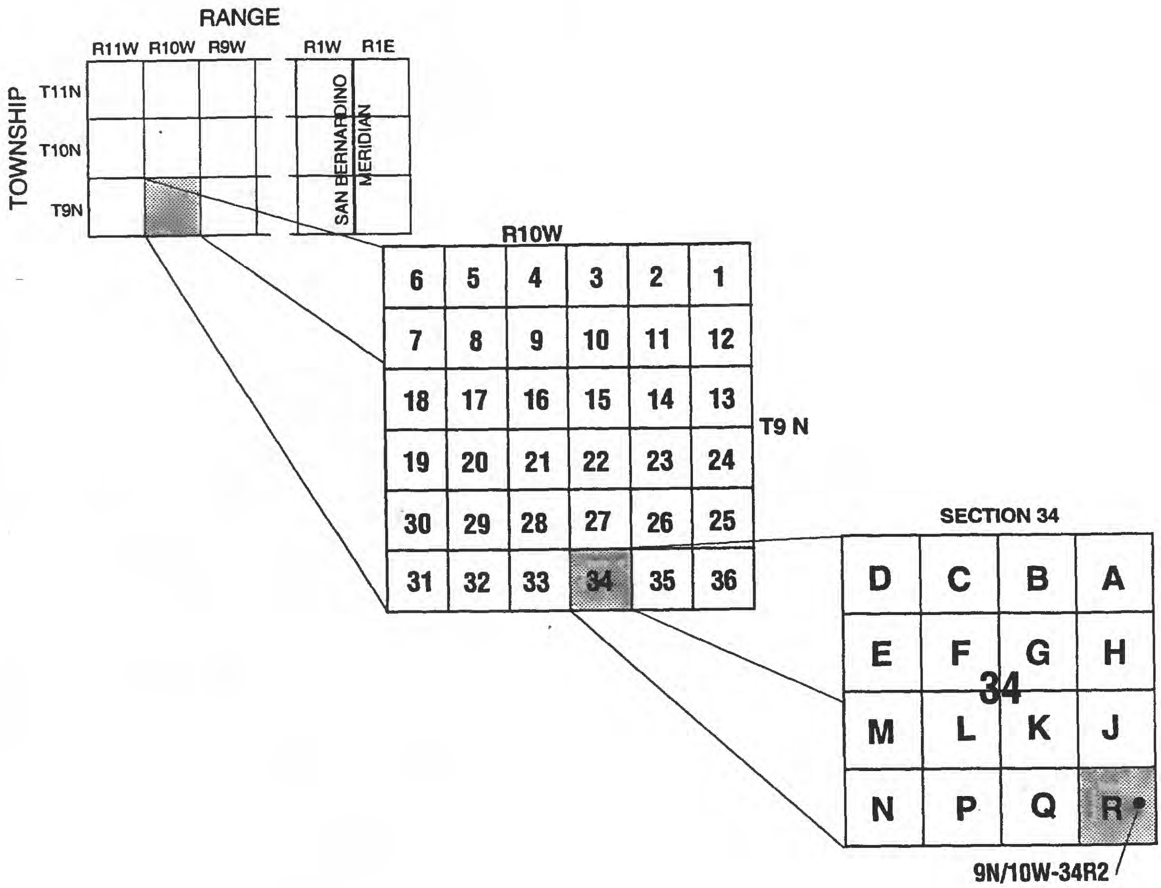

HYDROGEOLOGY AND LAND SUBSIDENCE, EDWARDS AIR FORCE BASE, ANTELOPE VALLEY, CALIFORNIA, JANUARY 1989-DECEMBER 1991

By C.J. Londquist, D.L. Rewis, D.L. Galloway, and W.F. McCaffrey

Abstract

Land subsidence has long been recognized as a problem in some parts of the Antelope Valley area of California. In 1988, the effects of subsidence were noted on Rogers Lake at Edwards Air Force Base in the form of sinklike depressions, fissures, and cracks, which have adversely affected the lakebed for landing airplanes and space shuttles. The land subsidence has been attributed to the pumping of ground water around the margins of the lakebed.

EAFB overlies two structural basins, East Antelope and Kramer, which have been filled to depths of more than 5,000 and 2,000 feet, respectively, with unconsolidated alluvium interbedded with lacustrine deposits. Lithologic and geophysical data indicate that these deposits become more consolidated with depth. Surface-geophysical information defines the East Antelope structural basin as a narrow northeast-trending trough, and indicates a possible fault zone that encompasses the Graham Ranch area.

Two alluvial aquifers are present in the Lancaster ground-water subbasin in Antelope Valley: the principal aquifer, which overlies the lacustrine deposits, is the major source of ground water for offbase users; and the deep aquifer is the major source of water at EAFB. Ground water in the Antelope Valley originates from the infiltration of surface-water runoff from the surrounding mountains. Estimates of the average annual recharge to the valley range from 40,200 to 81,400 acre-feet. In 1988, estimated pumpage in the valley was about 62,000 acre-feet and in 1990 the pumpage at Edwards Air Force Base was about 6,000 acre-feet. The long-term water-level trend at EAFB generally has been downward, and the greatest measured declines, as much as 90 feet, have occurred in the South Base well field. At the Holly site near the South Track well field, south of Rogers Lake, the hydraulic head in the overlying principal aquifer is about 100 feet higher than in the deep aquifer. The quality of ground water near Rogers Lake and in the Graham Ranch area ranges from soft to moderately hard, and commonly has a high dissolved-solids concentration. At the Buckhorn site, west of Rogers Lake, the water is characterized as very hard and slightly saline.

More than 1 foot of land subsidence has occurred since 1961 over the southern part of EAFB. The maximum measured subsidence for this period was 3.3 feet at benchmark P1155 near the South Track well field. Aquifer-system compaction measured at the Holly site showed a current average annual rate of compaction of 5.57×10^{-2} feet from May 1990 to November 1991.

INTRODUCTION

Land subsidence has long been recognized as a problem in some parts of the Antelope Valley area of California. In 1988, its effects were noted on Rogers Lake at Edwards Air Force Base (EAFB, fig. 1) in the form of sinklike depressions, fissures, and cracks, which have adversely affected the lakebed for landing airplanes and space shuttles. In 1988, the U.S. Geological Survey (USGS), in cooperation with the U.S. Department of the Air Force, began a study at EAFB to determine the causes of land subsidence and lakebed deformation on EAFB. During the early stages of the study, the distribution of land subsidence near Rogers Lake was correlated with the distribution of ground-water level declines resulting primarily from ground-water withdrawals from base production wells. In late 1989, the USGS began a second study to determine the relation between ground-water withdrawals and land-surface deformation near Rogers Lake and to explore other potential ground-water resources whose development would minimally affect the lakebed. In 1991, the two studies were merged.

The purpose of this report is to describe geologic and hydrologic data collected by the USGS during 1989-91 and to document the results and interpretations of the hydrogeologic investigation through December 1991. The report briefly summarizes the regional hydrogeologic setting of Antelope Valley, relying mainly on previously published reports, and also describes the specific hydrogeologic data that were collected: geologic logs, borehole and surface geophysics, and ground-water levels and quality. This report includes interpretations regarding land subsidence and aquifer-system compaction. Data presented in this report are interpreted in the context of previously published findings and discussed in terms of the characterization of the aquifer system at EAFB.

The investigations reported on here focus on the area of EAFB; however, because the hydrologic processes under study are governed by physical, hydrologic, and geologic boundaries that occur at the scale of Antelope Valley, the investigations necessarily include areas of Antelope Valley outside of the boundaries of EAFB (fig. 1).

LOCATION AND GEOGRAPHIC DESCRIPTION

Edwards Air Force Base is in Antelope Valley in the western part of the Mojave Desert of southern California about 60 mi north-northeast of the city of Los Angeles, astride the Los Angeles, Kern, and San Bernardino County lines (fig. 1). The Mojave Desert is part of the Basin and Range province of the Western United States which, in this area, is characterized by faulted mountain blocks separating basins of internal drainage. Antelope Valley is a closed topographic basin with its lowest point at Rogers Lake (fig. 1). This lake, like others in the Mojave Desert, is a dry lake or playa and forms a prominent desert feature. The term playa, as used in this report, refers only to the dry lakebed surface as defined by Motts (1970, p. 9).

Antelope Valley covers about 2,200 mi^2; the alluvial fans, valley floor, interior mountain, and foothill altitudes range from about 2,270 to 3,500 ft above sea level. Altitudes of the San Gabriel and Tehachapi Mountains rise to about 10,064 and 9,731 ft above sea level, respectively. In addition to Rogers Lake, Antelope Valley contains two other dry lakes, Rosamond and Buckhorn Lakes, which also are within the boundaries of EAFB (fig. 1).

Lancaster and Palmdale are the largest population centers in Antelope Valley, having a combined population of about 128,000 in 1989 (Lancaster Chamber of Commerce, oral commun., February 1991) and about 156,000 in 1990 (U.S. Department of Commerce, Bureau of the Census, 1990). Rosamond, located west of EAFB, had a population of about 12,000 in 1989 and about 18,000 in 1990 (Rosamond Chamber of Commerce, oral commun., 1991). The 1990 census figures for the unincorporated community of Boron is 2,101. The military resident population of EAFB is 7,423 (U.S. Department of Commerce, Bureau of the Census, 1990). The employed population of EAFB was about 15,100 during 1989 and 1990 (Cost and Business Management Division of Edwards Air Force Base, written commun., 1990).

The boundaries of EAFB encompass about 470 mi^2. EAFB is operated by the U.S. Air Force Flight Test Center, whose primary mission is to train

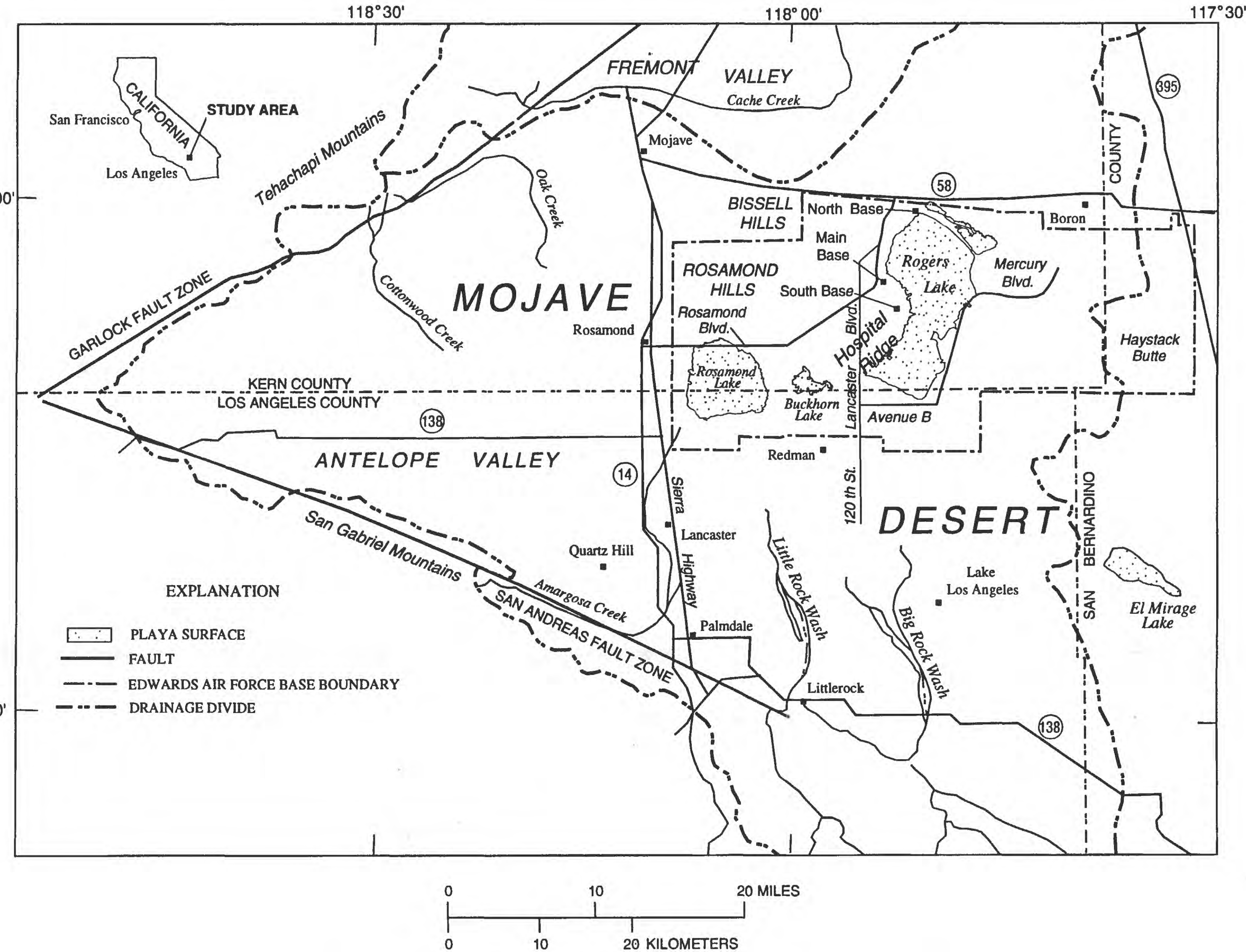

Figure 1. Location of study area.

Air Force flight test personnel and to conduct aviation development through experimental and test flight activities. EAFB is host to several tenant organizations. The National Aeronautics and Space Administration (NASA) operates the Ames-Dryden Flight Research facility at EAFB. Test facilities for the Jet Propulsion Laboratory, the Phillips Laboratory, formerly the Astronautics Laboratory, and the U.S. Air Force Rocket Propulsion Laboratory also are on EAFB. Runways on Rogers Lake are used to stage flight tests and land NASA's space shuttles; the entire lakebed surfaces of Rogers and Rosamond Lakes are designated as emergency landing surfaces.

CLIMATE AND VEGETATION

Antelope Valley is in the rainshadow of the Tehachapi and San Gabriel Mountains (fig. 1) and has a semiarid to arid climate. The average annual precipitation at EAFB is 4.8 in. for the 1933-89 period of record (Larry Plews, Project Manager, Edwards Air Force Base, oral commun., 1990). The total precipitation measured at the Lancaster Flight Service Station was 2.43 in. in 1989 and 1.85 in. in 1990 (National Oceanic and Atmospheric Administration, 1989, 1990). Most of the precipitation in Antelope Valley is in the late autumn and early winter months as a result of low-pressure frontal systems that move inland from the Pacific Ocean. Winter temperatures often cause precipitation to occur in the form of snow. Occasional summer storms occur in the area as a result of warm humid air masses moving northward from the Gulf of California or the Pacific Ocean. However, summer precipitation does not occur in significant quantities to impart a bimodal distribution to the precipitation pattern at EAFB.

Temperature variations at EAFB are characteristic of a desert climate with wide seasonal temperature extremes. During 1989 through 1990, temperatures ranged from the maximum summer high of 110°F to the minimum winter low of 3°F. The average annual temperatures were 62.7°F for 1989 and 61.0°F for 1990 (National Oceanic and Atmospheric Administration, 1989, 1990). Prevailing winds are from the west and southwest and are sustained at times as high as 30 to 40 mi/h, with occasional gusts of 60 to 70 mi/h or more.

The native vegetation throughout EAFB area is dominated by a sparse cover of xerophytes, plants whose root systems normally do not extend to the water table or capillary fringe. The most common of these are creosote bush (*Larrea tridentata*) and big sagebrush (*Artemisia tridentata*), with occasional Joshua trees (*Yucca brevifolia*) and prickly pear cacti (genus *Opuntia*). Vegetation changes at the transition between the coarse bedrock grus of the low-lying interior hills and the finer alluvial fill of the valley floor. Creosote bush generally does not occur below this area; whereas the more alkali tolerant big sagebrush (Meinzer, 1927) is abundant.

There also are some phreatophytes, plants whose roots usually penetrate the water table, such as mesquite (genus *Prosopis*), tamarisk (genus *Tamarix*), saltbush (genus *Atriplex*), and rabbitbrush (genus *Chrysothamnus*). These plants are in areas where the water table is or was near land surface in recent years, in areas of shallow perched water zones, and at dry springs. Playa surfaces and smaller clay pans are devoid of vegetation except where earth fissures and sinklike depressions provide intermittent sources of water by pooling rainfall and runoff.

PREVIOUS STUDIES

The earliest hydrogeologic reconnaissances of Antelope Valley were by Johnson (1911) and subsequently by Thompson (1929). These surveys focused on mapping ground-water resources of Antelope Valley. Their observations of the ground-water levels and the areal extent of flowing wells in Antelope Valley provide a snapshot of the ground-water conditions in Antelope Valley during the early period of ground-water development.

Thayer (1946) mapped the Antelope Valley ground-water-flow system into specific ground-water subbasins based on postulated lateral ground-water-flow boundaries. From 1947 to 1967, additional studies describing the ground-water resources of Antelope Valley and specifically the ground-water resources of EAFB were made by the State of California and the USGS. These studies have been summarized in reports by the California Department of Water Resources (1947), California Department of Public Works, (1955), Snyder (1955), Dutcher and Worts (1963), and Bloyd (1967). The number, size, and boundary locations of the ground-water subbasins originally described by Thayer (1946) were redefined using these studies by the State of California and the USGS.

The general geologic structure of the Antelope Valley was inferred on the basis of a gravity survey of the western Mojave Desert (Mabey, 1960). Geologic mapping of sections of the Antelope Valley was done by Dibblee (1952, 1957, 1958a, 1958b, 1959a, 1959b, 1959c, 1959d, 1960a) and Noble (1953). Dibblee (1960b, 1963) described the surface geology in the area of EAFB and later summarized the geology of Antelope Valley (Dibblee, 1967, 1981).

The USGS studies at EAFB between 1953 and 1969 produced eight data reports documenting ground-water conditions: Moyle (1960), Weir (1962, 1963, 1965), Giessner and Robson (1965), Giessner and Westphal (1966), Tyley (1967), and Koehler (1969). The objectives of these studies at EAFB were to (1) provide for periodic water-level measurements, (2) provide for periodic ground-water-quality analyses to monitor water-quality trends and to determine ground-water circulation patterns, and (3) provide technical advice on ground-water supply to EAFB.

Hughes (1975) evaluated the hydrogeology of the Haystack Butte area on EAFB for the U.S. Air Force Rocket Propulsion Laboratory. The previous studies in Antelope Valley formed the basis for the development and calibration of a mathematical model of the ground-water-flow system (Durbin, 1978). Duell (1987) reviewed the available ground-water-quality data for the Antelope Valley for the purpose of designing a water-quality monitoring network. Land subsidence in the Antelope Valley resulting from ground-water withdrawals for agricultural, municipal, and industrial water use was reported by Lewis and Miller (1968), McMillan (1973), Thomas and Phoenix (1976), Holzer (1984), and Blodgett and Williams (1992). As early as 1947, the California Department of Water Resources (1947), California Department of Public Works (1955) and Snyder (1955) documented that the annual ground-water pumpage in Antelope Valley exceeded the estimated average annual ground-water recharge.

REGIONAL HYDROGEOLOGIC SETTING

GEOLOGY

The Mojave Desert is a wedge-shaped block bounded by the San Andreas Fault Zone and San Gabriel Mountains to the southwest, the Garlock Fault Zone and Tehachapi Mountains to the northwest (fig. 1), and the Colorado River on the east (Hewett, 1954). Uplifts of the San Gabriel and Tehachapi Mountains isolated the Mojave Desert from the Pacific coast and created the interior or closed drainage basins of the western Mojave Desert.

Antelope Valley overlies three large sediment filled structural basins, which are separated by areas of extensively faulted, elevated bedrock (Dibblee, 1967) (fig. 2). These basins are the result of two periods of deformation (Burchfiel and Davis, 1981; Dibblee, 1981). The first of these was a period of crustal extension that occurred about 32 million years ago during the Tertiary Period and created structurally closed basins. The second period of deformation superimposed predominantly northwest-trending right-lateral faulting over the northeast-trending faults of the Basin and Range topography (Dokka, 1986, 1989; Glazner and others, 1989; Bartley and others, 1990) and ended about 700,000 years ago (Bortugno and Spittler, 1986).

EAFB overlies parts of two of these structural basins, the East Antelope basin and the Kramer basin (fig. 2). These basins have been filled to depths of more than 5,000 and 2,000 ft, respectively, with Tertiary and Quaternary sediments eroded from the adjacent bedrock highlands (Benda and others, 1960; Mabey, 1960). Borehole and gravity data indicate that the depth of fill in the East Antelope Basin could be as much as 10,000 ft (Mabey, 1960).

FAULTS

Strike-slip and normal faults are the major structures in the western part of the Mojave block with some minor, localized folding. The San Andreas and Garlock Faults are currently active, strike-slip faults. The San Andreas is a 1-mile wide, right-lateral, northwest-trending fault zone separating the Mojave Desert and the San Gabriel Mountains. The Garlock is a 1- to 2-mile wide, high-angle, left-lateral, northeast-trending fault zone, extending to the northeast about 250 mi from its junction with the San Andreas Fault (fig. 2).

Major fault traces of the Mojave Desert that extend into EAFB area include the Willow Springs, El Mirage, Blake Ranch, Spring, Kramer Hills, and Muroc Faults, an unnamed fault separating the Rosamond and Bissell Hills, and an unnamed inferred fault beneath Rosamond Lake (fig. 2). All the faults at some location along their trace display evidence of

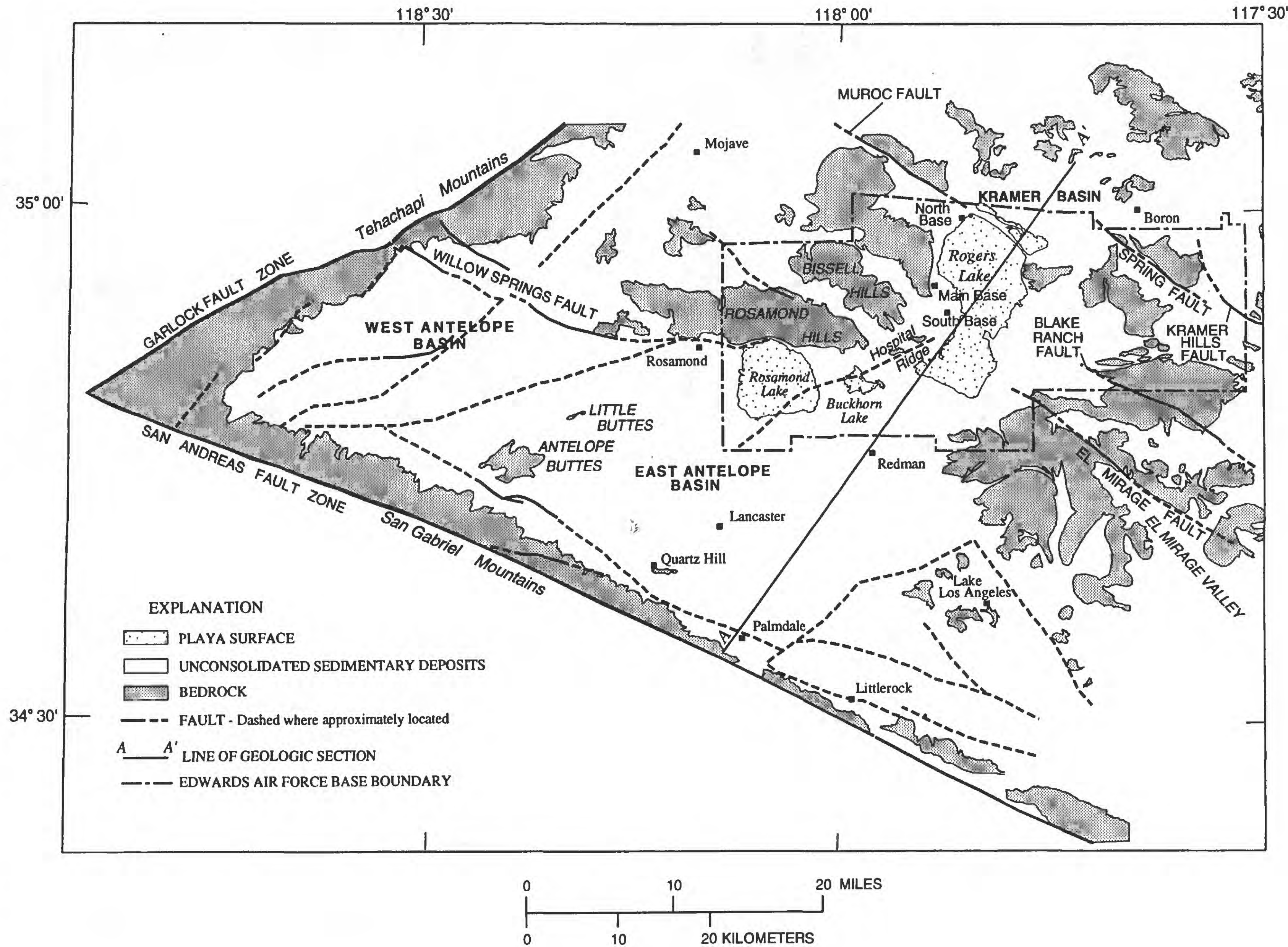

Figure 2. Generalized surficial geology and major faults in Antelope Valley. Modified from Mabey (1960) and Bloyd (1967).

Quaternary displacement. The Willow Springs Fault, also known as the Rosamond Fault, is described by Dibblee (1963) as an east-west-trending, normal fault, much of which is buried under alluvium along the southern edge of the Rosamond Hills. The El Mirage, Blake Ranch, Spring, Kramer Hills, and Muroc Faults are northwest-trending, right-lateral faults. The El Mirage Fault crosses the hills southeast of Rogers Lake and extends into the upper limits of the alluvial fan above the lake (Dibblee, 1960b). The Blake Ranch Fault is northeast of and subparallel to the El Mirage Fault (Dibblee, 1960b). The Spring and Kramer Hills Faults are in the northeast section of EAFB (Dibblee, 1960b). The Muroc Fault is northwest of Rogers Lake (Dutcher and Worts, 1963). Movement on the Kramer Hills, Spring, and Blake Ranch Faults has occurred within the past 2 million years, and on the El Mirage Fault within the past 700,000 years (Bortugno and Spittler, 1986). The existence of an unnamed fault buried beneath Rosamond Lake along the northwest flank of the East Antelope structural basin was inferred by Mabey (1960) on the basis of gravity and borehole data. A northeast extension of the fault (fig. 2), as originally mapped, is inferred on the basis of additional surface-geophysical data, and hydrogeologic information.

STRATIGRAPHY

The bedrock complex on and near EAFB consists of pre-Cenozoic igneous rocks and consolidated Tertiary sedimentary rocks (Hewett, 1954; Dibblee, 1963). Quartz monzonite is the predominant igneous rock type exposed in the hills at EAFB (Dibblee, 1960b, 1963). The sedimentary series of rocks of Tertiary age generally consists of well-indurated volcano-clastic flows and fluvial-lacustrine sediments (Dibblee, 1963). In the few local outcrops, the Tertiary sediments form very resistant hills or ridges. The existence of Tertiary sedimentary rocks in the subsurface in the basins has been interpreted from seismic-reflection data (Cheadle and others, 1986).

A series of unconsolidated deposits of Quaternary age overlie the consolidated rocks. These deposits are the result of rapid uplift and erosion of the San Gabriel and Tehachapi Mountains during a wet, pluvial climate. Dutcher and Worts (1963) mapped these deposits as either alluvial or lacustrine, based on the mode of deposition. The alluvium is composed of unconsolidated to moderately indurated, poorly sorted gravel, sand, silt, and clay. Older units within the alluvium are typically more compacted and indurated than the younger units (Dutcher and Worts, 1963; Durbin, 1978). The lacustrine deposits are composed of fine-grained sands, silts, and clays that accumulated in a relatively large lake or marsh that at times covered large parts of the Antelope Valley (Dibblee, 1967). These lacustrine deposits consist primarily of thick layers of blue-green silty clay and a brown clay containing interbedded sand and silty sand layers. The brown clay generally overlies the blue-green clay. The transition from blue-green to brown clay may represent a change in the depositional environment from relatively deep water to shallow, intermittent submergence (Dutcher and Worts, 1963). Individual clay beds are locally as much as 100 ft thick and are interbedded with lenses of coarser material as much as 20 ft thick. The lacustrine deposits are believed to be transgressive from south to north, across Antelope Valley, lapping northward onto the older alluvium and in turn being overlapped from the south by younger alluvium (Dutcher and Worts, 1963) (fig. 3). Near the southern limit of the valley, the lacustrine deposits are buried beneath as much as 800 ft of alluvium, but near the northern limit the lacustrine deposits are exposed at land surface.

The most prominent surface features on EAFB are the lacustrine deposits that form the playa surfaces of Rogers, Rosamond, and Buckhorn Lakes. Rogers Lake is the largest of the three playas covering an area of about 46 mi^2 near the geographic center of EAFB. The playa surfaces consist of very fine-grained lacustrine sediments. Particle-size analysis of material obtained from the surface of Rogers Lake indicates that 85 percent of the particles are finer than 7.9×10^{-5} in., which is in the range of clay-sized particles. Montmorillonite and illite clays are predominant in the near surface of Rogers and Rosamond Lakes (Droste, 1961; Neal and others, 1968). Motts and Carpenter (1970) reported that surface clay deposits extend more than 75 ft beneath the southern part of the lake and 45 ft beneath the northern part of the lake on the basis of data from 14 test holes drilled on Rogers Lake. Near the center of Rogers Lake, the clay beds thin to a depth of 25 ft. According to Motts and Carpenter (1970), the relatively thin surface clay layer overlies a thick sequence of sand, which overlies a fanglomerate.

Motts and Carpenter (1970) reported a 200-foot thick sequence of clay beneath Rosamond Lake. The thickening of the clay from Rogers to Rosamond Lake is accompanied by an increase in the amount of

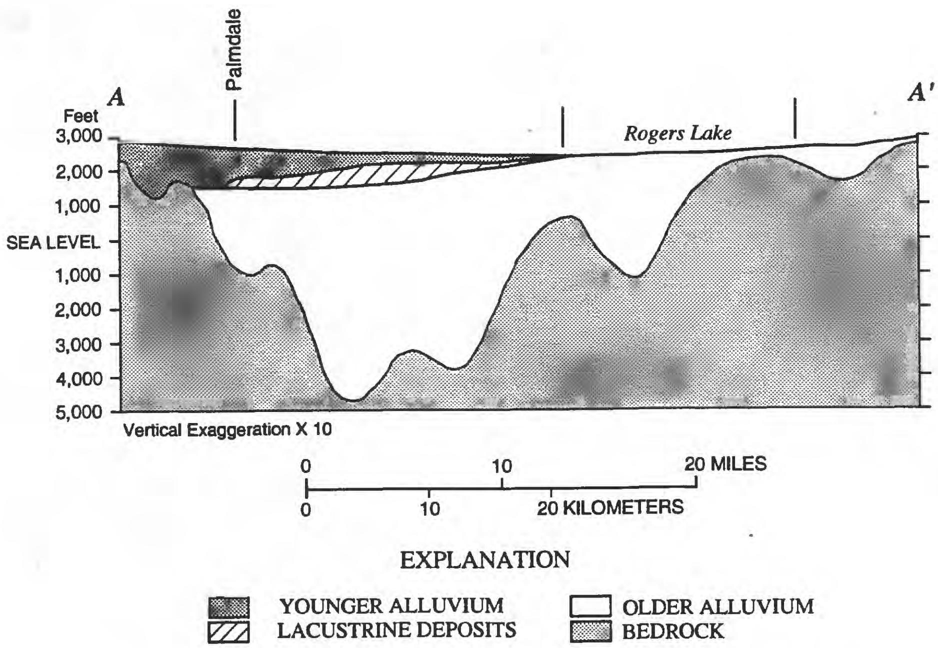

Figure 3. Generalized geologic section showing relation of lacustrine deposits to younger and older alluvium. Line of section is shown on figure 2.

blue-green clay. Motts and Carpenter (1970) attribute the increase in blue-green clay and the preservation of unaltered pollen samples to deposition under deep-water reducing conditions in the area of Rosamond Lake. Depths of the playa and lacustrine clays of Buckhorn Lake are unknown, and neither clay mineralogical information or pollen analysis are available.

Coarser grained alluvial deposits of sand, gravel, and cobbles and some silt form bajadas that skirt all the highlands near the playas. South of Buckhorn and Rosamond Lakes is a broad, sandy alluvial plain that grades gradually into the alluvial fans extending from the San Gabriel Mountains 18 mi to the south. To the west of Rosamond Lake, this plain extends 20 mi to EAFB of the Tehachapi Mountains.

AQUIFER SYSTEM

Previous investigators have defined two major ground-water-flow systems in the western Mojave Desert associated with Antelope Valley and Fremont Valley. Thayer (1946) mapped the Antelope Valley area into a series of ground-water subbasins bounded laterally by faults, consolidated rock, ground-water divides, and in some instances by arbitrary boundaries. Bloyd (1967) refined Thayer's subbasin maps on the basis of additional information, retaining the original names of the subbasins wherever possible (fig. 4). Bloyd's boundaries are the boundaries referred to in this report. EAFB overlies the Lancaster and North Muroc ground-water subbasins. The Lancaster subbasin is the largest and currently the most developed ground-water resource in Antelope Valley.

The aquifer system in the Lancaster subbasin consists of two alluvial aquifers known as the principal aquifer and the deep aquifer (Dutcher and Worts, 1963; Bloyd, 1967; Durbin, 1978). Both aquifers consist of interbedded heterogeneous mixtures of silt, sand, and gravel. The principal aquifer is unconfined and overlies lacustrine clay deposits within the sediments. This aquifer extends over most of the Lancaster subbasin south and southwest of Rogers Lake and provides most of the ground water pumped in Antelope Valley. The deep aquifer underlies the lacustrine clay beds and extends beneath Rogers Lake to the North Muroc subbasin. This aquifer is confined where overlain by the lacustrine deposits and unconfined elsewhere. Where unconfined, the deep aquifer grades upwards into the alluvium of the principal aquifer. The grading of the two aquifers provides a direct hydraulic connection between the two aquifers along the southern, western, and northeastern margins of the Lancaster subbasin

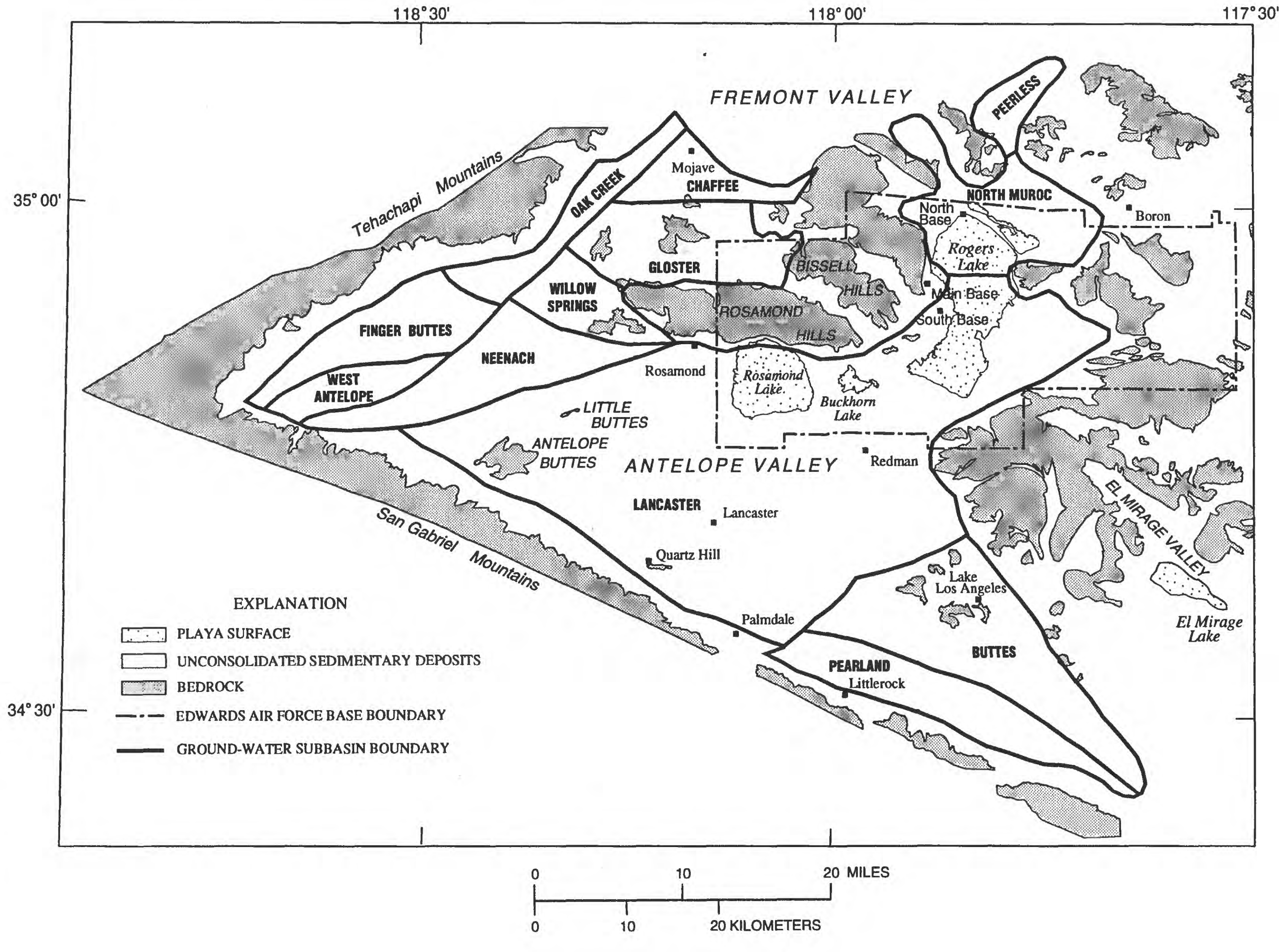

Figure 4. Ground-water subbasins in Antelope Valley (from Bloyd, 1967).

(Thompson, 1929). The deep aquifer is presumed to be underlain by low-permeability, consolidated sedimentary, and igneous rocks.

Ground water in the Antelope Valley area originates primarily from precipitation in the San Gabriel and Tehachapi Mountains. A portion of the surface runoff from precipitation infiltrates into the aquifer system at EAFB of the mountains and along the courses of the major stream channels extending onto the valley floor. Estimates of natural average annual recharge to the Antelope Valley ground-water basin range from 40,280 to 81,400 acre-ft (table 1) and are based on estimates of surface-water discharge from the surrounding mountains. The more recent estimates of Bloyd (1967) and Durbin (1978) probably are more representative of the actual recharge because they are based on longer term discharge and climatological data. Bloyd (1967) estimated the annual recharge rate for all ground-water subbasins in the Antelope Valley to be 58,000 acre-ft (fig. 4), however, Durbin (1978) only included those subbasins south and east of the Rosamond Hills (fig. 4) in his estimate of 40,700 acre-ft. Duell (1987) showed that most of the ground water north of the Rosamond Hills discharges northward from the Antelope Valley directly into the Fremont Valley and, therefore, is not available for use in either the Lancaster or North Muroc subbasins.

Prior to extensive ground-water development in Antelope Valley, ground water in the principal aquifer moved from the recharge areas near the mountain fronts toward the north central part of the valley where it was discharged by springs and evapotranspiration. Before the 1940's, ground water in the deep aquifer moved northward under the lacustrine deposits and Rogers Lake, and eventually was discharged from the Lancaster subbasin into the North Muroc subbasin (Durbin, 1978) (fig. 4). Data from recent gravity studies indicate the presence of a notch within the bedrock buried beneath the lakebed sediments at the north end of Rogers Lake. This feature may have provided the pass by which ground water, circulating within the Lancaster subbasin, moved into the North Muroc subbasin and then into the Fremont Valley as suggested by Thompson (1929).

With the extensive development of the ground-water system in the valley during the 1950's and 1960's, water levels in the principal aquifer declined to below the threshold level where evapotranspiration losses become significant. Ground-water pumpage became the primary source of discharge from the principal aquifer. This extensive ground-water development also caused changes in the flow patterns of the deep aquifer. Durbin (1978) estimated that by 1961, the direction of ground-water flow out of the northern Lancaster subbasin had been reversed, and that ground water in the deep aquifer flowed toward the major pumping centers in the central part of the subbasin. Movement of ground water between the two aquifers also occurs as leakage through the lacustrine beds and is dependent on the heads in the two aquifers. The water moves from the aquifer with the higher hydraulic head into the aquifer with the lower hydraulic head. Durbin's mathematical model indicated that the direction of leakage was downward from the principal aquifer into the deep aquifer along the western and southern periphery of the lacustrine deposits and upward from the deep aquifer to the principal aquifer in the north-central part of the Lancaster subbasin.

Table 1. Estimates of average annual recharge to Antelope Valley ground-water basin based on estimates of surface-water discharge from the surrounding mountains

[acre-ft, acre-foot; acre-ft/mi^2, acre-foot per square mile; mi^2, square mile]

Average annual recharge (acre-ft)	Surface-water drainage area (mi^2)	Recharge per unit discharge area (acre-ft/mi^2)	Source
81,400	558	146	Wright (1924)
68,800	483	142	Backman (1928)
50,000	558	90	Thompson (1929)
63,000	558	113	California Department of Water Resources (1947)
40,280	497	81	Snyder (1955)
58,000	558	104	Bloyd (1967)
40,700	385	106	Durbin (1978)

The potentiometric surfaces in the spring of 1990 for the Lancaster and North Muroc subbasins are shown in figure 5. Water-level data were collected by the USGS during the spring of 1990 as part of the the Antelope Valley-East Kern Water Agency (AVEK) monitoring program. The wells in figure 5 are shown in table 2 with their respective water-level altitudes. The potentiometric depressions north and east of Little Buttes and south of Redman are similar to those shown by Bloyd (1967) and Duell (1987),

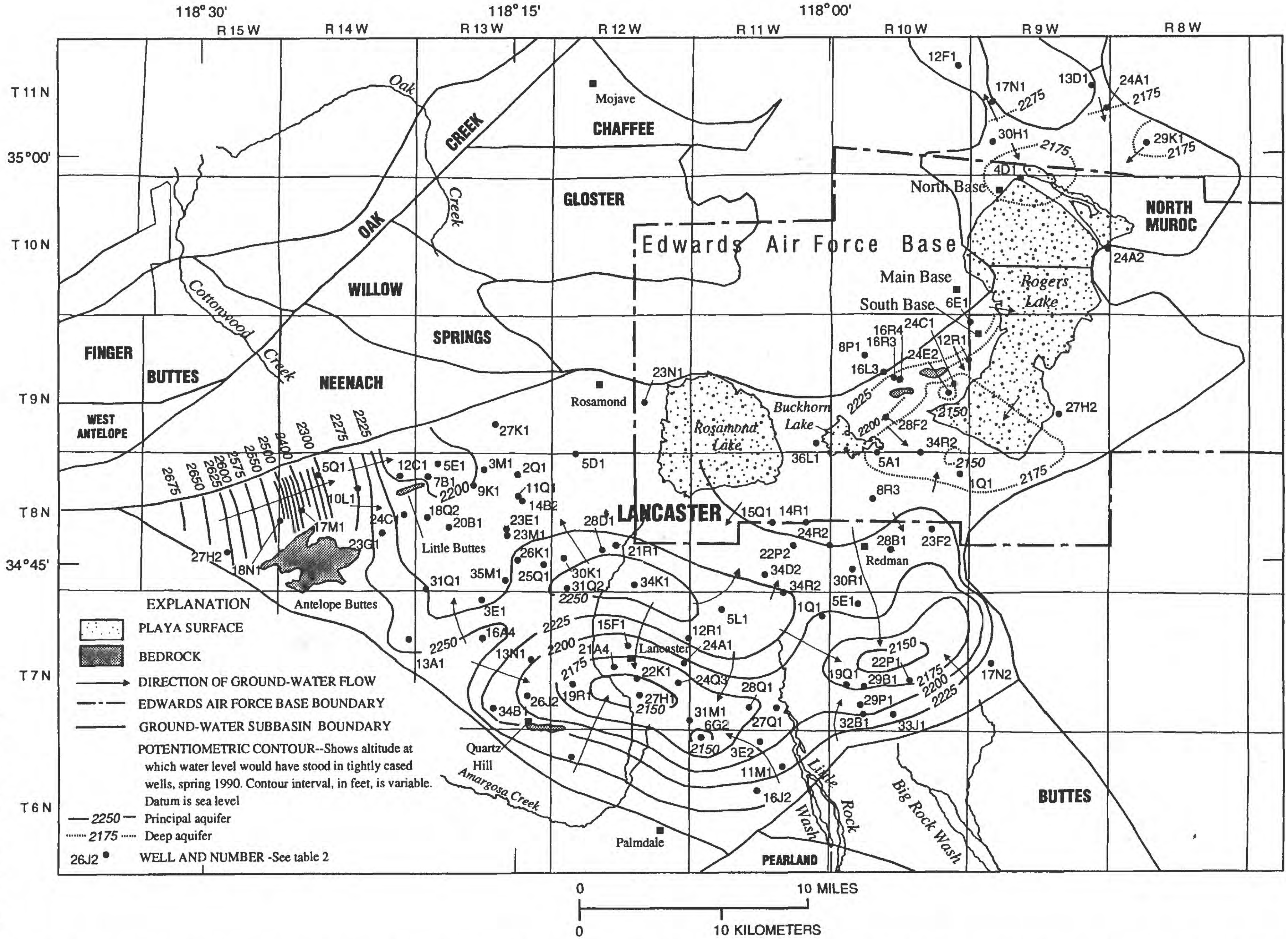

Figure 5. Potentiometric surfaces for the principal and deep aquifers of Lancaster and North Muroc ground-water subbasins spring 1990.

Table 2. Water-level altitudes for selected wells in the Lancaster and North Muroc ground-water subbasins, spring 1990

[Water-level altitudes, rounded to the nearest foot, are calculated from interpolated land-surface altitude from USGS topographic maps in feet above sea level, minus depth to water measured in hundredths of a foot]

State well No.	Water-level altitude	State well No.	Water-level altitude	State well No.	Water-level altitude
6N/11W- 3E2	2,195	8N/10W- 1Q1	2,157	8N/13W- 35M1	2,224
6G2	2,139	5A1	2,159	8N/14W- 5Q1	2,303
11M1	2,222	8R3	2,231	10L1	2,274
16J1	2,233	23F2	2,213	12C1	2,196
6N/12W- 7A1	2,250	28B1	2,207	17M1	2,419
7N/9W- 17N2	2,248	30R1	2,213	18N1	2,531
7N/10W- 5E1	2,217	8N/11W- 14R1	2,231	23G1	2,235
19Q1	2,169	15Q1	2,228	24C1	2,222
22P1	2,161	22P2	2,223	8N/15W- 27H2	2,639
29B1	2,175	24R2	2,229	9N/9W- 6E1	2,241
29P1	2,180	24R3	2,225	27H2	2,190
32B1	2,197	34D2	2,217	9N/10W- 8P1	2,290
33J1	2,217	34R2	2,227	12R1	2,182
7N/11W- 1Q1	2,196	8N/12W- 5D1	2,216	16L1	2,215
5L1	2,232	21R1	2,227	16R3	2,211
27Q1	2,178	28D1	2,249	16R4	2,219
28Q1	2,170	30K1	2,246	24C1	2,173
31M1	2,155	31Q2	2,253	24E2	2,130
33N1	2,175	34K1	2,261	28F2	2,201
7N/12W- 12R1	2,244	8N/13W- 2Q1	2,207	34R2	2,156
15F1	2,166	3M1	2,203	9N/11W- 36L1	2,186
19R1	2,158	5E1	2,198	9N/12W- 23N1	2,223
21A4	2,179	7B1	2,194	9N/13W- 27K1	2,220
22K1	2,149	9K1	2,202	10N/9W- 4D1	2,180
24A1	2,179	11Q1	2,206	24A2	2,210
24Q3	2,165	14B2	2,225	11N/8W- 29K1	2,168
27H1	2,127	18Q2	2,212	11N/9W- 13D1	2,172
7N/13W- 3E1	2,223	20B1	2,207	17N1	2,165
13N1	2,204	23E1	2,208	24A1	2,175
16A4	2,260	23M1	2,218	30H1	2,181
26J2	2,188	25Q1	2,247	36R1	2,192
34B1	2,214	26K1	2,230	11N/10W- 12F1	2,165
7N/14W- 13A1	2,229	31Q1	2,225		

but differ from those of Durbin (1978). Compared to Duell (1987), the more recent data show a steepening cone of depression between Lancaster and Palmdale (fig. 5). A potentiometric high, similar to that shown by Durbin (1978) and Duell (1987), is north of Lancaster at the terminus of Amargosa Creek. This probably is an area of recharge from surface runoff when amounts are significant enough to reach the valley floor. The recent trend of water levels in the area around Redman, an area of historically intensive ground-water pumping for agriculture irrigation, indicates slight recoveries in water levels. In this area, ground water in the principal aquifer flows southward toward an area where ground water is being pumped to supply agriculture irrigation; ground water in the deep aquifer flows northward toward EAFB water-supply wells (fig. 5).

GROUND-WATER USE

Ground-water use in Antelope Valley began in the 1880's (Thompson, 1929; Snyder, 1955) with only a few widely scattered shallow, small-diameter wells. Drilling of large-diameter production wells did not begin until about 1915. Several estimates of ground-water pumpage for Antelope Valley have been made using various indirect techniques (fig. 6). The only systematically measured and recorded pumpage data for the valley has been for EAFB; consequently, records of ground-water pumpage for Antelope Valley are incomplete. In addition, differences in estimates are significant where periods of different indirect techniques or investigators overlap.

Snyder (1955) estimated annual ground-water pumpage for Antelope Valley from 1924 through 1951 on the basis of electric-power consumption. He showed a very rapid increase in pumpage from about 55,000 to 173,000 acre-ft between 1924 and 1930. During the early 1930's, pumpage decreased somewhat and then began to increase rapidly into the 1950's (fig. 6). By 1951, the last year for which he made an estimate, the pumpage had increased to about 401,000 acre-ft. The California Department of Public Works (1955) estimated that ground-water pumpage in 1953 was about 480,000 acre-ft (fig. 6).

Investigators working during the 1970's estimated pumpage on the basis of land use and reported totals for various periods from 1950 to 1975 (fig. 6). The California State Water Resources Control Board (1974) estimated annual pumpage from 1950 through 1971. Their estimates for the early 1950's are considerably less than those of Snyder (1955) and California Department of Public Works (1955) and show a declining trend in pumpage as opposed to the rapidly increasing pumpage estimated by previous investigators. The California Department of Water Resources (K.W. Mido, written commun., 1973) estimated pumpage for 1958 through 1971. These estimates agree somewhat with those of the California State Water Resources Control Board for this period but show a more rapid decline in the annual pumpage. The Antelope Valley-East Kern Water Agency (W.G. Spinarski, written commun., 1976) estimated pumpage for 1974 and 1975. Their estimates were much higher than what would be expected from projecting the estimates of the California State Water Resources Control Board and the California Department of Water Resources. In 1988, pumpage estimates reported to the California Department of Water Resources by Antelope Valley water purveyors was about 62,000 acre-ft (Zettlemoyer, 1990; W.E. Templin, U.S. Geological Survey, written commun., 1991). The decrease in pumpage in Antelope Valley primarily is due to the decrease in irrigated agricultural land use and the import of about 41,000 acre-ft of water from the State Water Project (Zettlemoyer, 1990).

Records of pumpage for EAFB have been kept since 1947 and are documented and analyzed in various reports. Pumpage increased steadily from less than 1,000 acre-ft in 1947 to a high of 6,700 acre-ft in 1965 (fig. 7). From 1966 through 1988, annual pumpage ranged between 3,600 and 6,300 acre-ft/yr (Roy F. Weston, Inc., 1988; fig. 7). Estimates of pumpage data for 1989 and 1990 are about 5,950 and 6,150 acre-ft, respectively (Sergeant Thomison, Edwards Air Force Base, written commun., 1991; Technical Sergeant Swanigan, Edwards Air Force Base, written commun., 1991).

Durbin (1978) estimated that the annual average recharge of ground water to the Antelope Valley aquifers was about 40,700 acre-ft (table 1, fig. 6). On the basis of estimates of ground-water pumpage shown in figure 6, pumpage has exceeded recharge every year since the early 1920's. This imbalance is indicated by the declining water levels that have been recorded in wells throughout the valley. Furthermore, natural springs and a large area of flowing wells in Antelope Valley mapped by Johnson (1911) are not known to exist today.

HYDROGEOLOGIC ASSESSMENT AT EDWARDS AIR FORCE BASE

WELL DRILLING AND CONSTRUCTION

The criteria for selecting sites for the collection of borehole data and the installation of wells were based on the need for information on subsidence, subsurface geology, ground-water levels, and ground-water quality. A total of eight boreholes were drilled using mud-rotary methods during 1989-90, at four cluster sites on EAFB (fig. 8). Lithologic logs were made of the drill cuttings for one borehole at each site and bottom-hole cores were taken from seven of the boreholes. In addition to the drilling at these four sites, EAFB drilled three production wells, using mud-rotary methods, during this period, two in the Graham Ranch well field and one in the South Base well field (fig. 8) to replace production wells that had recently failed due to collapsed well casings. These wells were drilled in locations readily accessible to existing water-supply pipelines.

Construction data for wells completed in 1989 and 1990 on EAFB are summarized in table 3. Single and clustered wells were completed in boreholes at the Buckhorn, Branch Park, Holly, and Graham Ranch sites (fig. 8). Each well was screened and gravel packed; at cluster sites, wells were isolated

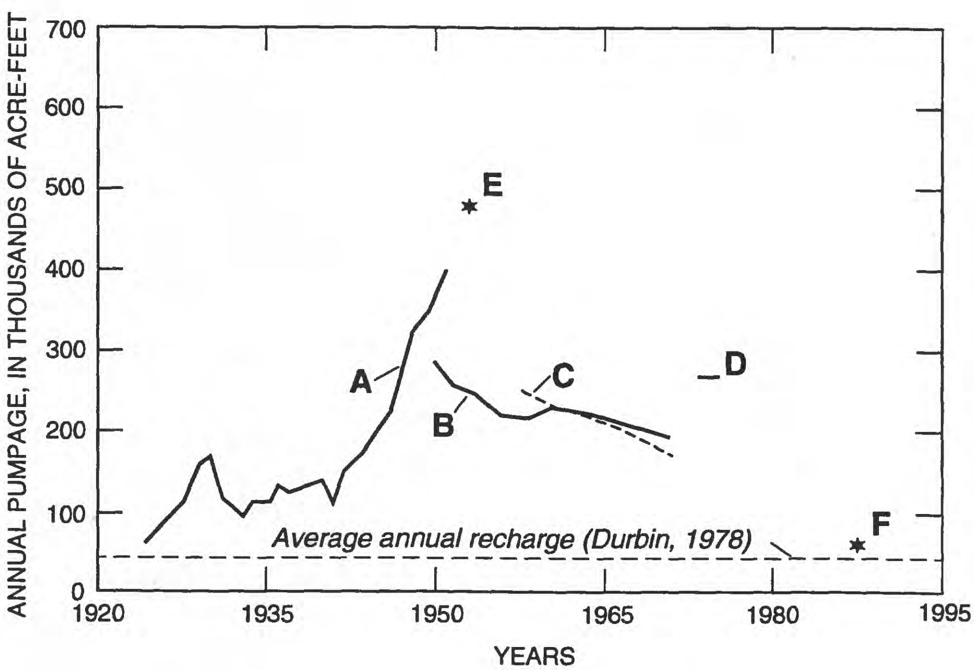

Figure 6. Estimated annual pumpage and average annual recharge for Antelope Valley, 1924-88. *A*, Snyder (1955; *B*, California State Water Resources Control Board (1974); *C*, California Department of Water Resources (K.W. Mido, written commun, 1973); *D*, Antelope Valley-East Kern Water Agency (AVEK) (W.G. Spinarski, written commun., 1976); *E*, California Department of Public Works (1955); *F*, Zettlemoyer (1990). Graph modified from Durbin (1978).

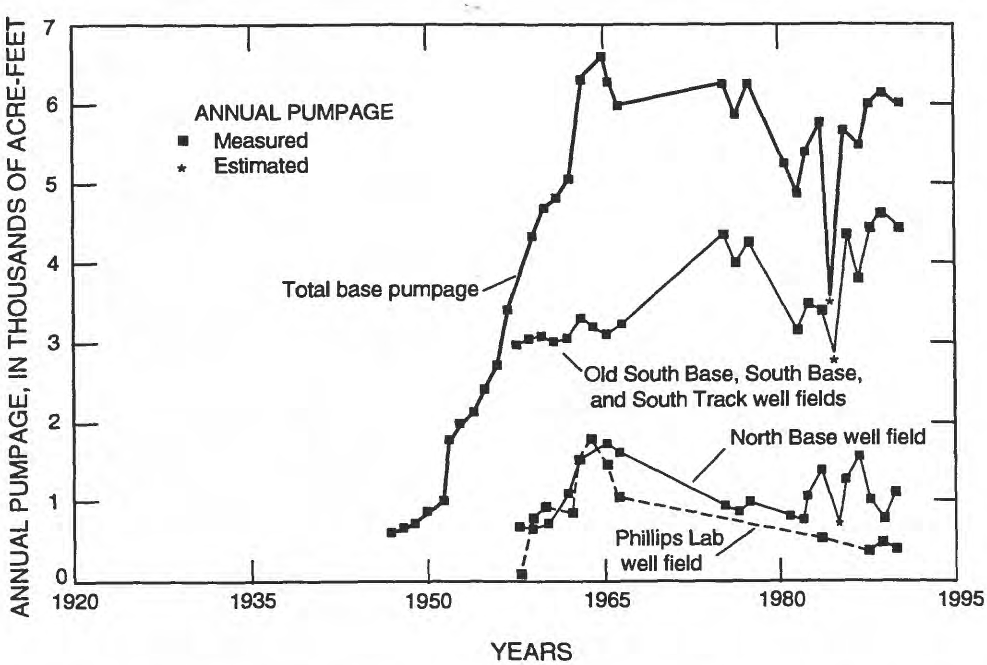

Figure 7. Annual pumpage at Edwards Air Force Base, 1947-90. Modified from Roy F. Weston, Inc. (1988).

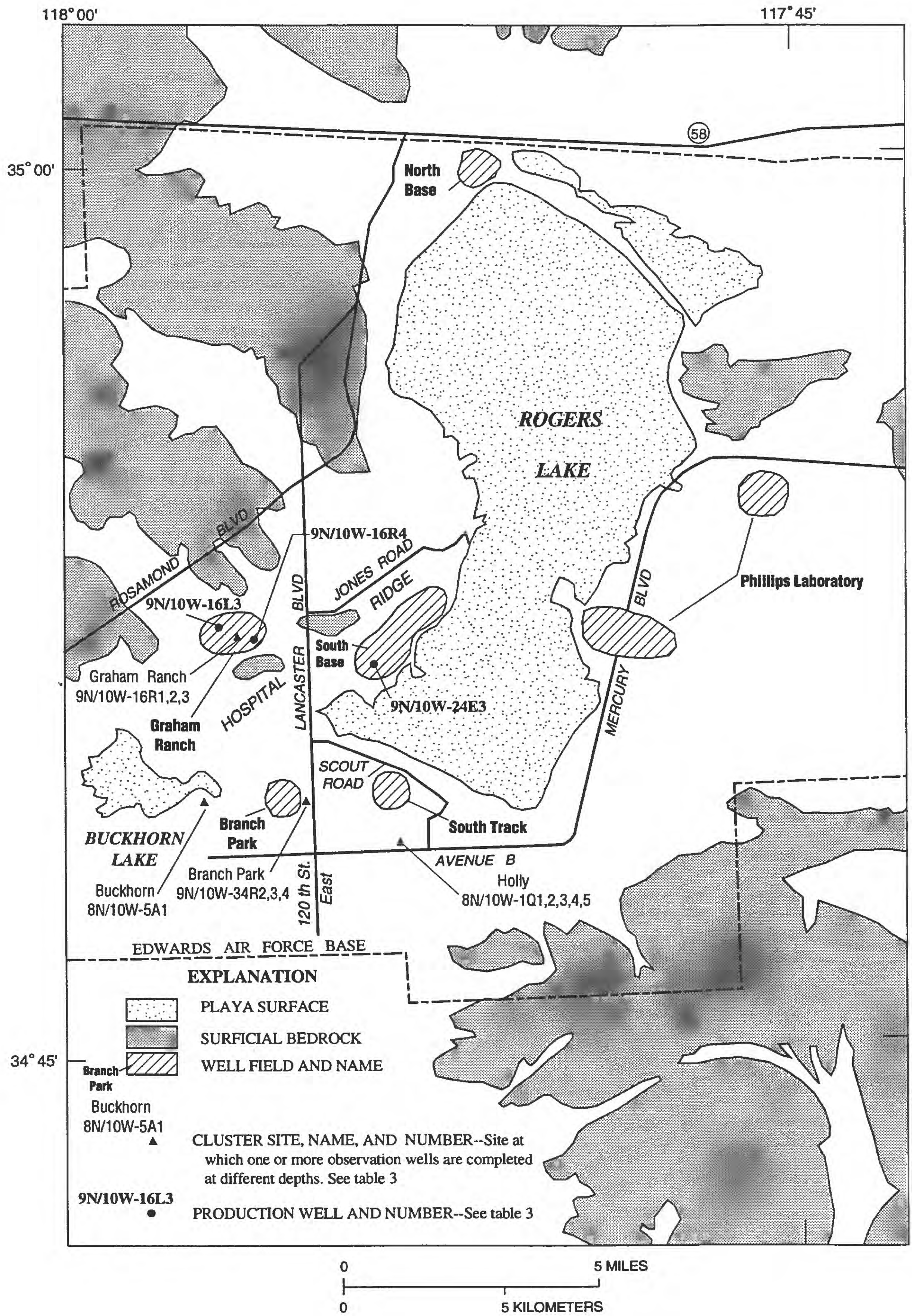

Figure 8. Location of well fields and cluster sites on Edwards Air Force Base.

Table 3. Construction data for wells completed in 1989 and 1990 on Edwards Air Force Base

[Altitude of land surface in feet above sea level. Primary use of well: Obs, observation well; Wtr, water-supply well. Depth drilled, casing depth, and gravel pack in feet below land surface. Type of finish: Grvl, gravel pack; Open, open hole. Screened interval and initial water level in feet below land surface. in., inch]

Site name and State well No.	Local well name	Altitude of land surface	Primary use of well	Depth drilled	Date of construction	Casing Diameter (in.)	Casing Depth	Gravel pack	Type of finish	Screened interval	Initial water level	Date of measurement
Buckhorn												
8N/10W- 5A1	BH1	2,287.2	Obs	958	10-31-89	2	947	884 - 947	Grvl	897 - 927	129.65	1-31-90
Branch Park												
9N/10W- 34R2	BP1	2,290.3	Obs	953	12-07-89	2	838	782 - 940	Grvl	788 - 808	136.76	2-06-90
34R3[1]	BP2	2,290.4	Obs	550	12-07-89	2	520	475 - 515	Grvl	480 - 510	136.08	2-06-90
34R4[1]	BP3	2,290.4	Obs	550	12-07-89	2	250	205 - 245	Grvl	210 - 240	136.08	2-06-90
Holly												
8N/10W- 1Q1	HO1	2,301.8	Obs	1,075	2-23-90	2	1,023	970 - 1,075	Grvl	980 - 1,010	147.37	5-09-90
1Q2[1]	HO2	2,301.7	Obs	1,107	3-01-90	3	643	600 - 640	Grvl	605 - 635	146.87	5-10-90
1Q3[1]	HO3	2,301.7	Obs	1,107	3-01-90	2	475	425 - 465	Grvl	430 - 460	145.46	5-10-90
1Q4[1]	HO4	2,301.7	Obs	1,107	3-01-90	2	130	80 - 120	Grvl	85 - 115	51.98	5-10-90
1Q5[2]	HO5	2,301.7	Obs	840	3-01-90	6	810	--	Open	--	--	--
Graham Ranch												
9N/10W- 16R1	GR1	2,315	Obs	965	11-12-89	2	840	790 - 840	Grvl	800 - 830	100.67	3-16-90
16R2[1]	GR2	2,315	Obs	650	11-12-89	2	584	485 - 580	Grvl	494 - 564	101.19	3-16-90
16R3[1]	GR3	2,315	Obs	650	11-12-89	2	360	290 - 350	Grvl	300 - 340	101.59	3-16-90
Graham Ranch well field												
9N/10W- 16L3	C-4 exploration well	2,325	Obs	270	8-31-89	16	270	50 - 270	Grvl	130 - 260	111.50	1-05-90
9N/10W- 16R4	C-4 production well	2,308.4	Wtr	709	6-30-90	16	700	0 - 702	Grvl	290 - 690	[3]110	4-15-90
South Base well field												
9N/10W- 24E3	S-7 production well	2,275	Wtr	706	8-03-89	16	700	0 - 700	Grvl	290 - 690	[4]140	8-03-89

[1]Clustered wells.
[2]Extensometer.
[3]Approximated from acoustic log.
[4]From driller's log.

from vertically adjacent screened intervals by bentonite grout placed in the annular space. At the Buckhorn site, one borehole was drilled and a single well 8N/10W-5A1, screened from 897 to 927 ft, was completed in it. Two boreholes were drilled at Branch Park, a single well 9N/10W-34R2 screened from 788 to 808 ft below land surface was completed in one of the boreholes and two cluster wells, one screened from 480 to 510 ft (9N/10W-34R3) and the other from 210 to 240 ft (9N/10W-34R4) were completed in the second borehole. Three boreholes were drilled at the Holly site. A single well, 8N/10W-1Q1, screened from 980 to 1,010 ft, was completed in one borehole. Three cluster wells, one screened from 605 to 635 ft (8N/10W-1Q2), the second from 430 to 460 ft (8N/10W-1Q3), and the third from 85 to 115 ft (8N/10W-1Q4), were completed in the second borehole. An extensometer was installed in the third borehole, 8N/10W-1Q5. The extensometer measures aquifer-system compaction in the interval from 15 to about 840 ft. Construction and operation of the Holly extensometer are further discussed by Blodgett and Williams (1992). At the Graham Ranch site, two boreholes were drilled. In the first borehole, a single well 9N/10W-16R1 was constructed with a screened interval from 800 to 830 ft. In the other borehole, two cluster wells were completed; one was screened from 494 to 564 ft (9N/10W-16R2) and the other from 300 to 340 ft (9N/10W-16R3). Each of the boreholes drilled by EAFB were completed with large diameter casings, long screen intervals, and gravel packs from the bottom of the hole to near land surface (table 3).

LITHOLOGIC LOGS

Lithologic logs were made of subsurface materials from drill cuttings collected at the surface during the drilling of the deepest borehole at Buckhorn, Branch Park, and Graham Ranch sites and the intermediate borehole at the Holly site (figs. 8 and 9*A-D*). Lithologic logs also were made during the drilling of three base boreholes, 9N/10W-16L3, 9N/10W-16R4, and 9N/10W-24E3 (figs. 9*E-G*).

The lithologic logs indicate that subsurface materials are largely heterogeneous arkosic alluvium consisting of varying thicknesses of interbedded clay, silt, sand, and gravel (figs. 9*A-G*). The only continuous horizons distinguishable from site to site on the basis of the drill cuttings were the brown, green, greenish-gray, and gray clays in the upper sections of the boreholes at the Buckhorn, Branch Park, and Holly sites (fig. 8).

Bottom-hole cores were collected from seven of the boreholes using a 10-foot core barrel. These cores, described in table 4, represent a small part of the stratigraphy of the sediments filling the basin in Antelope Valley, yet they delineate the variability, texture, composition, and degree of consolidation of the sampled horizons in the ground-water basin.

BOREHOLE GEOPHYSICS

Borehole-geophysical surveys were conducted at each of the four cluster sites (figs. 8, 9*A-9D*). EAFB supplied geophysical-log data for the three new production wells (figs. 8, 9*E-9G*). The surveys consisted of a set of four electric logs: spontaneous potential, 16- and 64-inch normal resistivity, and guard (focused) resistivity, in addition to natural gamma, acoustic, and caliper logs. Borehole-geophysical data were collected from the deepest borehole at each site except where noted. Acoustic surveys were not done at the Holly site, and only a partial acoustic log was done at the Branch Park site due to obstructions in the deepest borehole.

Electric logs measure the electrical properties of the formation around the borehole, the fluid in the formation, and the depth of borehole. Spontaneous potential (SP) and normal resistivity logs are used to distinguish between fine-grained sediments, silts and clays, and coarser grained sand and gravel (figs. 9*A-G*). For clays, the SP log had a positive deflection towards the right side of the scale; however, the resistivity log had a relatively negative deflection toward the left side of the scale. Sand and gravel beds have a negative deflection toward the left on the SP log and the resistivity logs have a high resistivity response toward the right side of the scale. A negative SP response with low resistivity generally indicates brackish water with a high dissolved-solids concentration. Guard resistivity is similar to the normal resistivity except the measurement is focused on a smaller interval thickness measuring discrete changes in resistivity, and capable of detecting thin layers in the section. The natural gamma log measures the amount of gamma emission from materials that have relatively high concentrations of potassium-40, uranium-238, uranium-235, and thorium-232. Clays, as well as feldspar-rich gravel, generally have higher concentrations of potassium-40. The acoustic log measures the velocity of an acoustic pulse between a transmitter and a receiver on the probe. The acoustic log gives an indication of the degree of consolidation of the formation, an approximate location of the water table, and is useful in the

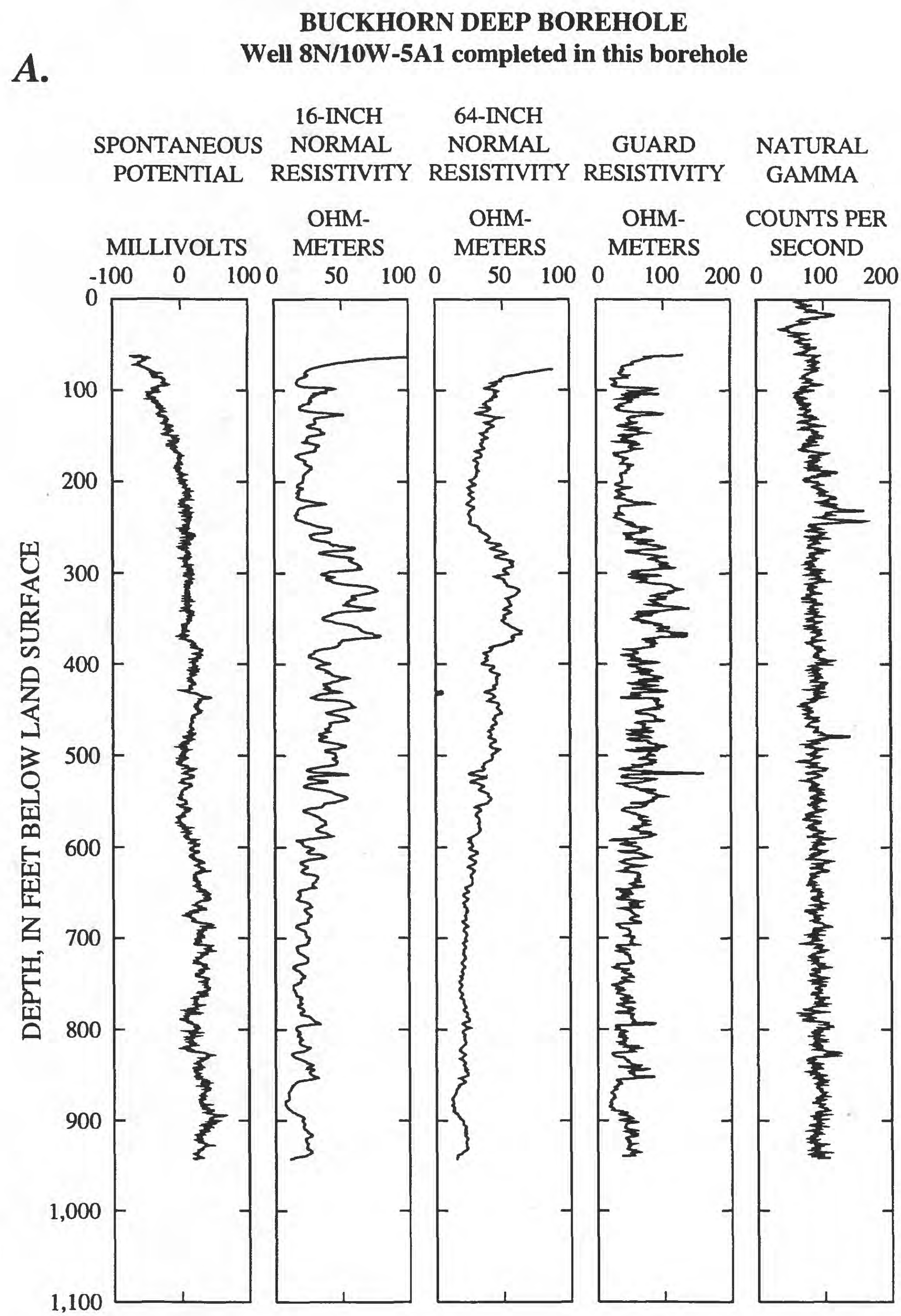

Figure 9. Geophysical and lithologic logs for boreholes drilled on Edwards Air Force Base during 1989 and 1990.

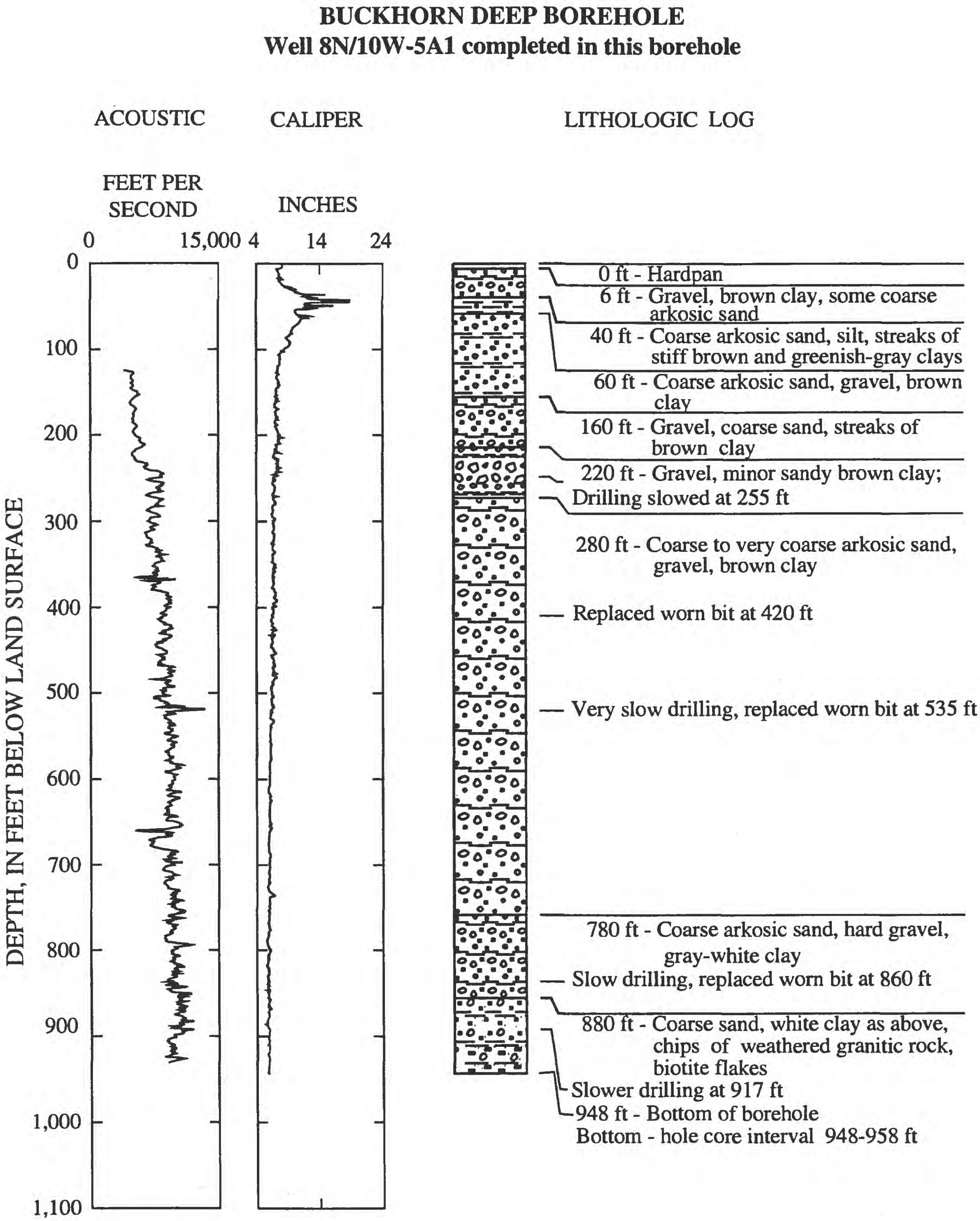

Figure 9. Geophysical and lithologic logs for boreholes drilled on Edwards Air Force Base during 1989 and 1990--*Continued.*

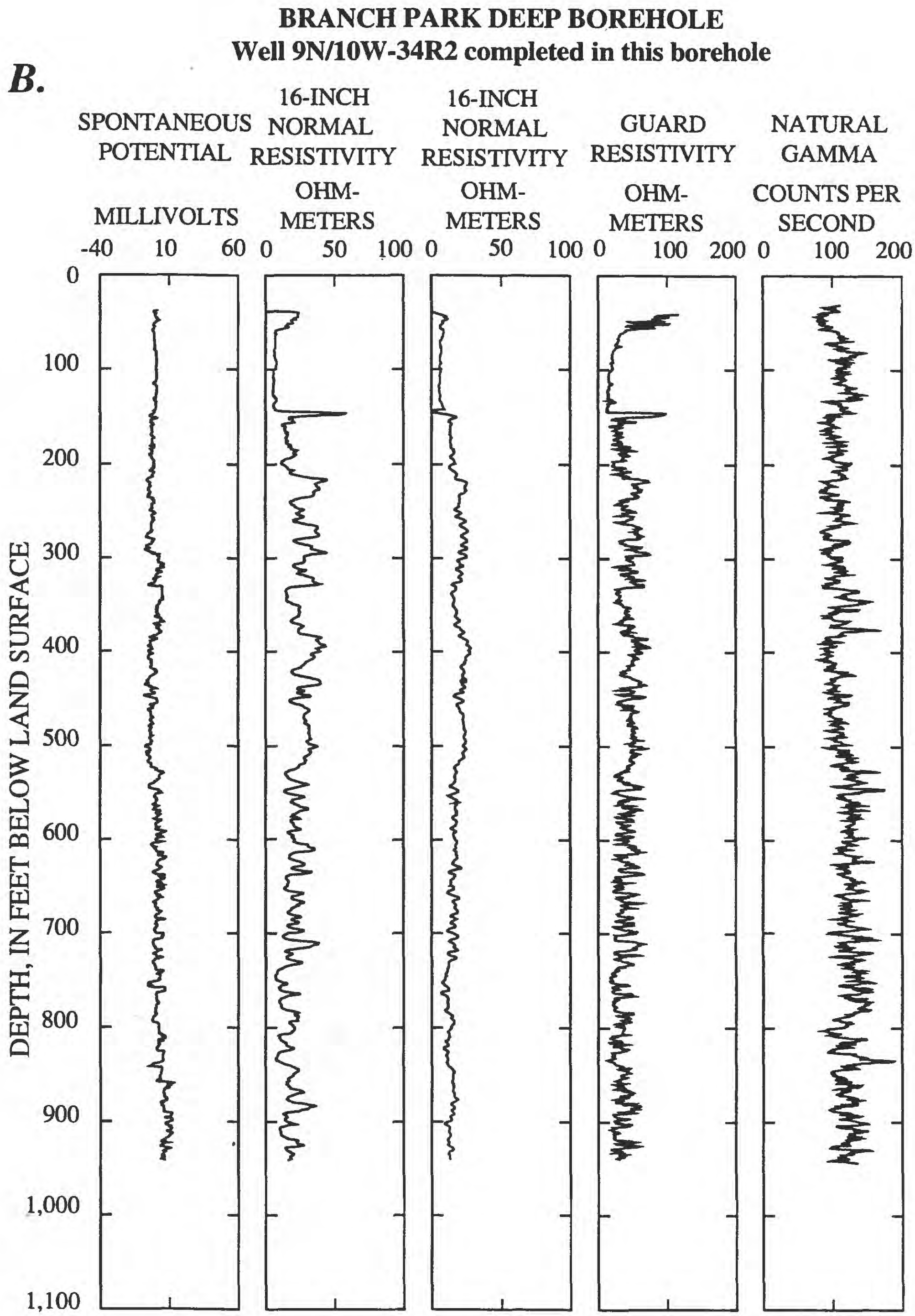

Figure 9. Geophysical and lithologic logs for boreholes drilled on Edwards Air Force Base during 1989 and 1990--*Continued.*

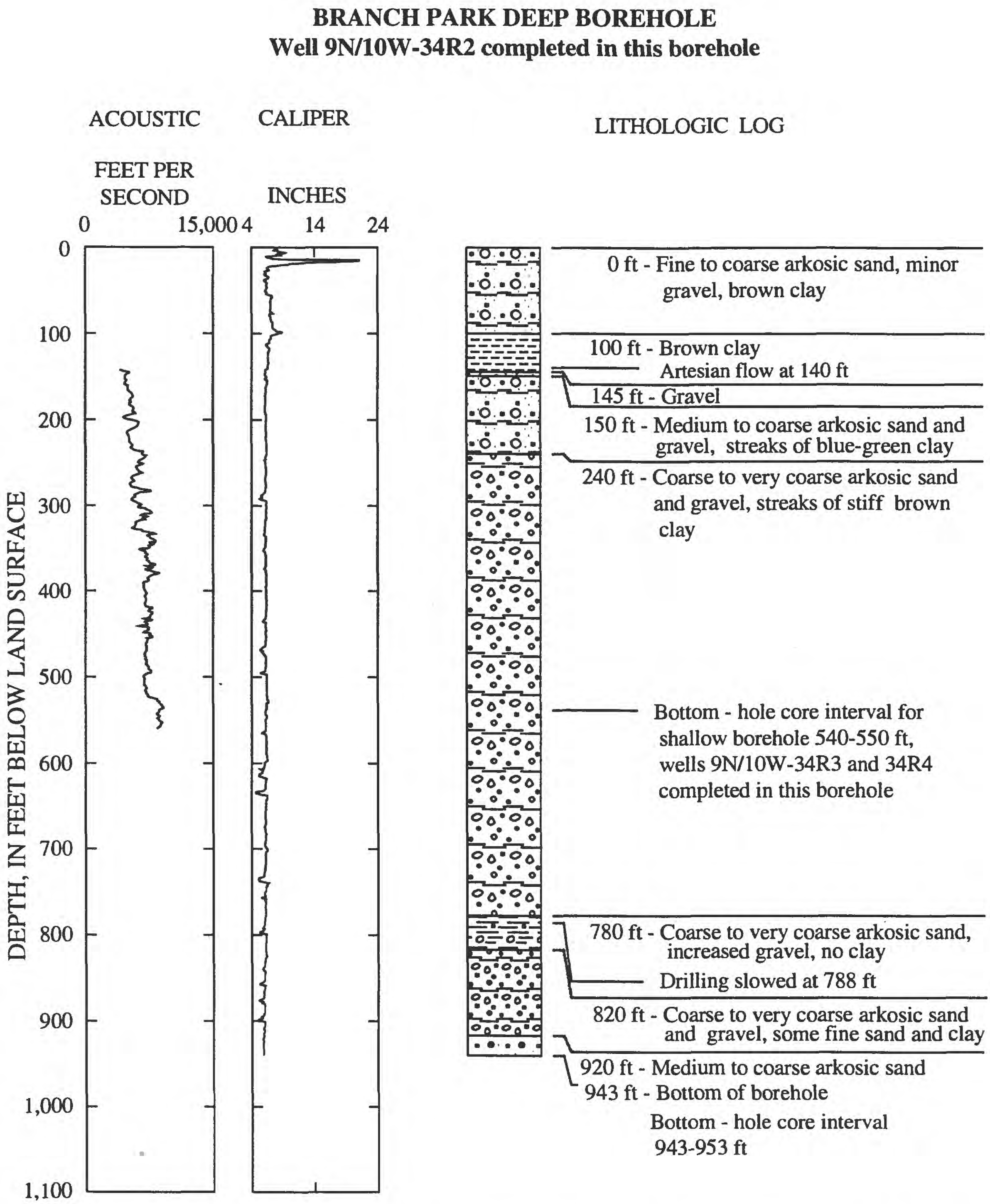

Figure 9. Geophysical and lithologic logs for boreholes drilled on Edwards Air Force Base during 1989 and 1990--*Continued.*

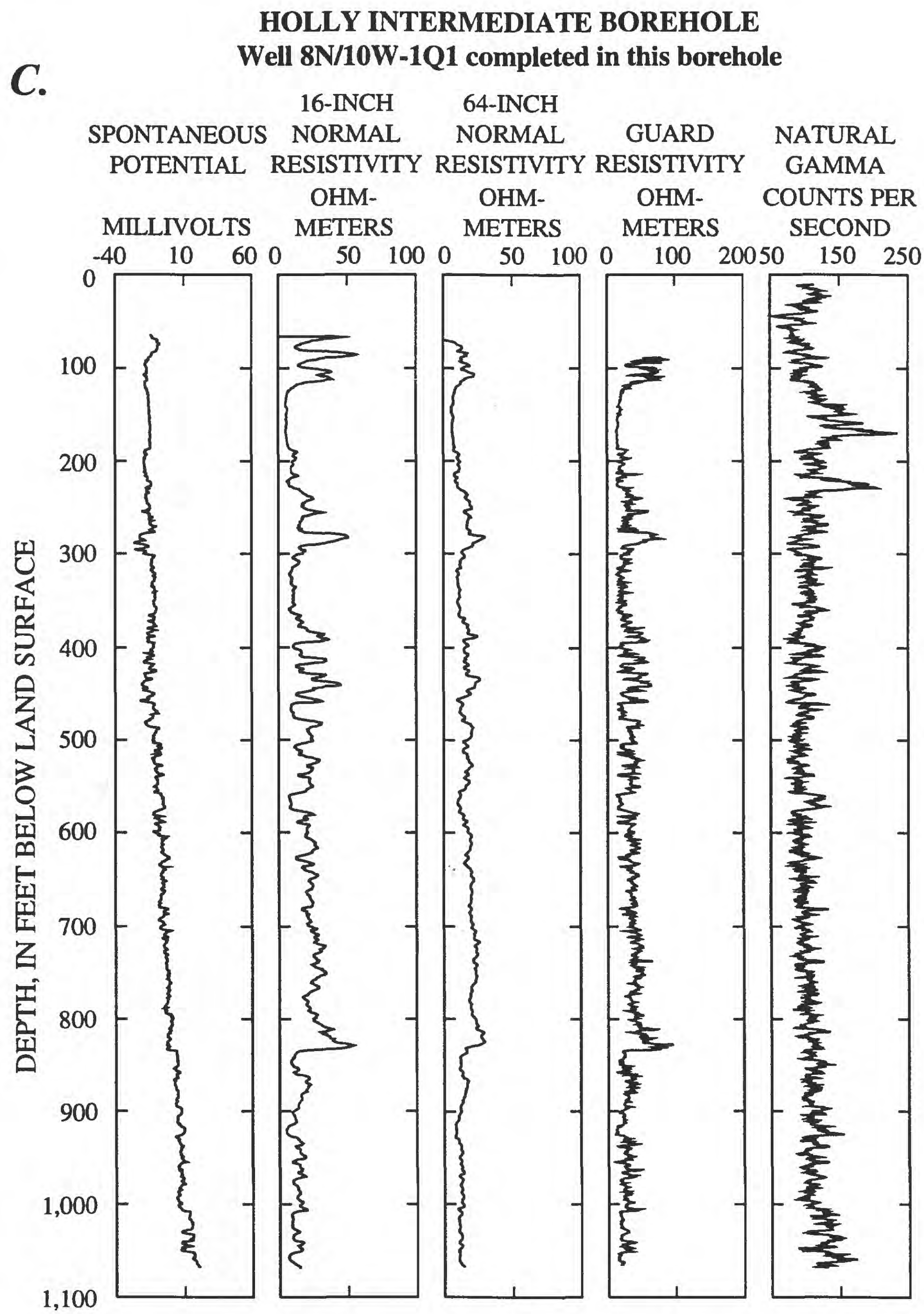

Figure 9. Geophysical and lithologic logs for boreholes drilled on Edwards Air Force Base during 1989 and 1990--*Continued.*

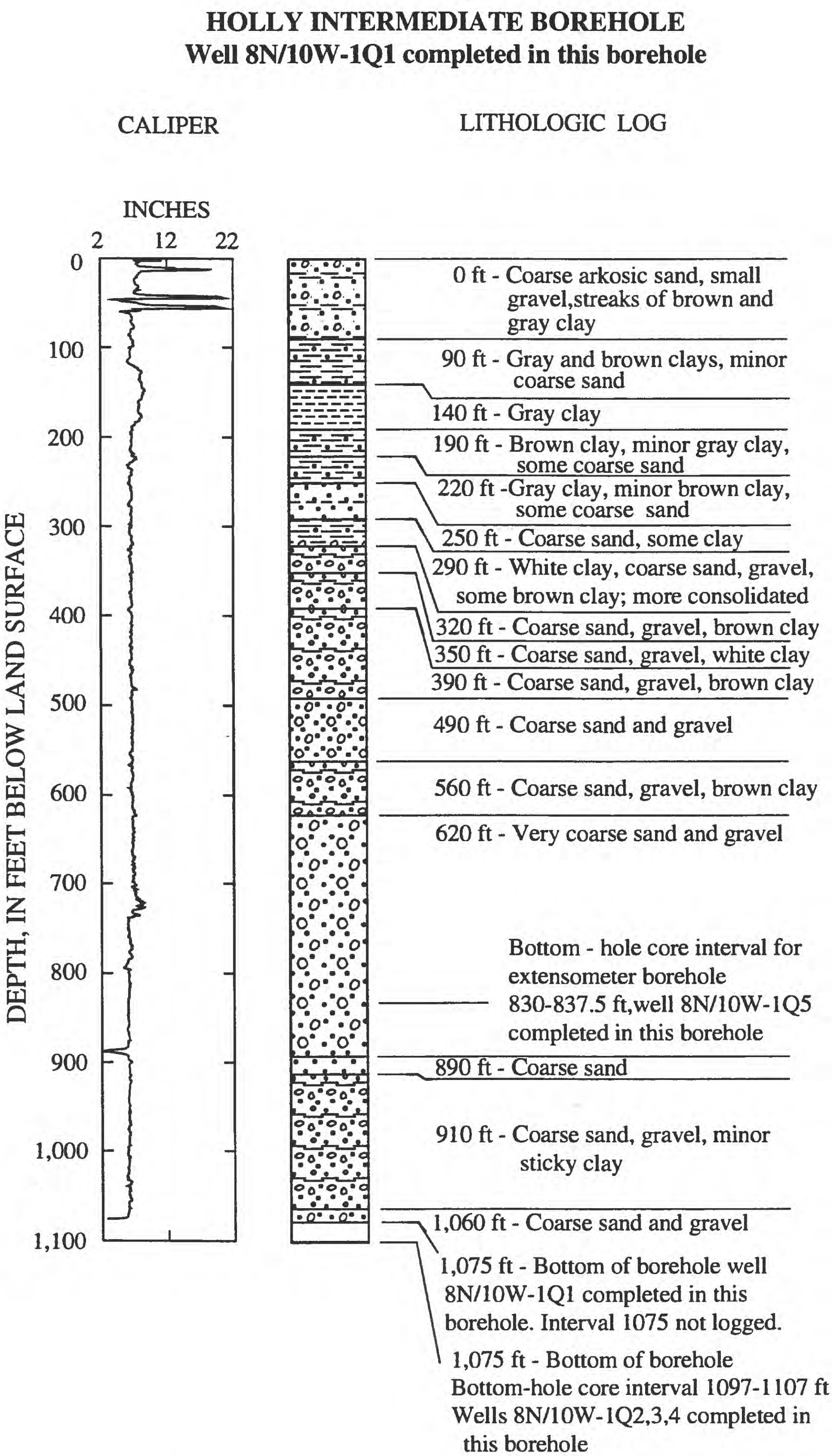

Figure 9. Geophysical and lithologic logs for boreholes drilled on Edwards Air Force Base during 1989 and 1990--*Continued.*

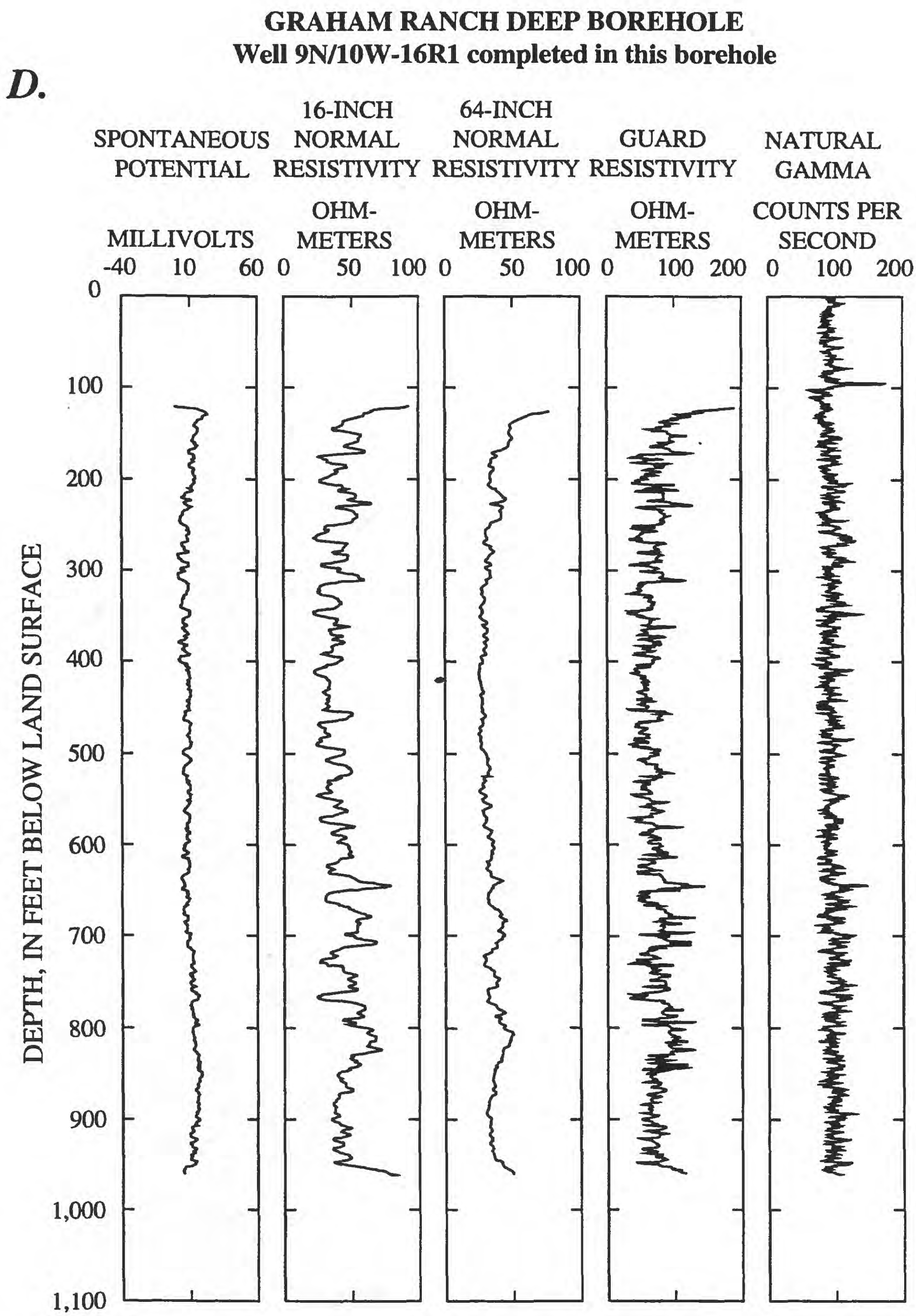

Figure 9. Geophysical and lithologic logs for boreholes drilled on Edwards Air Force Base during 1989 and 1990--*Continued.*

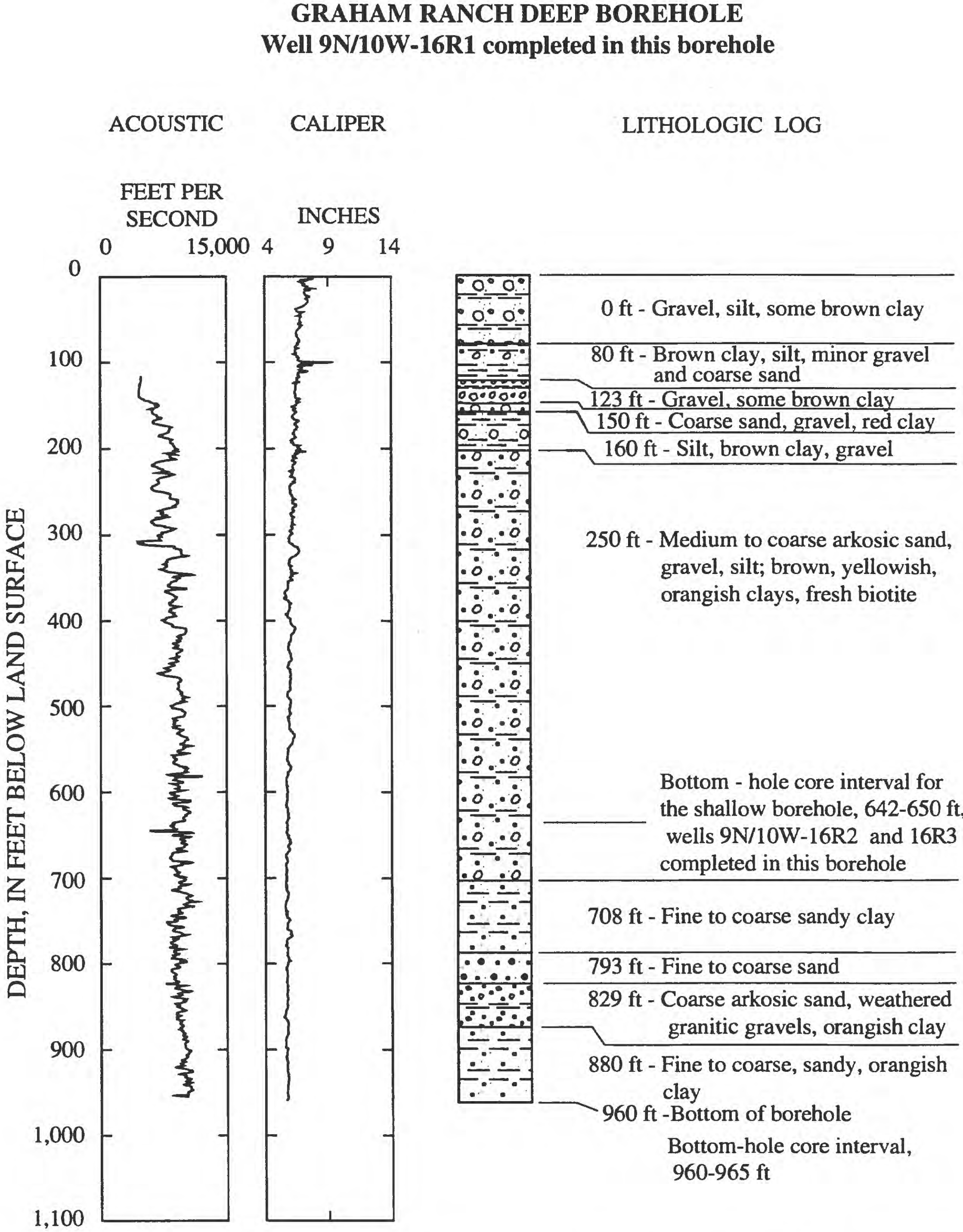

Figure 9. Geophysical and lithologic logs for boreholes drilled on Edwards Air Force Base during 1989 and 1990--*Continued.*

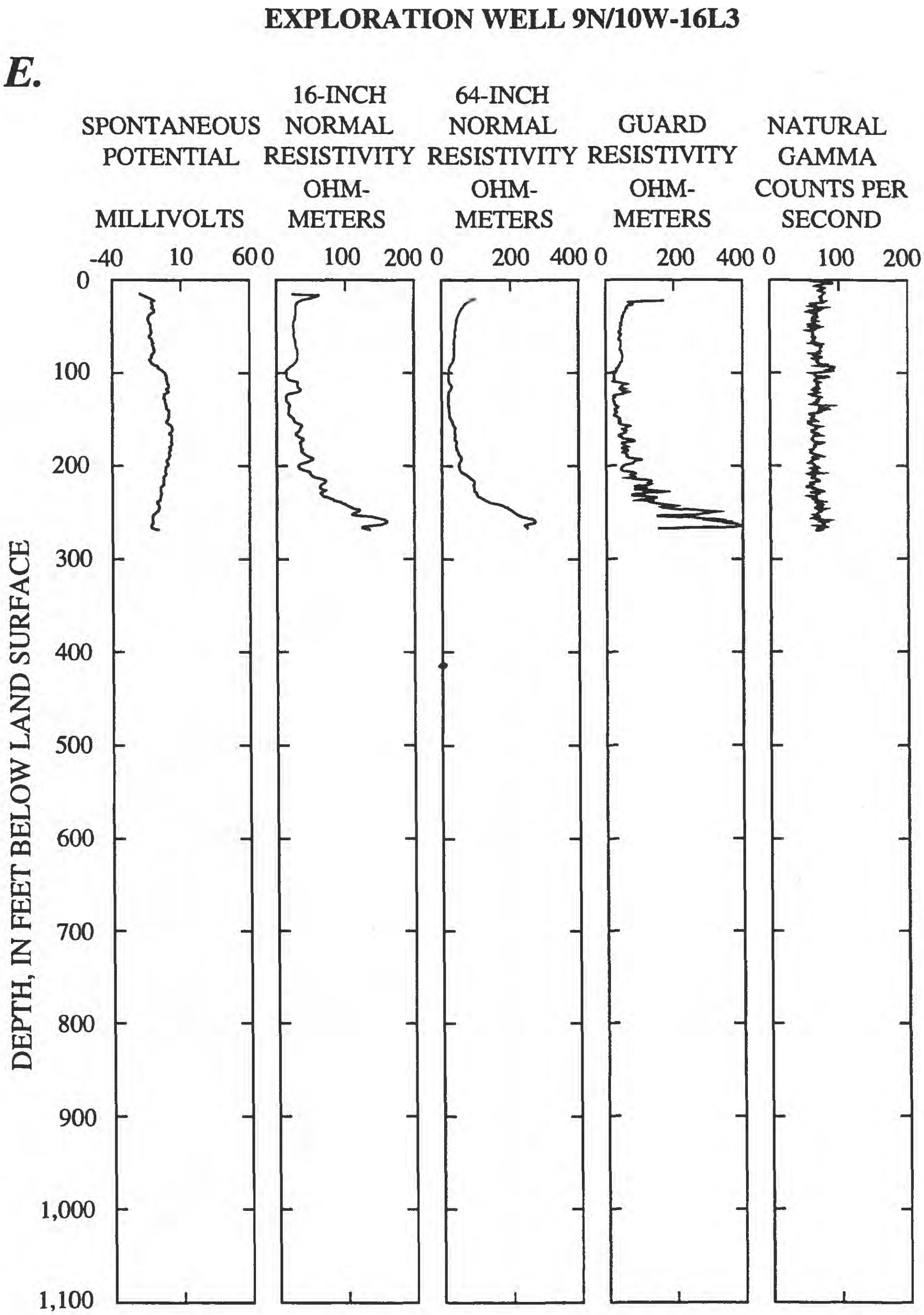

Figure 9. Geophysical and lithologic logs for boreholes drilled on Edwards Air Force Base during 1989 and 1990--*Continued.*

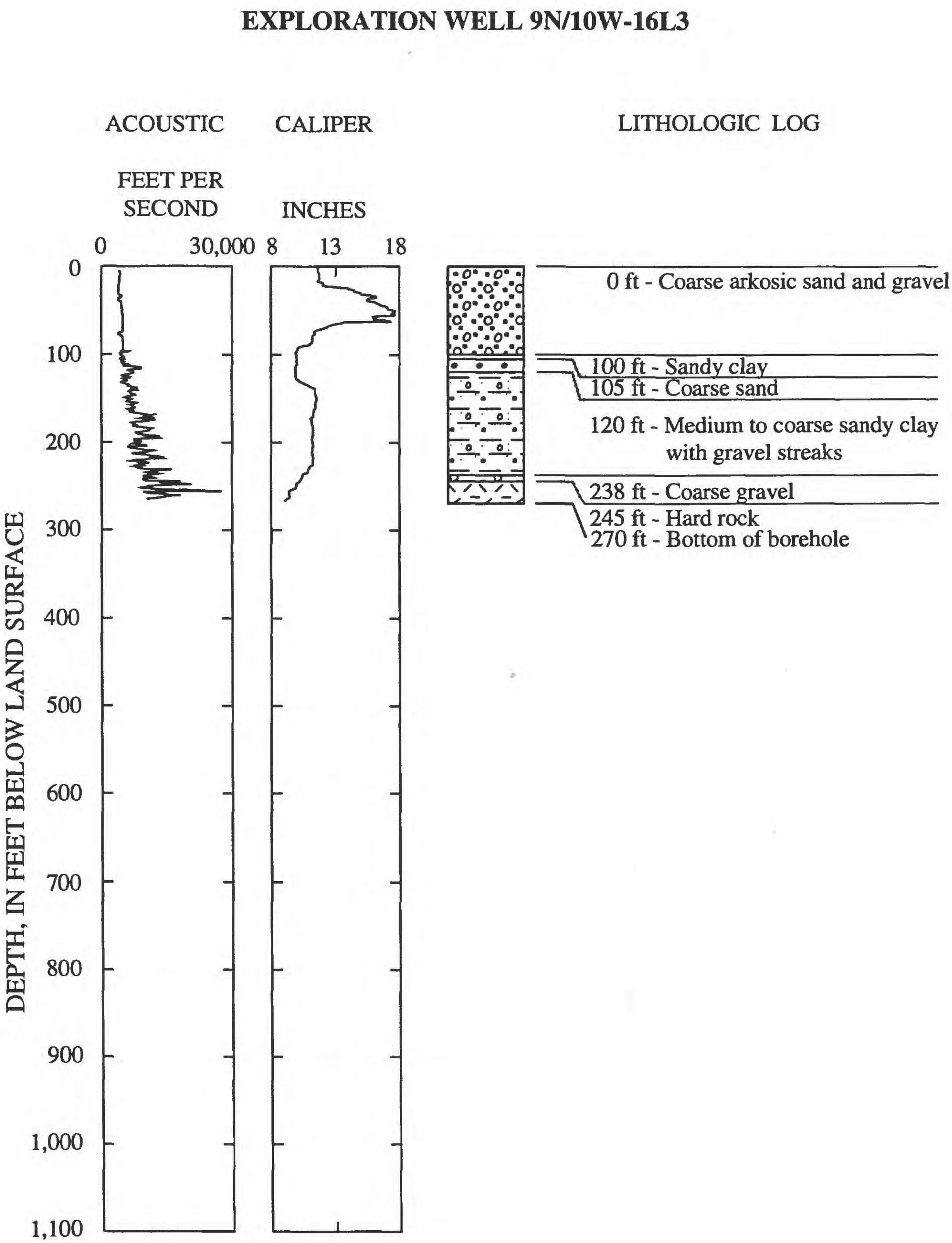

Figure 9. Geophysical and lithologic logs for boreholes drilled on Edwards Air Force Base during 1989 and 1990--*Continued.*

PRODUCTION WELL 9N/10W-16R4

F.

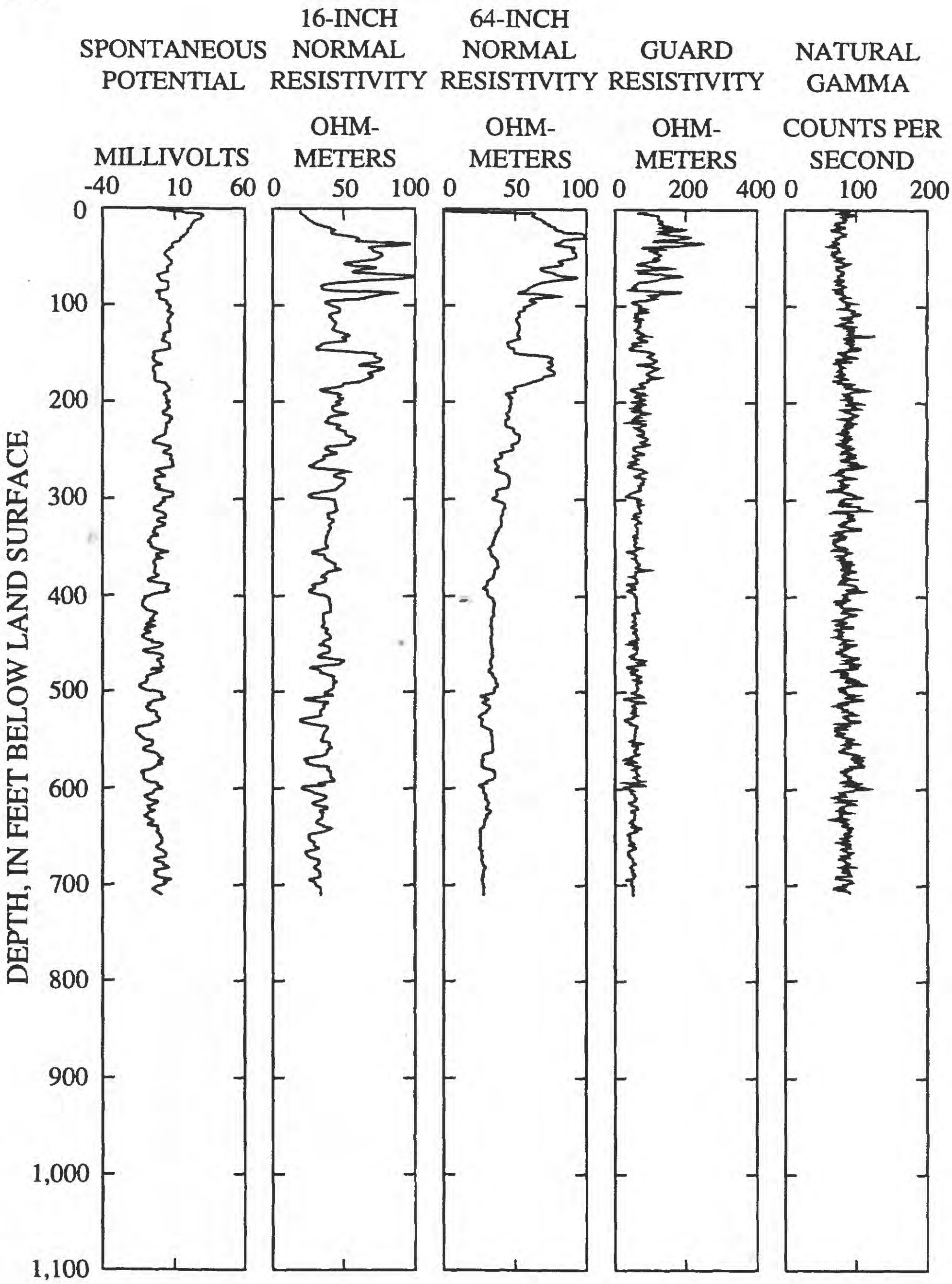

Figure 9. Geophysical and lithologic logs for boreholes drilled on Edwards Air Force Base during 1989 and 1990--*Continued.*

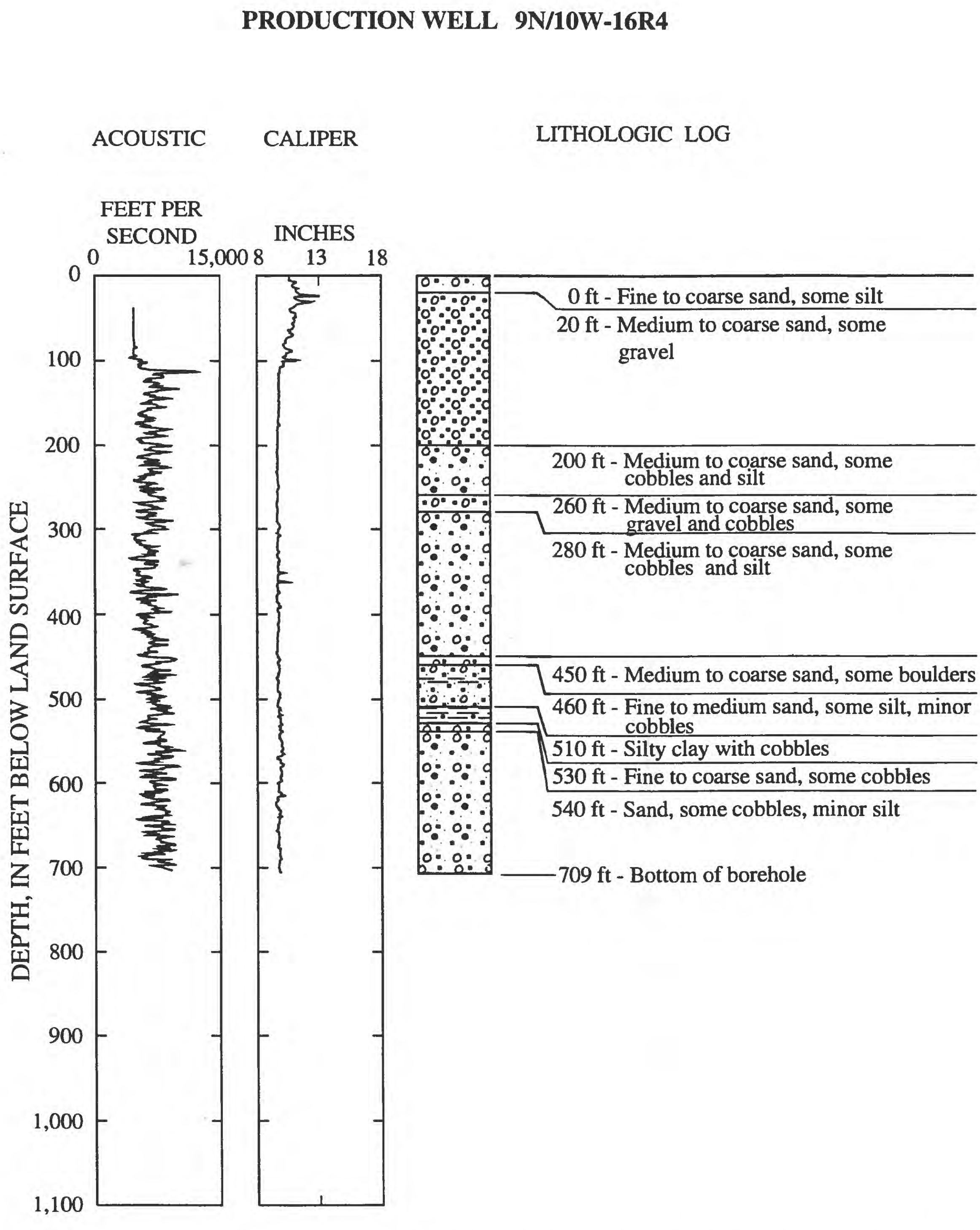

Figure 9. Geophysical and lithologic logs for boreholes drilled on Edwards Air Force Base during 1989 and 1990--*Continued.*

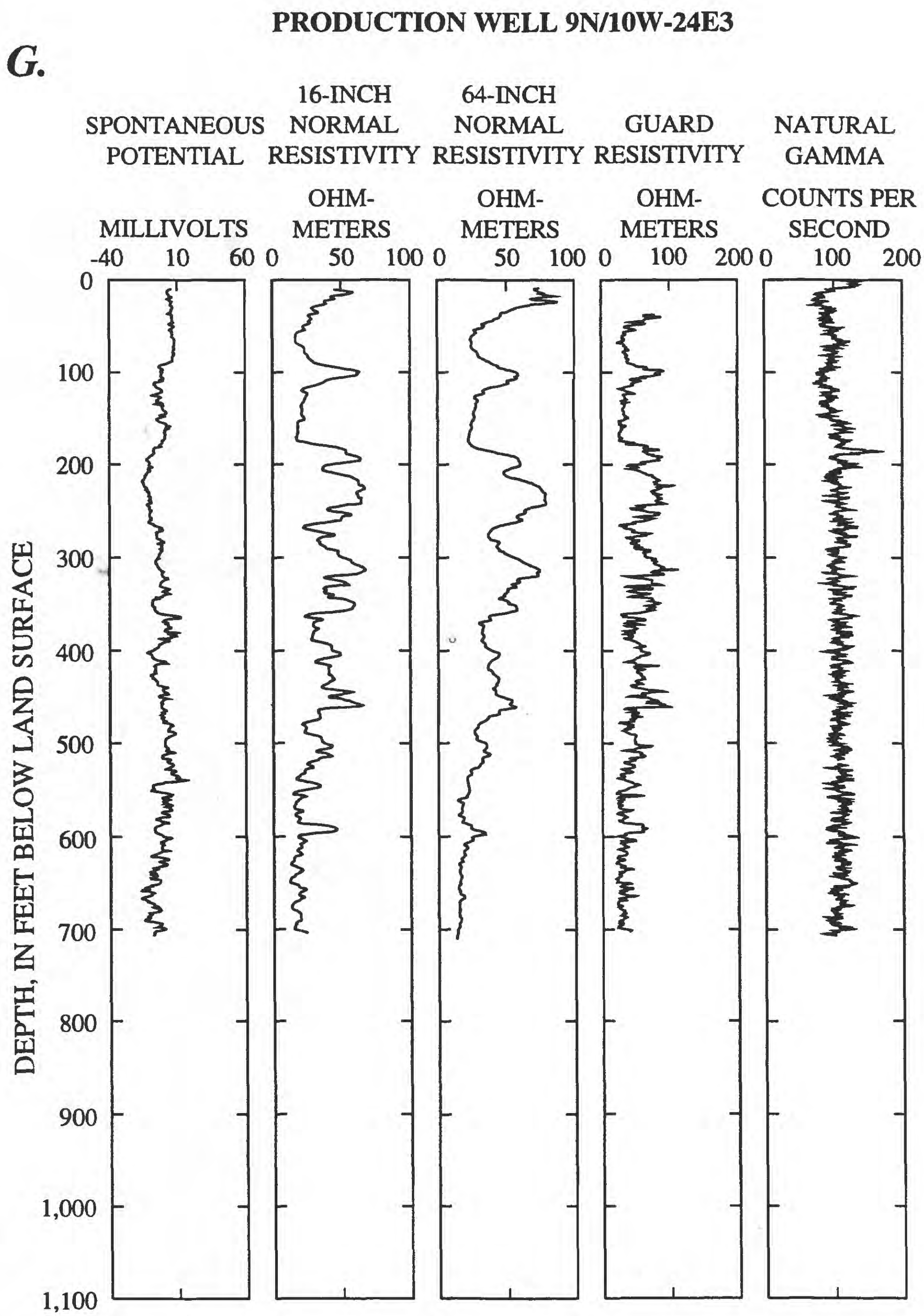

Figure 9. Geophysical and lithologic logs for boreholes drilled on Edwards Air Force Base during 1989 and 1990--*Continued.*

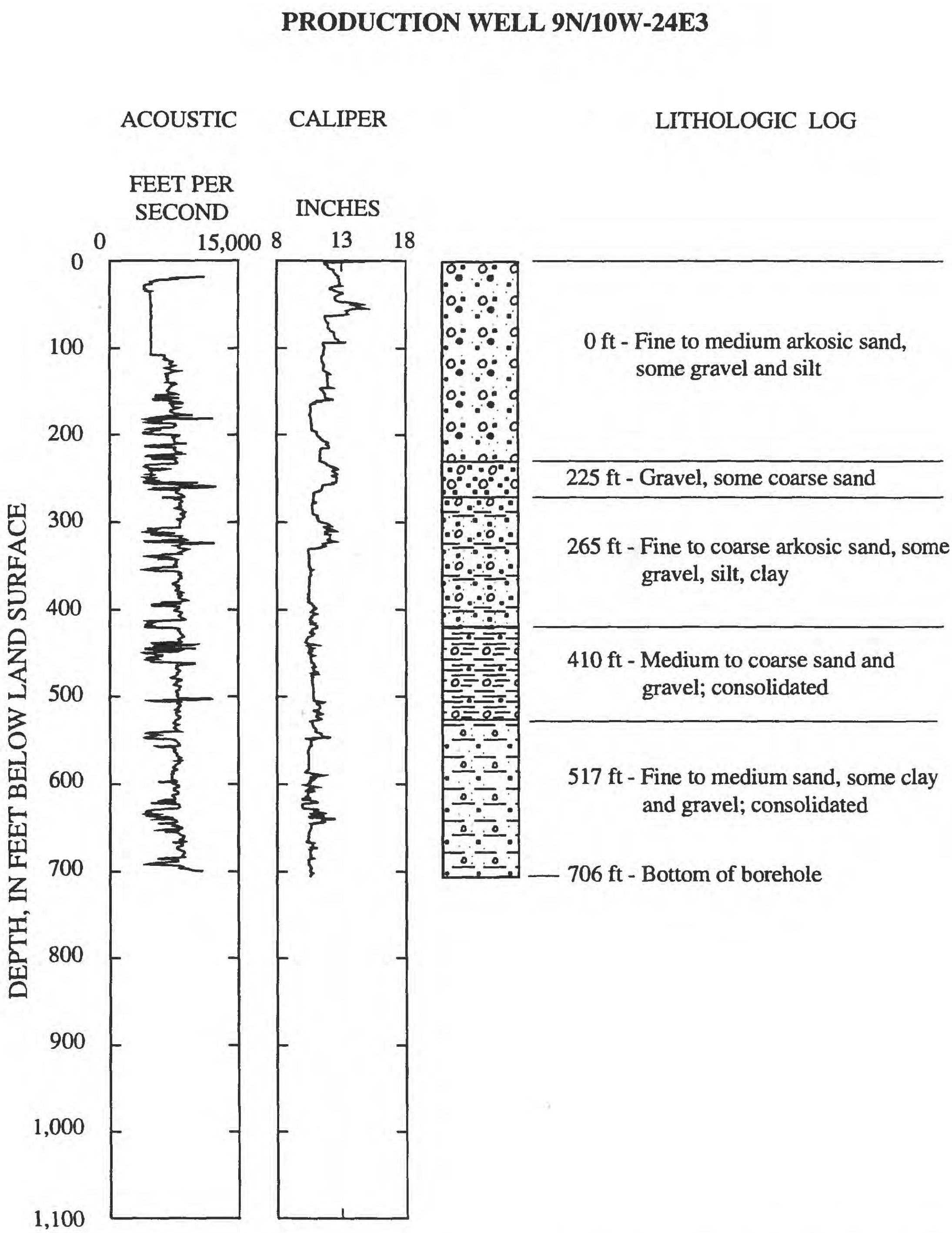

Figure 9. Geophysical and lithologic logs for boreholes drilled on Edwards Air Force Base during 1989 and 1990--*Continued.*

Table 4. Description of cores from boreholes drilled in 1989 and 1990 on Edwards Air Force Base

[Thickness and depth in feet. ft, foot; in., inch; ohm-m, ohm-meter]

Core description	Thickness	Depth
Buckhorn deep borehole. Core interval depth, 948-958 ft; 100 percent recovery. Core is a pale tan to medium orange brown, poor to well consolidated with siliceous cement, poorly sorted, frosted fine- to very coarse grained, subangular to very angular, granitic alluvium. Subhorizontal, coring-induced fractures occur randomly throughout the core. Resistivity values are unknown for this bottom hole core. Well 8N/10W-5A1 completed in this borehole.		
Alluvium is dark in color, black mica- and clay-rich, very coarse arkosic sand with occasional granitic and aplite pebbles to 0.4 in.	2	948
Upper alluvium grades into gravelly sand with decreased mica and clay, and increased silt. Clasts generally range from 0.1 to 0.2 in. with occasional pebbles from 0.7 to 3.1 in.	6.5	950
Core barrel penetrated a large, highly altered granitic cobble, 15 cm thick. Texture generally is equigranular with anhedral to euhedral grains of gray quartz, pink microcline, white altered orthocase, and black book biotite. Two induced fractures separate the cobble into three pieces.	0.5	956.5
Below the cobble, the alluvium changes into a light colored, sericitic-rich, poorly sorted, poorly consolidated, pebbly sand. The granitic clasts range from 0.6 to 2.0 in.	1	957
Branch Park deep borehole. Core interval depth, 943-953 ft; 50 percent recovery. Core is light grayish brown to medium grayish brown, of fine to medium coarse grained, angular to subrounded, arkosic alluvium that is well consolidated when dry with a siliceous cement, disintegrating when wet. No resistivity values available for this bottom hole core. Well 9N/10W-34R2 completed in this borehole.		
Alternating fine-grained, 6- to 8-inch thick, moderately sorted, pebbly, sandy silt and 1- to 3-inch, fine gravel layers.	4	943
Same as above with a higher clay content.	1	947
Branch Park shallow borehole. Core interval depth, 540-550 ft; 100 percent recovery. Core is medium grayish tan to medium grayish brown, well consolidated, poorly to moderately sorted arkosic alluvium with a siliceous cement. The 16-inch normal resistivity log for this borehole (fig. 9) shows that the 540- to 550-foot interval has resistivity values ranging from 12 to 19 ohm-m. Wells 9N/10W-34R3 and 34R4 were completed in this borehole.		
Alluvium is massive, with fine- to medium-grained, subangular to subrounded, gray quartz, white and pink feldspars, and bronze biotite grains and occasional quartz monzonite gravels 0.4 to 2.4 in. in diameter.	2	540
Gradation into a fine to coarse, subangular to rounded, alternating matrix- and clast-supported sandy conglomerate, ending with a thin 1-inch, thick gravel layer.	2.5	542
Alluvium is massive, finer grained, with few clasts larger than 0.2 in., and an increase in fine, black biotite.	5.5	544.5

Table 4. Description of cores from boreholes drilled in 1989 and 1990 on Edwards Air Force Base--*Continued*

Core description	Thickness	Depth
Holly deep borehole. Core interval depth, 1,097-1,107 ft; 60 percent recovery. Core is highly fractured, highly altered, coarse-grained quartz monzonite bedrock. Wells 8N/10W-1Q2, 1Q3, and 1Q4 completed in this borehole.		
Weathered bedrock fragments to 4.7 in., composed of white, altered feldspars, gray quartz, bronze biotite, and manganese oxide.	2.5	1,097
Decomposed bedrock with mineral composition of white, altered orthoclase, pink microcline, gray quartz, and bronze biotite. Fracture planes in this section show slippage, and limonite staining.	1.5	1,099.5
Pegmatite dike with very angular rock fragments to 1.6 in. of pink microcline and gray quartz.	1	1,101
Same composition and texture as 1,099.5-foot interval.	1	1,102
Holly extensometer borehole. Core interval depth, 830-840 ft; 80 percentage recovery. Core is light tan to light grayish orange, well consolidated when dry with siliceous cement. This core is correlated to the 830- to 837.5-foot interval of the 16-inch normal resistivity log of the Holly intermediate borehole (fig. 9*C*) about 50 ft to the southeast with resistivity values ranging from 14 to 18 ohm-m. This core is similar to the 600-foot zone of the Graham Ranch shallow borehole core. Well 8N/10W-1Q5 completed in this borehole.		
Alternating medium-grained, 6- to 8-inch thick, pebbly, sandy arkosic alluvium and 1- to 4-inch cobble layers. Matrix grains are frosted, angular to rounded, clear quartz, white, altered feldspar, and minor black biotite. Pebbles and cobbles, 5 to 10 percent, are subrounded to rounded, 0.2 to 2.4 in. granitoids with color index of 1-3, dense red, green, and purplish rhyolites, and white, banded rhyolites.	7.5	830
Gradation to a sandy silt with same composition as above.	0.5	837.5
Graham Ranch deep borehole. Core interval depth, 960-965 ft; 80 percent recovery. Well 9N/10W-16R1 completed in this borehole.		
Core is a light tan to light grayish tan, composed of poorly sorted, massive, coarse sandy arkosic alluvium with a fine-grained siliceous cementing matrix and occasional gravels. The mineral composition is subangular to subrounded, coarse sand of gray quartz, pink and white feldspars, and black biotite. Gravels are angular to well rounded, white quartz monzonite, pink granite, and pink and gray pegmatite clasts from 0.8 to 2.4 in. in diameter. Resistivity values are unknown for this bottom hole core. Well 9N/10W-16R1 completed in this borehole.	4	960
Graham Ranch shallow borehole. Core interval depth, 642-650 ft; 100 percent recovery. Core consists of light tan to grayish orange brown, poorly sorted, massive, angular to well rounded, medium- to coarse-grained arkosic alluvium. The material is well consolidated when dry, having a siliceous cement, but disintegrates when saturated. Occasional subangular to rounded, granitoid, aplite, and pegmatite gravels ranging from 0.4 to 1.6 in. throughout the core. Correlating this interval to the 16-inch normal resistivity log of the nearby deep borehole (fig. 9*D*), the resistivity values range from 33 to 38 ohm-m. Wells 9N/10W-16R2 and 16R3 completed in this borehole.		
Alluvium is darker in color and clay-rich.	1	642
Gradation into material lighter in color and rich in white, altered orthoclase.	7	643

identification of contrasting lithologic units that may cause seismic refractions along the contact. The caliper logs show the diameter of the borehole with depth.

The logs for the deep borehole at the Buckhorn site (fig. 9*A*) suggest unsaturated and saturated, unconsolidated, very fine-, fine-, and medium-grained alluvial sediments from the surface to about 240 ft below land surface; poor to moderately consolidated, medium- and coarse-grained beds to 540 ft; and moderate to moderately well-consolidated, clay-rich, fine-, medium-, and coarse-grained beds to the bottom of the borehole. At the Branch Park site, 2 mi to the east of the Buckhorn site (fig. 8), the logs for the deep borehole (fig. 9*B*) indicate unsaturated and saturated, unconsolidated to moderately consolidated, relatively thick sequences of very fine-, fine-, medium-, and coarse-grained sediments from the surface to about 530 ft below land surface, and moderate to moderately well-consolidated, narrower beds of fine-, medium-, and coarse-grained sediments to the bottom of the borehole. The logs for the intermediate borehole at the Holly site (fig. 9*C*) indicate unsaturated and saturated, unconsolidated to moderately well-consolidated, interbedded, very fine-, fine-, medium-, and coarse-grained alluvial sediments from the surface to about 838 ft below land surface. At depths greater than 838 ft to the bottom of the borehole, the logs indicate that the material becomes finer grained and perhaps more consolidated.

The borehole geophysical logs for the deep borehole at the Graham Ranch site (fig. 9*D*) indicate varying thicknesses of interbedded, fine-, medium-, and coarse-grained alluvial sediments that are unconsolidated at the surface, becoming more consolidated with depth. At about 770 ft to the bottom of the hole, the formation becomes moderately well- to well-consolidated. The logs for well 9N/10W-16L3 (fig. 9*E*), which is northwest of the Graham Ranch site (fig. 8), show unsaturated, unconsolidated, medium- to coarse-grained alluvium from the surface to about 95 ft below land surface; unsaturated and saturated moderately consolidated, fine- and coarse-grained beds to about 135 ft; poorly consolidated weathered bedrock to about 245 ft; and competent bedrock to the bottom of the borehole. Figure 9*F* illustrates the logs for well 9N/10W-16R4 and shows electrical, gamma, and acoustic responses for bedding thickness, grain-size distribution, and consolidation of the subsurface sediments similar to those for the deep borehole at the Graham Ranch site located just to the west (figs. 8, 9*D*) as in figure 9*D*. The logs illustrated in figure 9*G* for well 9N/10W-24E3 in the South Base well field (fig. 8) indicate unsaturated and saturated, unconsolidated, very fine-, fine-, medium-, and coarse-grained alluvial sediment from the surface to about 360 ft below land surface; poor to moderately consolidated medium- and coarse-grained beds to about 600 ft; and moderately consolidated fine-, medium-, and coarse-grained beds to the bottom of the borehole.

The Buckhorn, Branch Park, Holly sites and well 9N/10W-24E3 are near the southwestern shores of Rogers Lake (fig. 8). Normal resistivity for the subsurface materials at these locations generally range from about 5 ohm-meters (ohm-m) for very fine-grained clays to about 80 ohm-m for coarse-grained gravel (figs. 9*A*, 9*B*, 9*C*, and 9*G*). The Graham Ranch site and wells 9N/10W-16L3 and 9N/10W-16R4 are northwest of the other sites and topographically separated from the valley by Hospital Ridge (fig. 8). The normal resistivity in this area ranges from 15 ohm-m for fine-grained silts and clays to about 80 ohm-m for coarse-grained gravel to about 260 ohm-m for competent bedrock (figs. 9*D*, 9*E*, and 9*F*). The less consolidated sediments have relatively small acoustic velocity values for very fine- and fine-grained clays and silts, and larger acoustic velocity values for medium- and coarse-grained sands and gravel. The logs also indicate that the acoustic velocities generally increase with depth for fine- and coarser-grained sediments suggesting that the sediments become more consolidated, and perhaps less permeable, with depth (figs. 9*A*, 9*B*, 9*D*, 9*E*, 9*F*, and 9*G*).

The upper sections of the geophysical logs for the Branch Park and Holly sites and production well 9N/10W-24E3 show distinctive unconsolidated, very fine-grained layers that correlate with brown, blue-green, and gray clays, based on lithologic logs, (figs. 9*B*, 9*C*, and 9*G*) at depths of about 100 to 250 ft below land surface. Streaks of brown and greenish-gray clays also are present within the upper 200 ft at the Buckhorn site (fig. 9*A*). These clays may be similar to the thick, deeper, blue and green clays described in logs from wells drilled farther south near Redman and Lancaster (Dutcher and others, 1962) and may be part of the lacustrine sediments that separate the principal aquifer from the deeper aquifer in the Antelope Valley (Durbin, 1978). Another very fine- to fine-grained layer is at the 315- to 365-foot interval at the Holly site. The logs for Branch Park and Buckhorn sites indicate a westward facies change at this interval from very fine- and fine-grained sediments to medium- and coarse-grained sediments. Protrusions into the boreholes shown in the Branch Park and Holly borehole caliper logs (figs. 9*B*-9*C*) correspond to fine- to medium-grained layers that probably have a large percentage of very fine-grained matrix composed of expansive clay minerals, such as montmorillonite.

The geophysical logs for the Graham Ranch site and production well 9N/10W-16R4 show a deep sequence of corresponding fine-grained beds interbedded with varying thicknesses of medium- and coarse-grained beds, suggesting deposition of suspended fine-grained sediments over fan-deposit material eroded from adjacent highlands to the north and northwest. These two sites are in close proximity to the shallow exploration well 9N/10W-16L3 that penetrated competent bedrock at about 230 ft below land surface. This indicates that the bedrock plunges very steeply to the south or southeast between these two sites.

SURFACE GEOPHYSICS

Surface geophysical surveys were conducted and analyzed in the following sequence: (1) gravity surveys, (2) seismic-refraction surveys, and (3) vertical electric soundings. The purpose of the surveys was to define the shape and structure of the pre-Tertiary crystalline basement surface, and map the subsurface distribution of fine-grained and coarse-grained sediments in order to identify potential aquifers, and areas where ground-water withdrawals might further exacerbate land-subsidence problems. Because new sources of ground water are being explored in the Graham Ranch area, the focus is on Graham Ranch.

GRAVITY SURVEYS

Gravity surveys measure differences in the acceleration of gravity at the Earth's surface caused by differences in the mass of the material beneath the surface. The differences can be used to indicate the geologic structure and general shape of the basement complex beneath the sedimentary deposits. Because of density variations between bedrock types, isostatic residual gravity maps should not be directly interpreted as indicating the depth to basement complex. In general, a gravity low corresponds to an area with a thick sedimentary section of unconsolidated, hence low-density sediments. A gravity high corresponds to an area with high-density bedrock, whether igneous, metamorphic, or sedimentary, which crops out at the surface or is buried near the surface and covered only by a thin veneer of lower density unconsolidated sediments.

Gravity data at more than 1,100 new gravity stations (Morin and others, (1990) were used to supplement an existing gravity data base (Snyder and others, 1982) and to produce an isostatic residual gravity map of EAFB and vicinity (fig. 10). The gravity map illustrates the location of EAFB with respect to two of the major structural basins, East Antelope and Kramer, that underlie the eastern parts of Antelope Valley. The closed lines of equal isostatic gravity residuals provide an approximate shape of the basins. The East Antelope structural basin is an elongated northeast to southwest oriented trough, the northeast edge of which is beneath the southwestern end of Rogers Lake. A small, crudely triangular-shaped extension of the basin lies beneath the southern one-half of Rogers Lake. The identification of this structure as a separate trough attached to the East Antelope structural basin is a refinement of detail to previous gravity mapping (Mabey, 1960). The northwestern flank of the East Antelope basin is characterized by a steep gravity gradient extending from the middle of Rogers Lake southwestward to near the city of Lancaster. Mabey (1960) inferred the western segment of this steep gradient to be a fault in the pre-Tertiary basement rock now buried by Cenozoic sediments deposited in the basin. Data presented in this report suggest that this inferred fault extends farther east to near Rogers Lake (fig. 2). The interpreted form of the Kramer structural basin, northeast of Rogers Lake, is little changed from that interpreted by Mabey (1960).

Figure 11 shows a larger scale isostatic residual gravity map of the Graham Ranch area. The Graham Ranch area is a flat alluvial surface of very gentle slope extending from a northwest trending valley between the Rosamond and Bissell Hills to the north, to a low, northeast trending, granitic ridge (Dibblee, 1960b), bordering the area on the south and referred to in this report as Hospital Ridge. Separated from the main part of Antelope Valley by the granitic rocks of Hospital Ridge, the Graham Ranch area lies 30 ft higher than the playa surfaces south of the ridge. The gravity contours (fig. 11) suggest the existence of a small west-to-east oriented basin underlying the Graham Ranch area. The isostatic residual gravity decreases rapidly from -10 mgals (milligals) at the Bissell Hills to -22 mgals at Hospital Ridge, both mapped as quartz monzonite.

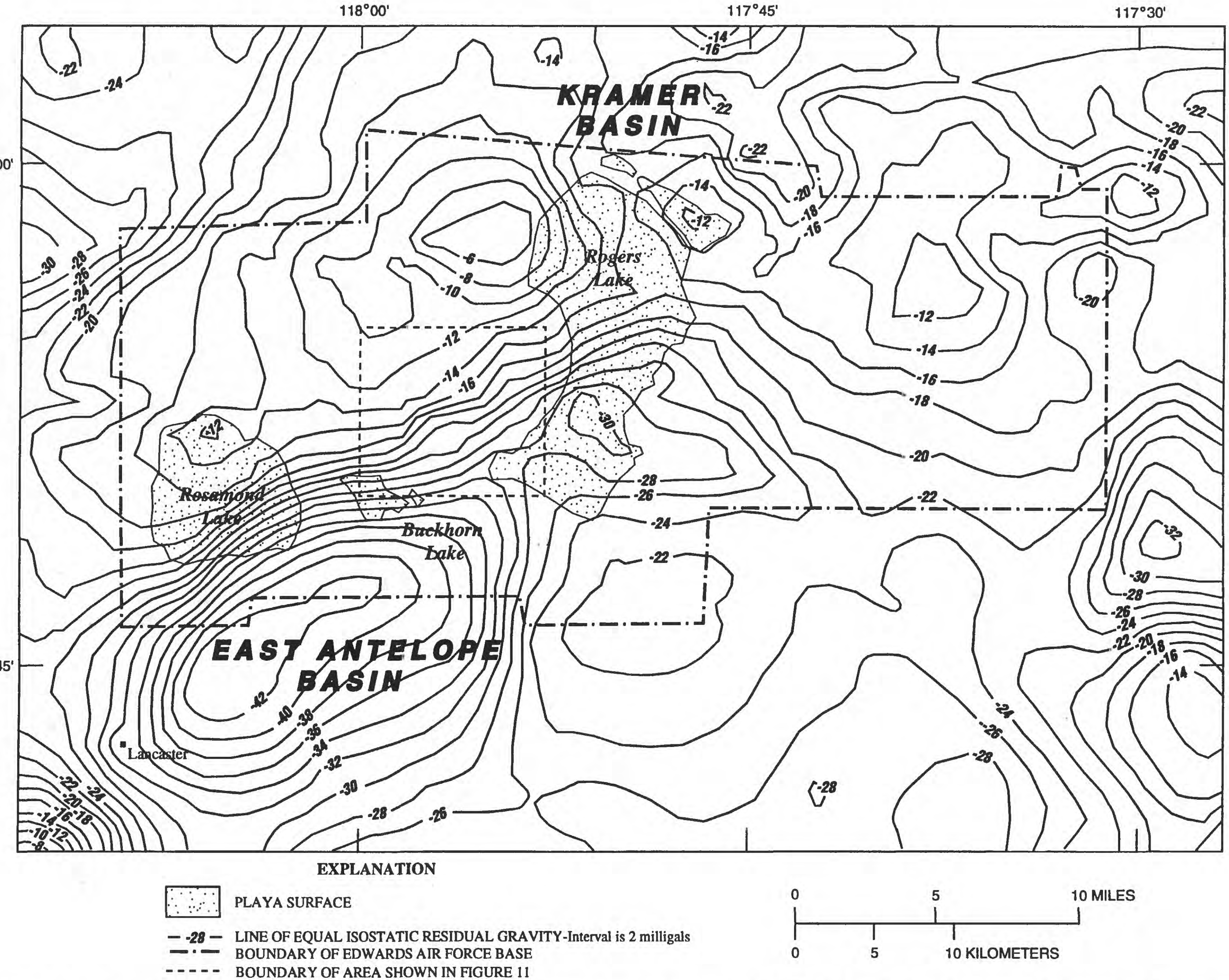

Figure 10. Isostatic residual gravity for Edwards Air Force Base and immediate vicinity. Modified from R.C. Jachens, U.S. Geological Survey, written commun., 1989.

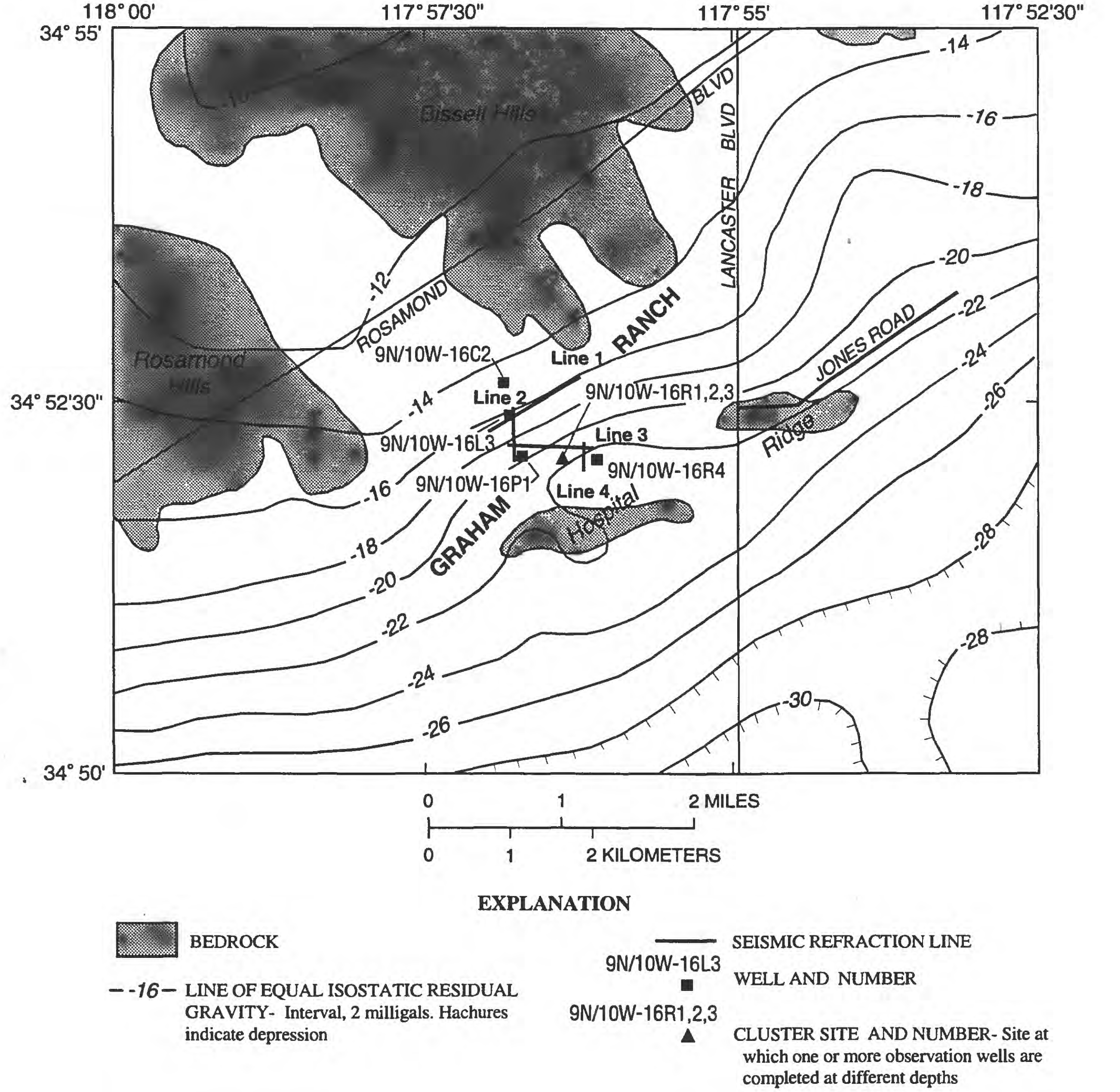

Figure 11. Isostatic residual gravity and seismic refraction lines for the Graham Ranch area on Edwards Air Force Base. Modified from Morin and others (1990).

This suggests that a prominent density variation in the pre-Tertiary basement rocks may occur along a northeast strike between the Bissell Hills and Hospital Ridge (John Mariano, U.S. Geological Survey, written commun., 1991) or that the bedrock outcrops that form Hospital Ridge are not connected to the bedrock basement but rather are isolated blocks of bedrock underlain by alluvium (Zohdy and Bisdorf, 1990).

SEISMIC-REFRACTION SURVEYS

A seismic-refraction survey measures the acoustic velocity of an elastic energy wave that has been imparted into the ground from an energy source. The spectrum of acoustic velocities measured range from several hundred feet per second for very loose unconsolidated sediments, usually found only at the surface, to more than 20,000 ft/s for very competent bedrock. In general, unconsolidated sediments have low acoustic velocities of only a few thousand feet per second, whereas consolidated rocks are characterized by acoustic velocities in excess of 15,000 ft/s. Water-saturated unconsolidated sand has an approximate acoustic velocity of 5,000 ft/s (Press, 1966).

In September 1989, seismic-refraction surveys were done in the Graham Ranch area to evaluate a depression in the bedrock surface suggested on the basis of the gravity surveys (fig. 11). Four seismic refraction lines (fig. 11) were implemented, with a total of 10 seismic spreads, each with 12 geophones at 100-foot spacings. To provide continuity between spreads, a two geophone overlap was used between continuous spreads and at each line intersection one geophone remained in place from a preceding spread. An additional spread was used to measure the characteristic acoustic velocity of quartz monzonite assumed to underlie the sedimentary deposits. This spread was laid out on a weathered outcrop of fractured and faulted quartz monzonite on Hospital Ridge, and an apparent velocity of 16,700 ft/s was measured. Traveltime data were collected for both forward and reverse directions along each spread. The seismic source consisted of a buried, two component explosive. The seismic refraction data were processed using an inverse modeling program, SIPT2 (Rimrock Geophysics, Inc., 1987-89).

Four refractors, layers 1 through 4, were identified in the Graham Ranch area (David Berger, U.S. Geological Survey, written commun., 1990). The interpreted seismic section beneath each refraction line is shown in figure 12. Table 5 shows the measured apparent acoustic velocities and the average modeled acoustic velocities for each layer. Layer 1 is a relatively thin, discontinuous layer from 3 to 35 ft thick and has an apparent velocity of about 1,940 ft/s (table 5). Layer 2 is laterally continuous, and ranges in thickness from about 50 to 200 ft (fig. 12) with apparent velocities ranging from 2,060 to 3,450 ft/s (table 5). The interface between layers 1 and 2 is represented by a compositional change indicated in the lithologic logs for the Graham Ranch site and exploration well 9N/10W-16L3 (figs. 9*D* and 9*E*). The measured apparent velocities in layers 1 and 2 are consistent with the unconsolidated, unsaturated alluvium logged in these wells.

Layer 3 ranges in thickness from about 140 to more than 850 ft (fig. 12) and has apparent velocities ranging from 7,740 to 12,150 ft/s. Velocities in this range are indicative of a fine-grained, semiconsolidated deposits (David Berger, U.S. Geological Survey, written commun., 1990). Water levels measured in well 9N/10W-16R1 at the Graham Ranch site and exploration well 9N/10W-16L3 (table 3) would indicate that the water table in this area is in layer 3. However, it was not discernible because of the high apparent velocities of the formation. The large apparent velocities are consistent with the lithologic and borehole geophysical data collected from the Graham Ranch site and exploration well 9N/10W-16L3, and the borehole geophysical data collected from production well 9N/10W-16R4. The acoustic logs for the Graham Ranch site and wells 9N/10W-16L3 and 16R4 (figs. 9*D*-9*F*) indicate a transitional increase in acoustic velocities from an average 4,500 ft/s for shallower logged intervals, to an average 7,100 ft/s at depths of about 150 ft at the Graham Ranch site, and 110 ft in wells 9N/10W-16L3 and 16R4. Below the transition, average acoustic velocities show a steady increase with increasing depth. Average bottom-hole acoustic velocities at the Graham Ranch site and in well 9N/10W-16R4 were about 10,000 and 8,330 ft/s, respectively. Cores collected from the boreholes at the Graham Ranch site at about 642 and 960 ft consisted of moderately consolidated, semicemented (siliceous cementation), poorly sorted, older alluvium (table 4).

Table 5. Seismic refraction acoustic velocities for layers 1-4 for the Graham Ranch area on Edwards Air Force Base

[Source of data: David Berger, U.S. Geological Survey, written commun., 1990. ft/s, foot per second]

Layer	Measured apparent velocities (ft/s)	Average modeled velocities (ft/s)
1	1,940	1,900
2	2,060 - 3,450	2,800
3	7,740 - 12,150	9,000
4	16,700 - 41,700	17,000

Layer 4 has apparent acoustic velocities in the large range from 16,700 to 41,700 ft/s. The smaller velocities in this range are consistent with the measured characteristic velocity of 16,700 ft/s for weathered quartz monzonite (David Berger, U.S. Geological Survey, written commun., 1990). The anomalously large velocity of 41,700 ft/s most likely

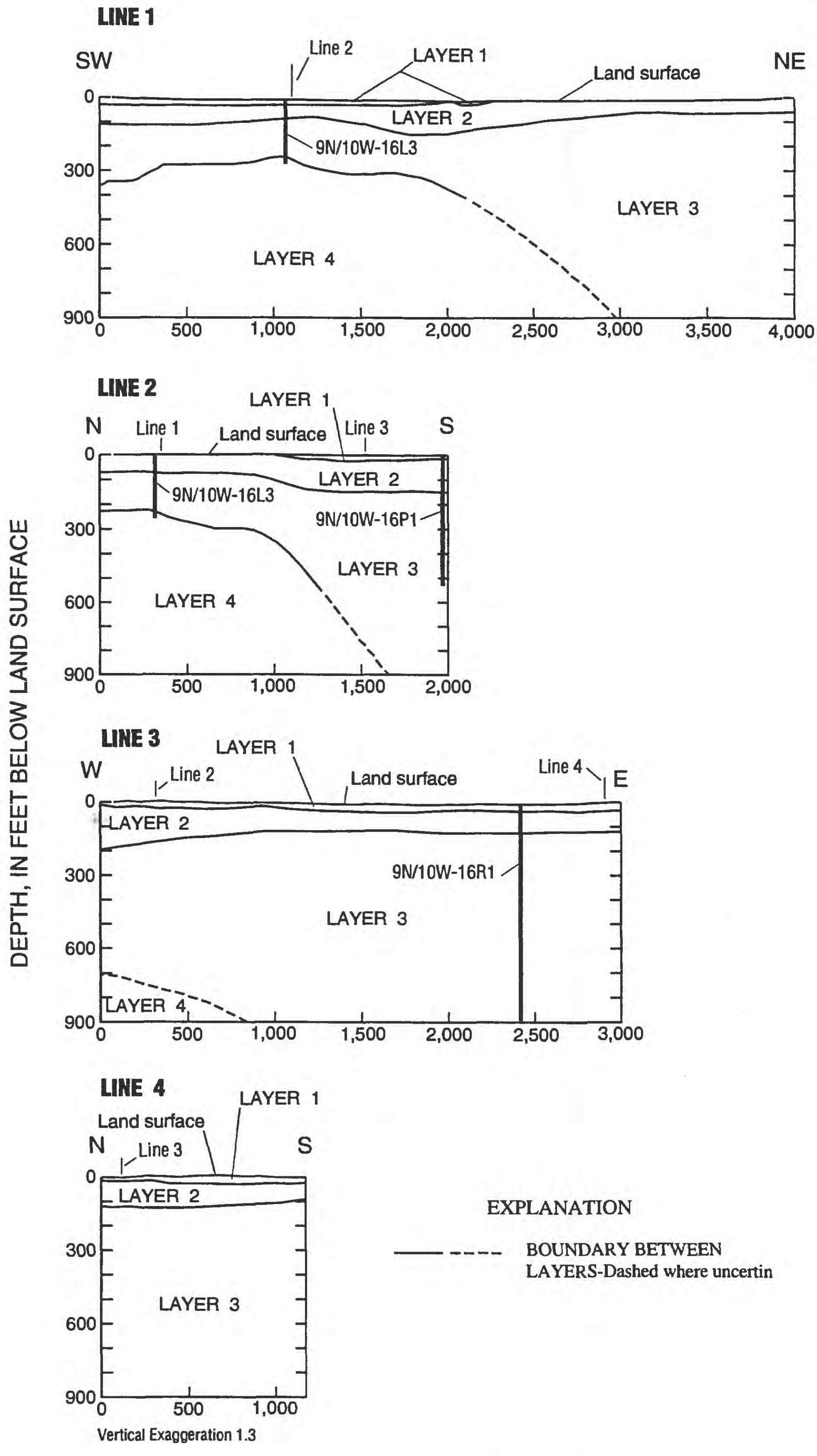

Figure 12. Seismic refraction lines in the Graham Ranch area on Edwards Air Force Base. Location of lines shown on figure 11. (Data from David Berger, U.S. Geological Survey, written commun., 1990).

resulted from shooting upslope on layer 4. The refracting bedrock surface beneath lines 1, 2, and 3 is irregular and slopes towards the east and south. The depths to the top of layer 4 ranged from 230 to greater than 900 ft. The top of layer 4 is below the sampling depth along line 4, along the eastern parts of lines 1 and 3, and along the central and southern parts of line 2. Bedrock depth control was provided by exploration well 9N/10W-16L3, northwest of the intersection of lines 1 and 2 (fig. 11), where the lithologic and borehole geophysical logs show that the depth to bedrock is 230 ft (fig. 9*E*).

VERTICAL ELECTRIC SOUNDINGS

Vertical electric soundings were made using direct current (DC) methods. The DC resistivity surveying technique involves the introduction of a very low frequency, direct current into the ground through two widely spaced electrodes, and the measurement of the potential difference between two electrodes placed near the center of the electrode array. This measured potential difference is then used to compute an apparent resistivity for the Earth materials beneath the array. Extending the distance between the electrodes in the array causes the flow path of the current to penetrate deeper into the Earth. The resulting apparent resistivities are considered averages of the actual resistivities of the individual layers of sediment and rock beneath the electrode array (Zohdy and others, 1974).

In October 1989, 67 vertical electric, deep soundings using the Schlumberger array configuration (Zohdy and others, 1974) were conducted at EAFB, 59 of which (numbers 1-58 and 67) were made in the Graham Ranch area and areas west and south of Rogers Lake (fig. 13). Eight additional electric soundings, numbers 59-66, were made on the northern part of Rogers Lake and are not discussed in this report. The purpose of these soundings was to determine the configuration of the bedrock surface and to provide information concerning the distribution and thickness of the unconsolidated sediments. The detailed survey, analysis, and interpretation of the Schlumberger data were made by Zohdy and Bisdorf (1990), and some of the results are summarized here.

The interpretation of the Schlumberger soundings at EAFB indicated that the electrical resistivity of the bedrock may be only a few hundred ohm-meters, and as low as 100 ohm-m. The relatively low resistivities for igneous rock may be related to the weathering and alteration of the quartz monzonite. Saturated, coarse-grained sediments, indicative of sand-and-gravel freshwater aquifers, are characterized by resistivities ranging from 30 to 70 ohm-m. Fine-grained clay-rich sediments are characterized by resistivities lower than 15 ohm-m. In general, for saturated, unconsolidated sediments, the higher the resistivity the coarser grained the material. However, the occurrence of brackish ground water will decrease the resistivity of the sediments and deviate from this generalization.

Interpreted resistivity at depths of 328, 656, 984, and 1,640 ft for the Graham Ranch area and the areas south and west of Rogers Lake are shown in figures 14*A*-14*D*. At the 328-foot depth (fig. 14*A*), a sharp northeast trending resistivity contrast occurs between an area of larger resistivities (greater than 100 ohm-m) northwest, and an area of lower resistivities (less than 70 ohm-m) southeast of the contrast. The resistivity contrast represents the northern edge of a small, buried structural basin in the Graham Ranch area, and suggests the existence of a geologic fault (Zohdy and Bisdorf, 1990). Two regions of relatively intermediate to high resistivity, 70 to greater than 100 ohm-m, material occur about 1 mi south of the northern edge of the basin, at the 328-foot depth beneath Hospital Ridge and probably represent the southern edge of this small basin. A short resistivity sounding 31 made on Hospital Ridge measured resistivities from 33 to 150 ohm-m in the upper 130 ft, and 60 ohm-m at depths greater than 130 ft. The interpreted resistivities near Hospital Ridge are lower than expected for quartz monzonite. Zohdy and Bisdorf (1990) concluded that the low resistivities of 60 ohm-m measured at depth beneath Hospital Ridge indicated that the ridge is composed of floating, weathered granitic blocks. An alternative interpretation is that Hospital Ridge is rooted, and the low interpreted resistivities may be attributed to the highly fractured, altered bedrock exposures. Field observations of Hospital Ridge, and other exposures of quartz monzonite on EAFB indicate that many fractures and faults in these outcrops are in-filled with clay-sized quartz and feldspar minerals.

At the 656-foot depth (fig. 14*B*), the zone between 70 to 100 ohm-m has migrated southeastward from the region of high resistivity contrast and has coalesced with the regions of 70 to 100 ohm-m material near Hospital Ridge to form the crude outline of a basin. Geoelectrically, the basin appears to be open to the south and east at this depth. A region

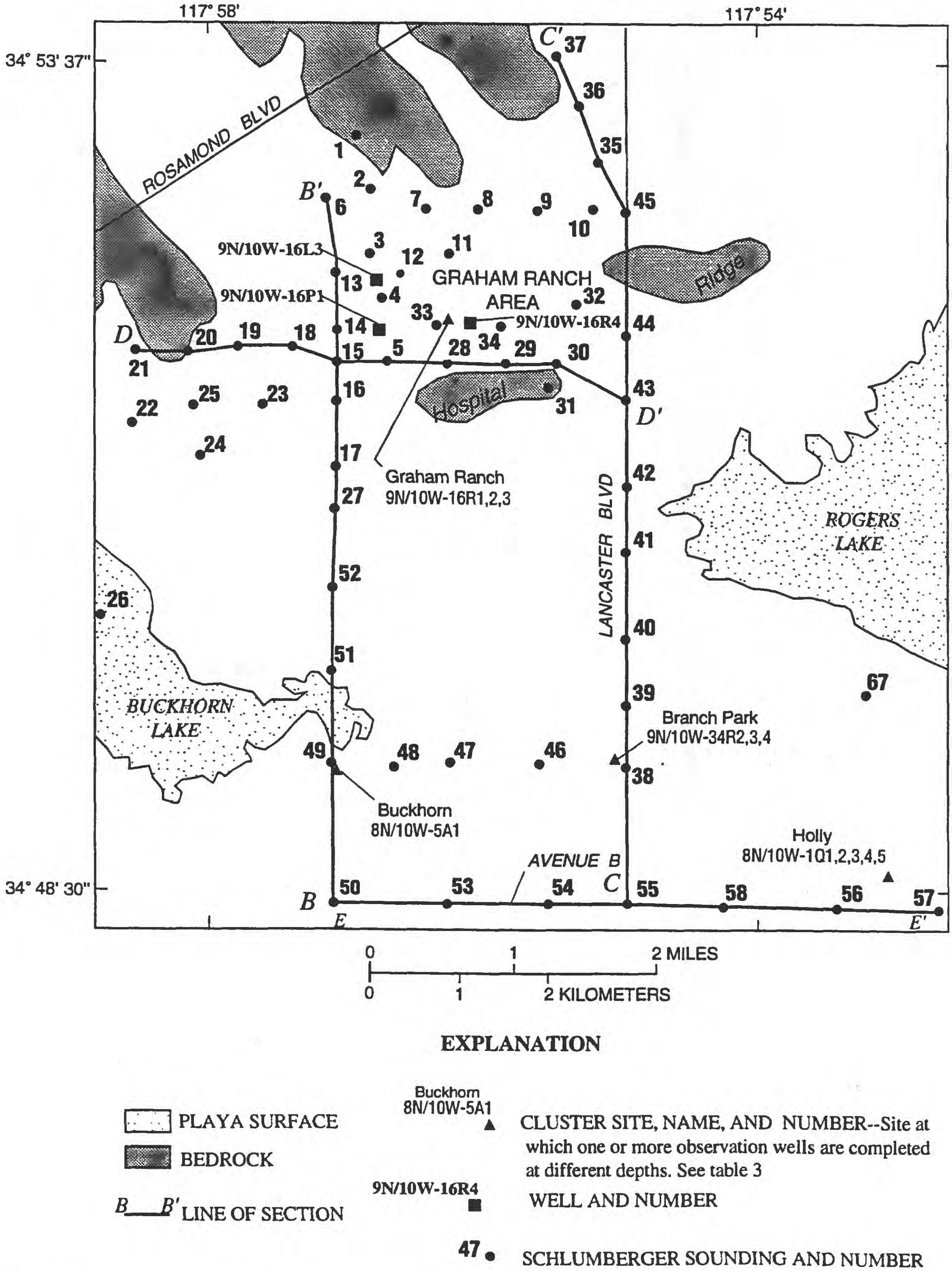

Figure 13. Location of 59 vertical electric soundings and cross sections *B-B', C-C', D-D', and E-E'* in the Graham Ranch area and vicinity on Edwards Air Force Base. Modified from Zohdy and Bisdorf (1990).

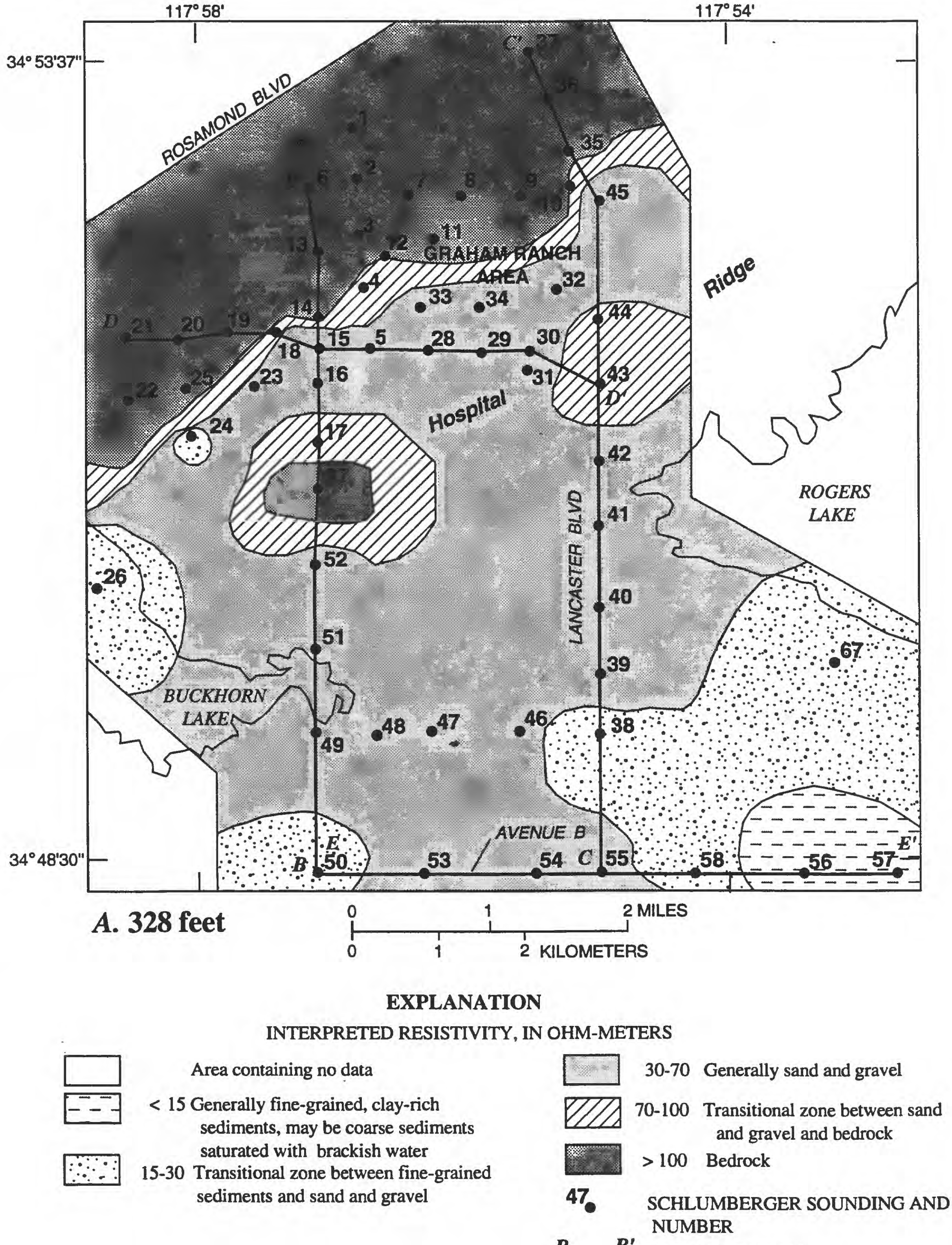

Figure 14. Interpreted resistivities of rock formations and associated rock types at depths of 328, 656, 984, and 1,640 feet below land surface for the Graham Ranch area and vicinity on Edwards Air Force Base. Modified from Zohdy and Bisdorf (1990).

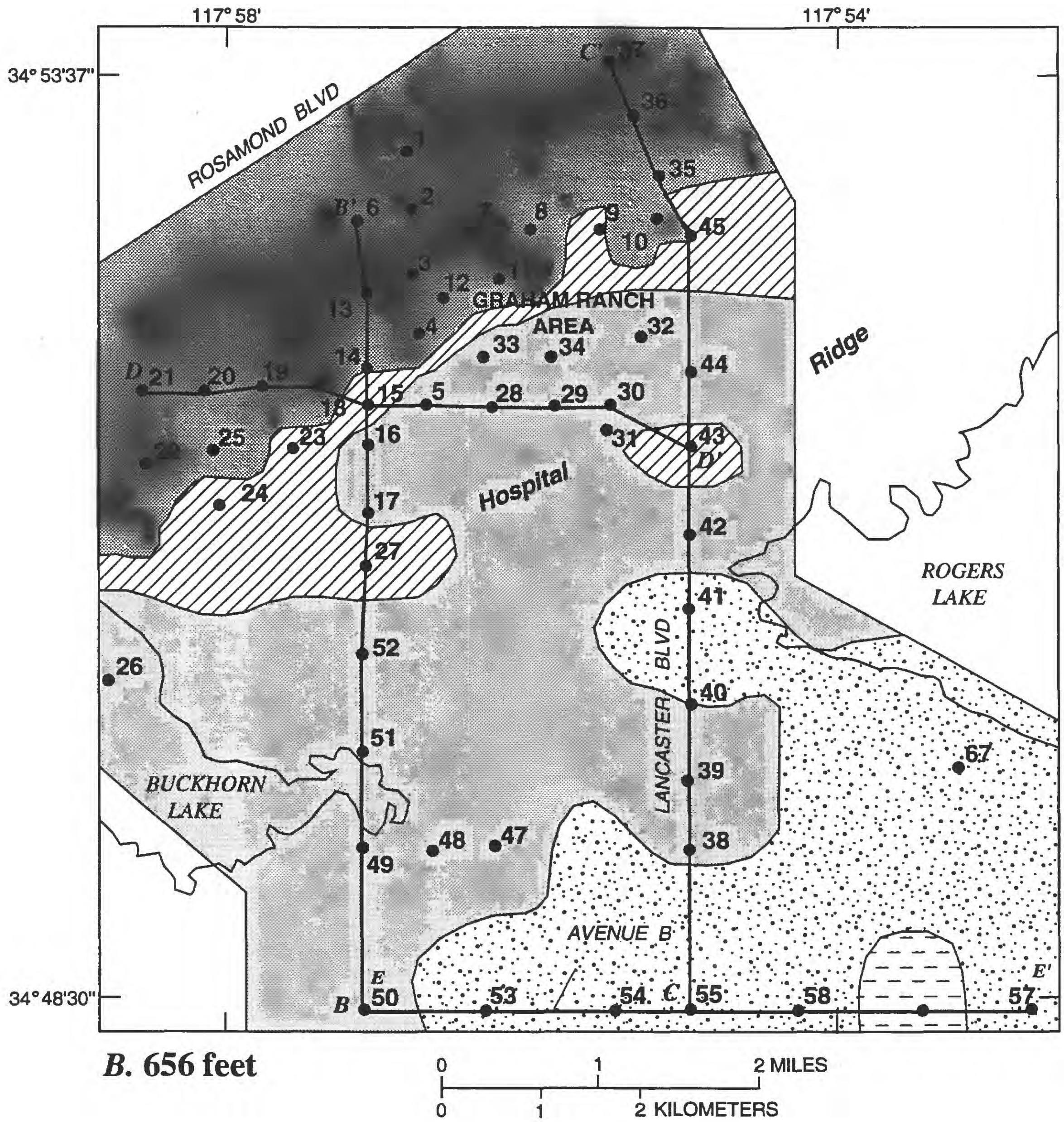

B. **656 feet**

EXPLANATION

INTERPRETED RESISTIVITY, IN OHM-METERS

- Area containing no data
- < 15 Generally fine-grained, clay-rich sediments, may be coarse sediments saturated with brackish water
- 15-30 Transitional zone between fine-grained sediments and sand and gravel
- 30-70 Generally sand and gravel
- 70-100 Transitional zone between sand and gravel and bedrock
- > 100 Bedrock
- 47 ● SCHLUMBERGER SOUNDING AND NUMBER
- B——B' LINE OF SECTION

Figure 14. Interpreted resistivities of rock formations and associated rock types at depths of 328, 656, 984, and 1,640 feet below land surface for the Graham Ranch area and vicinity on Edwards Air Force Base. Modified from Zohdy and Bisdorf (1990)--*Continued.*

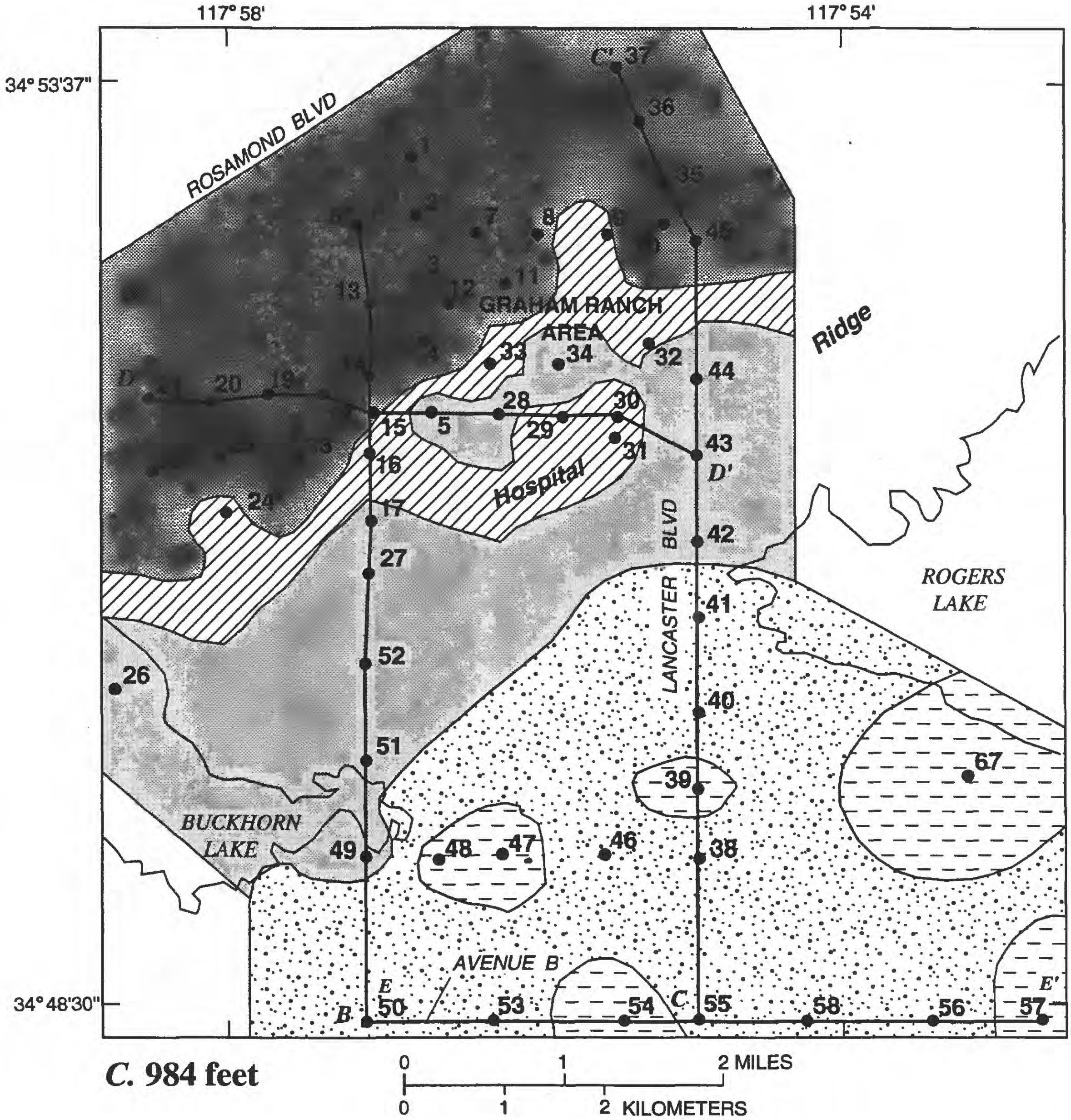

C. **984 feet**

EXPLANATION

INTERPRETED RESISTIVITY, IN OHM-METERS

Area containing no data

< 15 Generally fine-grained, clay-rich sediments, may be coarse sediments saturated with brackish water

15-30 Transitional zone between fine-grained sediments and sand and gravel

30-70 Generally sand and gravel

70-10 Transitional zone between sand and gravel and bedrock

> 100 Bedrock

47 SCHLUMBERGER SOUNDING AND NUMBER

B ___ B' LINE OF SECTION

Figure 14. Interpreted resistivities of rock formations and associated rock types at depths of 328, 656, 984, and 1,640 feet below land surface for the Graham Ranch area and vicinity on Edwards Air Force Base. Modified from Zohdy and Bisdorf (1990)--*Continued.*

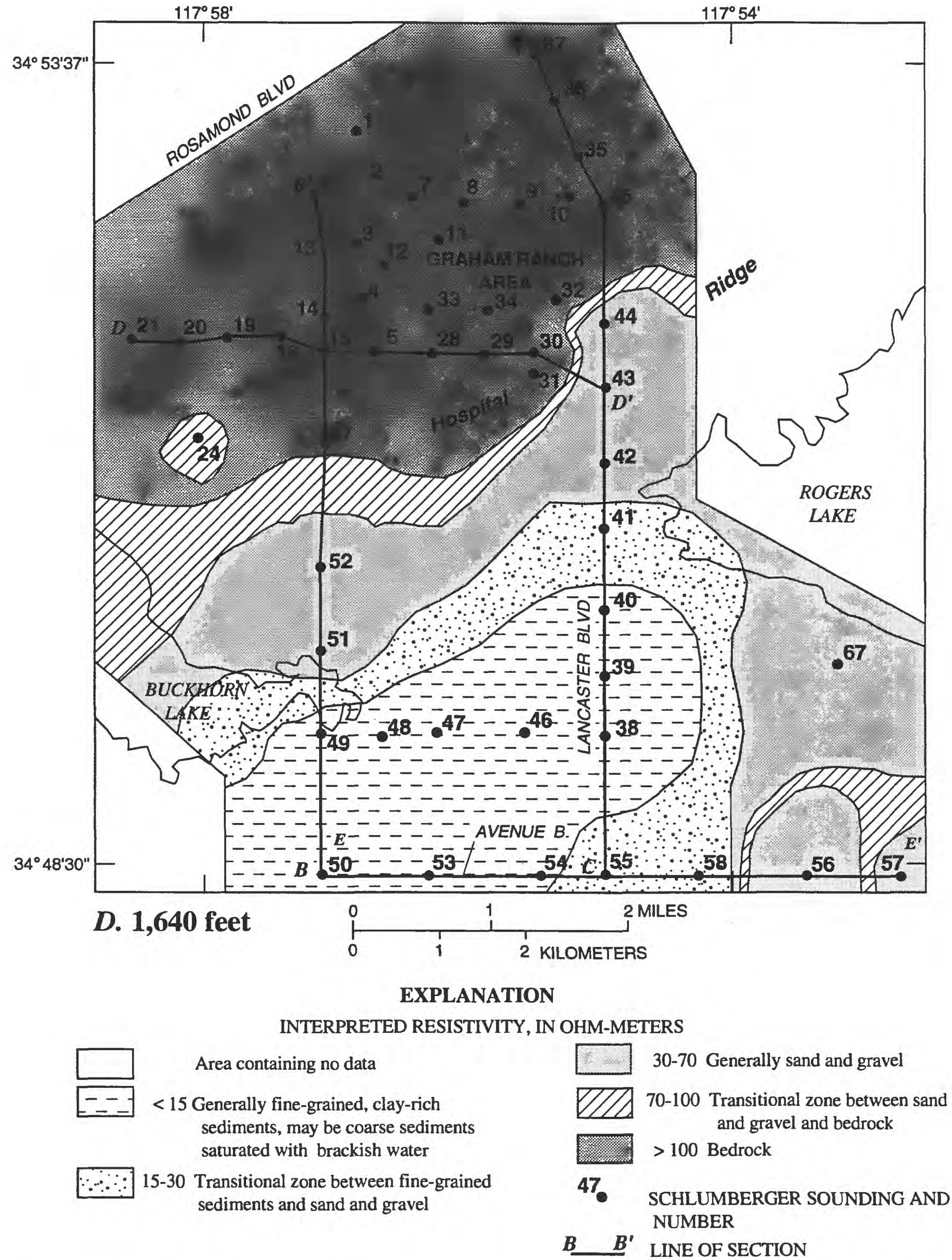

Figure 14. Interpreted resistivities of rock formations and associated rock types at depths of 328, 656, 984, and 1,640 feet below land surface for the Graham Ranch area and vicinity on Edwards Air Force Base. Modified from Zohdy and Bisdorf (1990)--*Continued.*

of less than 30 ohm-m resistivity south and west of Rogers Lake has expanded from its coverage at the 328-foot depth. On each of the 328- and 656-foot depth maps, there is a large region of resistivities between 30 and 70 ohm-m material which encompasses the principal sediments from which ground water is produced by base production wells near Branch Park and in the Graham Ranch area.

At the 984-foot depth (fig. 14*C*), the small basin in the Graham Ranch area appears closed. The low-resistivity region south and west of Rogers Lake has extended southwestward, increasing the areal distribution of fine-grained sediments in this part of the East Antelope structural basin. At this depth, the coarse-grained deposits indicated by the 30 to 70 ohm-m zone are primarily restricted to a narrow northeast-trending band south of Hospital Ridge, and north and west of Branch Park.

The deepest part of the small basin in the Graham Ranch area probably is less than 1,640 ft as indicated in figure 14*D*. At this depth, the region of high resistivities greater than 100 ohm-m extends from the northwest to south of Hospital Ridge, west of Lancaster Boulevard. A second region of high resistivity is present at the 1,640-foot depth in the southeast corner of the surveyed area. Between these regions, there is a large region of resistivities less than 15 ohm-m that extends to the southwest. To the north and east of this low-resistivity region, there is a region of resistivities of 30 to 70 ohm-m. Distribution of interpreted resistivities at the 1,640-foot depth is well correlated to the distribution of isostatic gravity residuals (fig. 10). The regions of interpreted low resistivities are associated with the regions of larger negative residuals on the gravity map and generally conform to the shape of the northeast corner of the East Antelope structural basin. The regions of interpreted high resistivities are associated with the regions of smaller negative residuals on the gravity map and generally conform to the northeast boundaries of the structural basin.

The altitude and shape of the interpreted bedrock surface is shown in cross sections in figures 15*A-D*. The surface of the granitic basement is delineated by the contact between the 70 to 100 ohm-m zone and the greater than 100 ohm-m zone. The south to north cross sections, *B-B′* and *C-C′*, indicate shallow basement rocks north of the Graham Ranch area (figs. 15*A* and 15*B*). This is confirmed by the penetration of poorly consolidated, weathered bedrock at an altitude of about 2,190 ft above sea level and competent bedrock at about 2,080 ft above sea level in exploration well 9N/10W-16L3, near sounding 13. Proceeding from north to south, the bedrock surface deepens, indicating the subdued impression of the small basin in this area near sounding 45 to 44 and sounding 14 to 16 (figs. 15*A* and 15*B*). The bedrock surface continues to deepen, except for a bedrock ridge detected beneath sounding 43 (fig. 15*B*), and more subtly beneath sounding 17 (fig. 15*A*). The bedrock surface slopes steeply into the East Antelope structural basin beneath soundings 42 (fig. 15*B*) and 51 (fig. 15*A*), where the interpreted altitude of the basement surface is about 2,000 ft below sea level. Another ridge is encountered beneath soundings 39 (fig. 15*B*) and 49 (fig. 15*A*), and beyond this, the interpreted bedrock surface deepens southward to the ends of the cross sections.

The west to east cross sections, *D-D′* and *E-E′* (figs. 15*C* and 15*D*) also show the transition from a shallow to a deep basement. Cross section *D-D′* runs along the northern flank of Hospital Ridge, from west of the Graham Ranch area east to Lancaster Boulevard (fig. 13). This cross section shows the small basin identified in the southern part of the Graham Ranch area, deepening from west to east to a minimum altitude of about 1,000 ft above sea level beneath sounding 28 (fig. 15*C*). At the Graham Ranch site (fig. 13) at wells 9N/10W-16R1, 16R2, and 16R3, 1,800 ft north-northeast of sounding 28 and about 500 ft east of sounding 33 (not shown on fig. 15*C*) bedrock was not encountered at a bottom hole altitude of 1,350 above sea level. This is consistent with the resistivity measurements, which indicate that the altitude of the basement surface is less than 1,330 ft above sea level (fig. 15*C*). Furthermore, lithologic and borehole geophysical logs of alluvium penetrated in well 9N/10W-16R1 were consistent with the interpreted resistivities from sounding 33. This information was used to site production well 9N/10W-16R4 1,200 ft east of the Graham Ranch site (fig. 8).

Cross section *E-E′* runs along Avenue B from sounding 50 to 57 across the northeast part of the East Antelope structural basin (fig. 13), where the minimum altitude of the basement surface is less than 2,500 ft below sea level beneath sounding 53 (fig. 15*D*). East of sounding 53, the bedrock surface slopes upward to an altitude of about 1,250 ft above sea level at sounding 57 on the rim of the East Antelope structural basin (fig. 15*D*). The Holly site boreholes, drilled about 1,000 ft northeast of

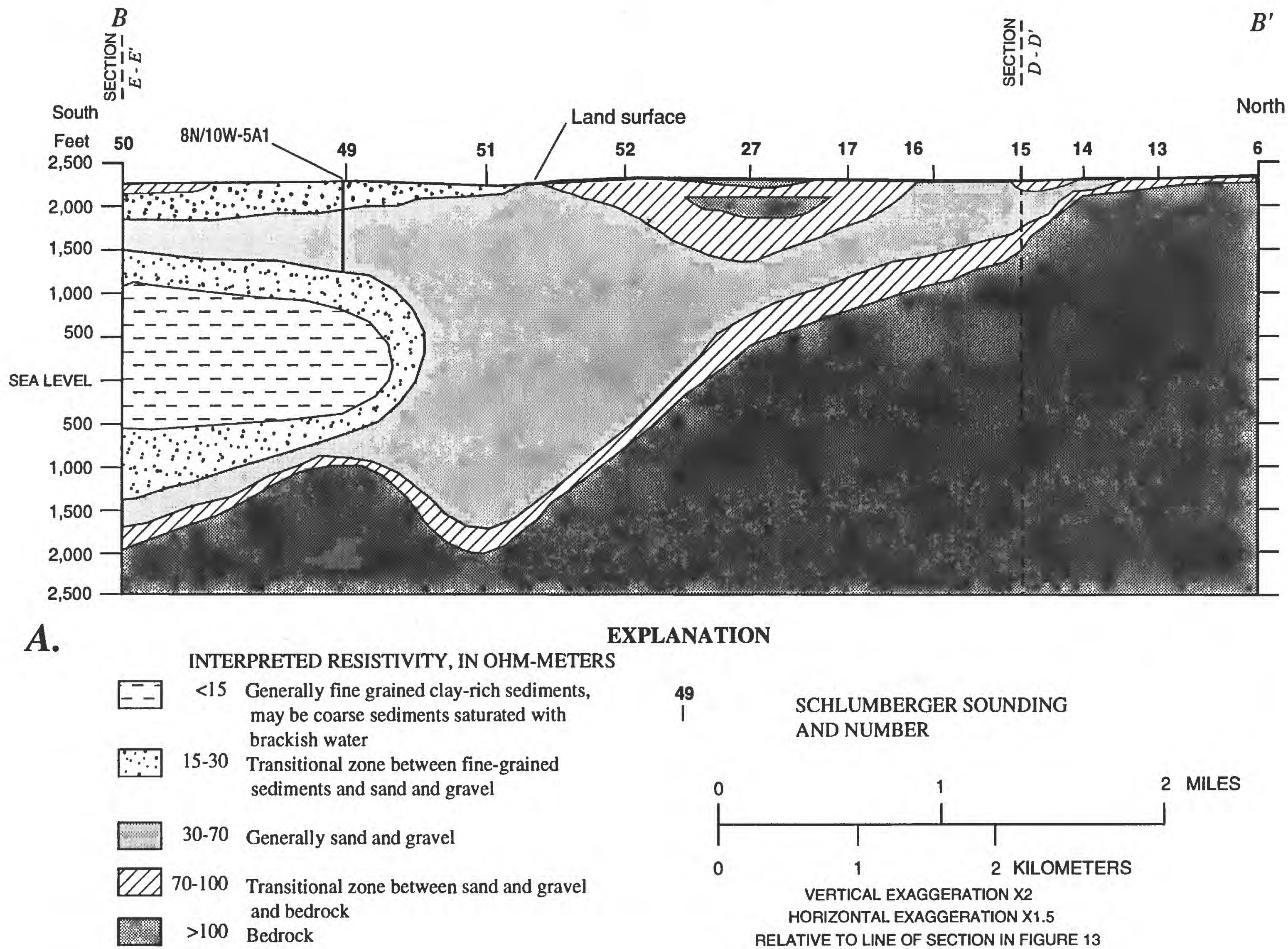

Figure 15. Interpreted resistivities of rock formations and associated rock types for the Graham Ranch area and vicinity on Edwards Air Force Base.

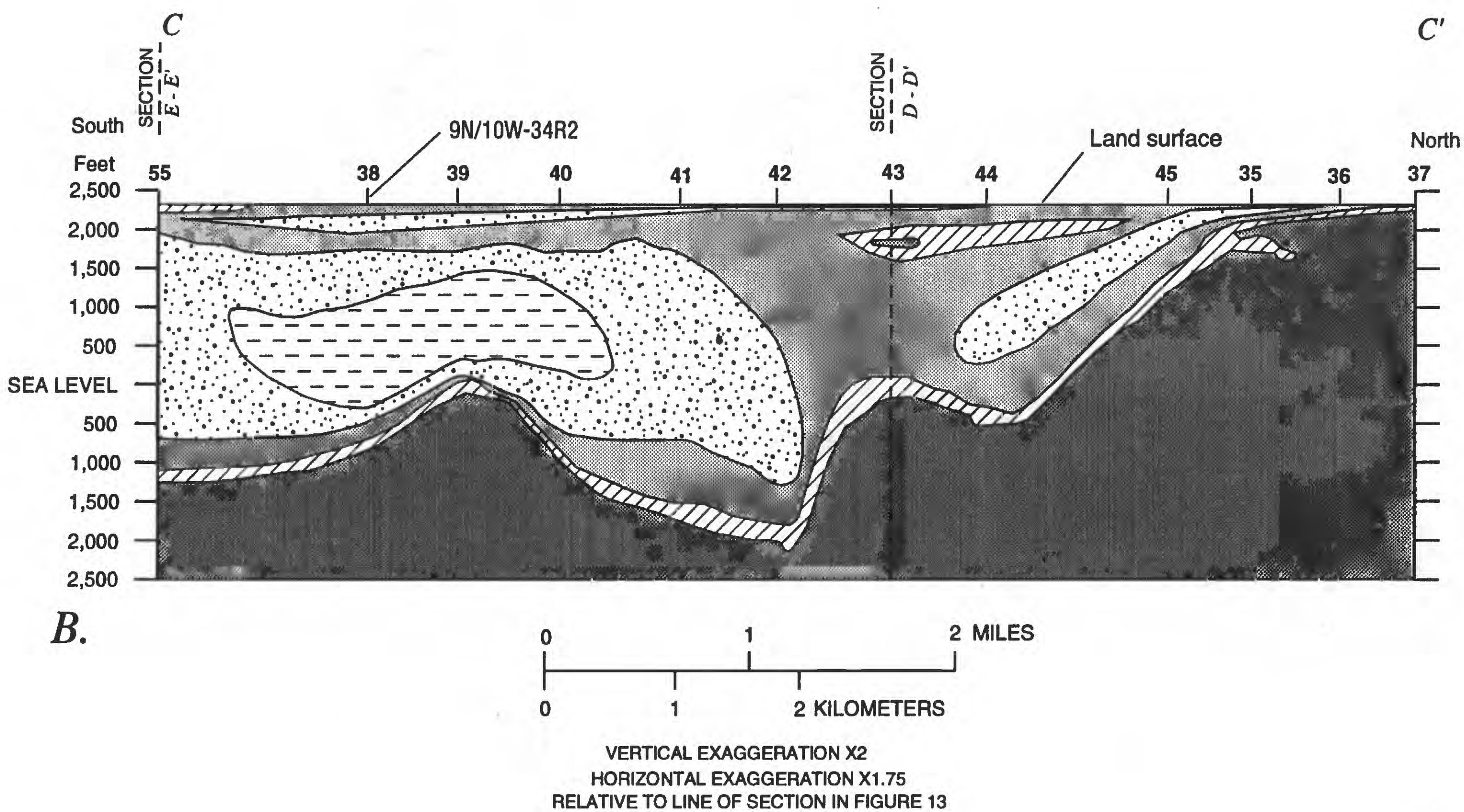

Figure 15. Interpreted resistivities of rock formations and associated rock types for the Graham Ranch area and vicinity on Edwards Air Force Base--*Continued.*

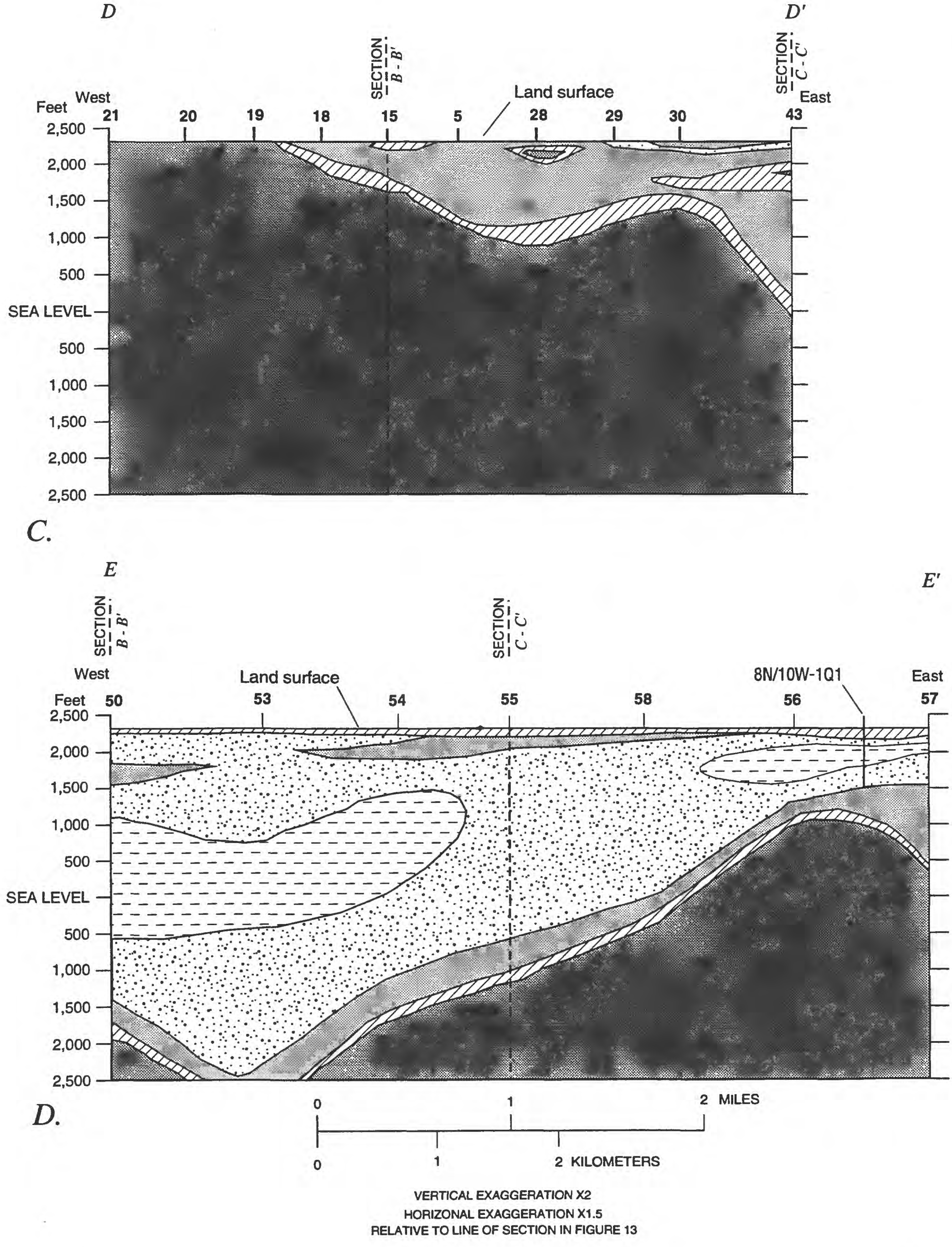

Figure 15. Interpreted resistivities of rock formations and associated rock types for the Graham Ranch area and vicinity on Edwards Air Force Base--*Continued*.

sounding 56 (fig. 13), penetrate weathered quartz monzonite at an altitude of about 1,000 ft above sea level. Because of the proximity of the alluvium/weathered basement contact to the bottom of the hole, the borehole resistivity survey could not measure the contact. The interpreted geoelectric section indicates that the deep boreholes at the Holly site should have bottomed in the 70 to 100 ohm-m material, which may be consistent with the lithology depending on the interpreted resistivity of weathered quartz monzonite. However, the thick section of low resistivity (less than 15 ohm-m material interpreted in the cross section above an altitude of 1,600 ft) near sounding 56 (fig. 15*D*) does not agree well with the borehole logs, which show a homogeneous clay interval from 2,214 to 2,092 ft above sea level underlain by sands, gravels, and interbedded clays (fig. 9*C*).

The boundary between the granitic bedrock and the overlying sediments is mantled with 70 to 100 ohm-m material suggesting a gradual transition from the more competent, unweathered bedrock through a section of weathered bedrock to the overlying unconsolidated sediments. Other 70 to 100 ohm-m and greater than 100 ohm-m material is near the surface, beneath soundings 30, 43, 44, 17, 27, and 52 (figs. 15*A*, 15*B*, and 15*C*), and is underlain by lower resistivity, 30 to 70 ohm-m material. This gives the appearance that the granitic rock exposed in outcrops on Hospital Ridge do not connect with the bedrock underlying the basin, and supports the inference made from the resistivity profiles that the three northeast-trending topographic ridges, collectively referred to as Hospital Ridge, may be floating blocks of weathered quartz monzonite (Zohdy and Bisdorf, 1990). The 70 to 100 ohm-m material beneath soundings 15 and 28 (fig. 15*C*) may represent buried stream channels (Zohdy and Bisdorf, 1990).

Cross section *E-E′* (fig. 15*D*) also shows a thick section of low resistivity, material (less than 15 ohm-m) extending from west to east up the bedrock slope of the East Antelope structural basin. This is spatially correlated with the less than 15 ohm-m material occurring in cross sections *B-B′* and *C-C′* (figs. 15*A* and 15*B*). The resistivity cross sections, *B-B′* and *C-C′*, delineate the northern part of a lenticular zone of low resistivity, which is between 1,500 and 2,000 ft thick in this section of the basin. The termination of the northern boundary of the zone (fig. 15*A*) suggests that the associated deposits may be related to the inferred fault (fig. 2) or faults striking about N. 50° to 60° E. forming the northern boundary of the East Antelope structural basin in this area. Zohdy and Bisdorf (1990) suggest two possibilities for this zone: (1) the zone predominantly consists of clay beds with some clean sand and gravels interbedded within the clays or (2) the zone may consist of a number of sand and gravel beds containing brackish to saline ground water. An overlying, 15 to 30 ohm-m material thins eastward beyond sounding 58, and extends northward as far as sounding 41 (figs. 15*B* and 15*D*). The 30 to 70 ohm-m material, indicative of coarse-grained material and a potential ground-water resource, is widely distributed at depths less than 700 ft. A 4,000-foot thick section of these sediments is near soundings 51 and 42 (figs. 15*A* and 15*B*).

WATER-LEVEL MEASUREMENTS

Ground-water levels are routinely measured on an annual or semiannual basis in 19 wells (fig. 16) on EAFB as part of the Antelope Valley-East Kern Water Agency (AVEK) ground-water monitoring program. Long-term hydrographs for 16 of these wells (figs. 16, 17*A-B*, 17*E-H*, 17*J-S*) show a general long-term downward water-level trend from 1947 to 1990. The rates and amounts of these declines vary greatly for the area of EAFB. The largest documented declines were in well 9N/10W-24C1 (figs. 16 and 17*K*), where short-term declines of as much as 180 ft have been recorded and there has been a general long-term decline of about 90 ft (fig. 17*K*). Hydrographs for two of the wells, 8N/11W-14R1 and 8N/11W-15Q1 (figs. 16, 17*C*, and 17*D*), show a slight long-term increase in water levels. The water table in these wells is perched from the deeper water table by a thick sequence of clay (Dutcher and others, 1962). The hydrograph for well 9N/10W-8P1 (figs. 16 and 17*I*) shows very little water-level change over the period of record and may be isolated from the rest of the basin.

At the Holly site (fig. 8), two distinct potentiometric surfaces are separated by a thick lacustrine unit. The water level in well 8N/10W-1Q4, which is completed above the lacustrine unit, is at an altitude of about 2,249 ft and shows very little fluctuation, except for a slight downward trend from May 1990 to November 1991 (fig. 18*A*). In wells 8N/10W-1Q1, 1Q2, and 1Q3, which are completed below the lacustrine unit, the water-level altitudes fluctuated from a low of about 2,152 ft to a high of about 2,164 ft during this same period (fig. 18*B*).

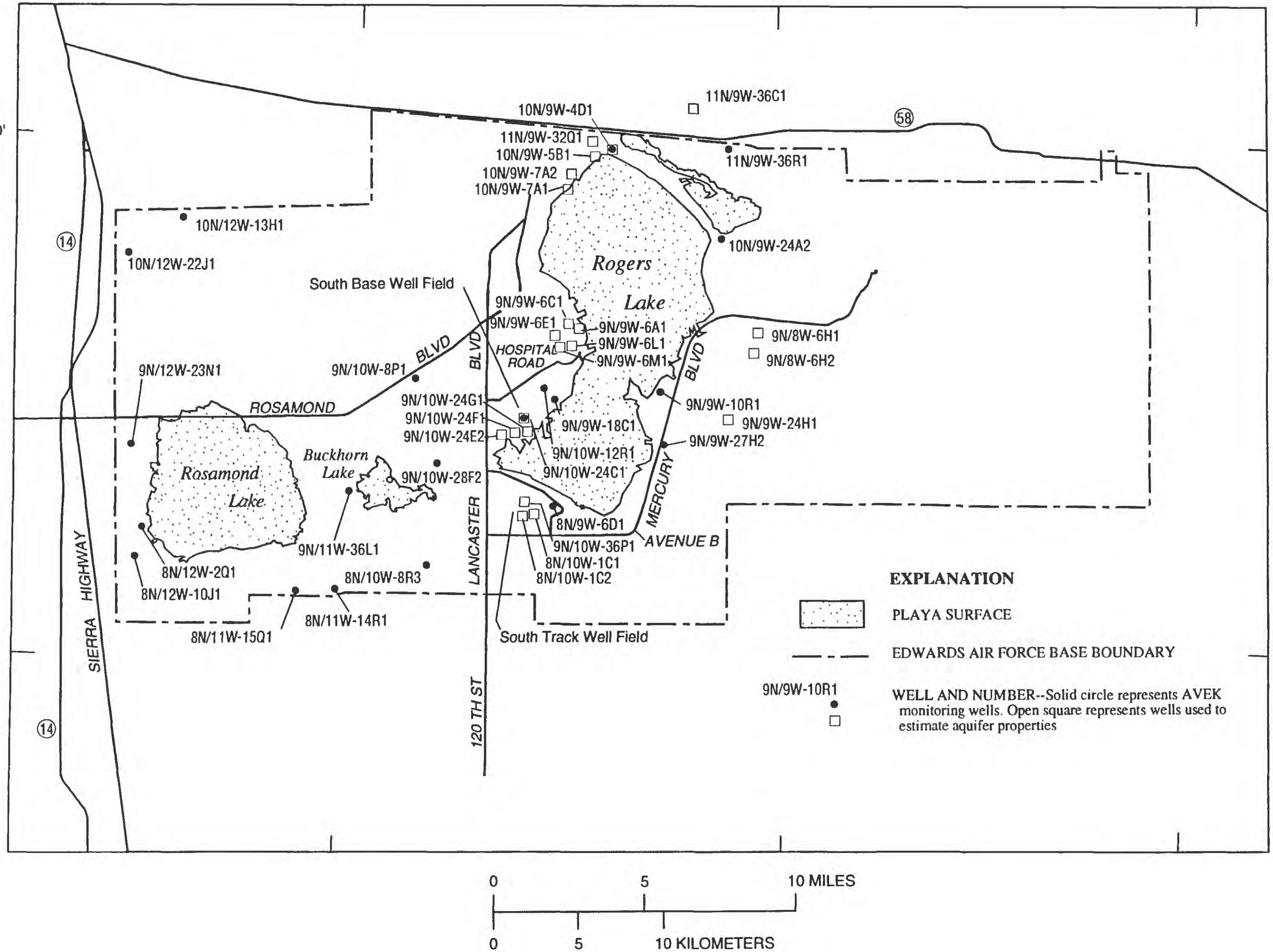

Figure 16. Location of wells routinely monitored by the U.S. Geological Survey as part of the Antelope Valley-East Kern Water Agency (AVEK) monitoring program and location of wells used to estimate aquifer properties on Edwards Air Force Base.

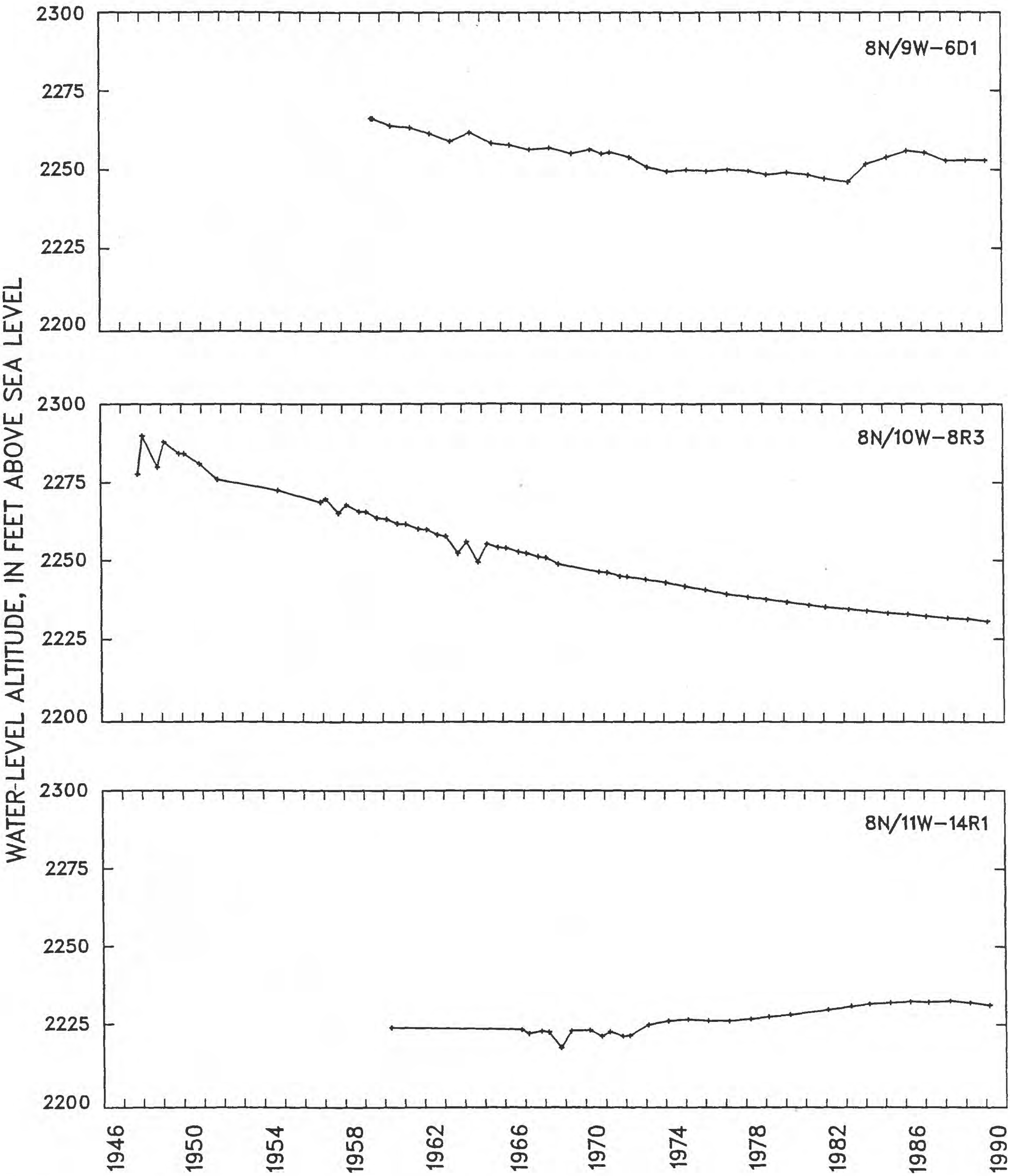

Figure 17. Water levels monitored by U.S. Geological Survey as part of the Antelope Valley-East Kern Water Agency (AVEK) monitoring program for wells on Edwards Air Force Base, 1947-90. Location of wells are shown on figure 16.

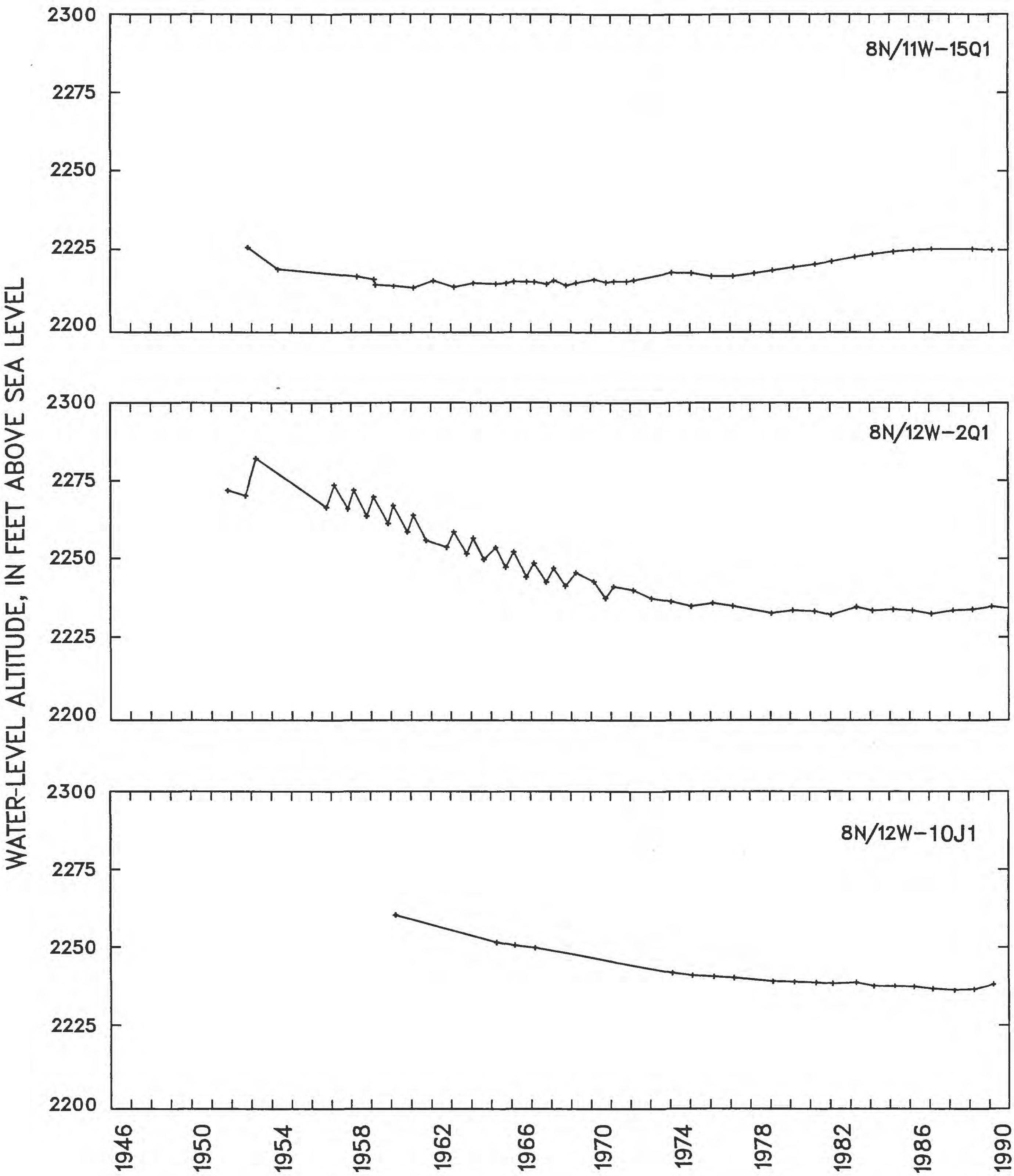

Figure 17. Water levels monitored by U.S. Geological Survey as part of the Antelope Valley-East Kern Water Agency (AVEK) monitoring program for wells on Edwards Air Force Base, 1947-90--*Continued.*

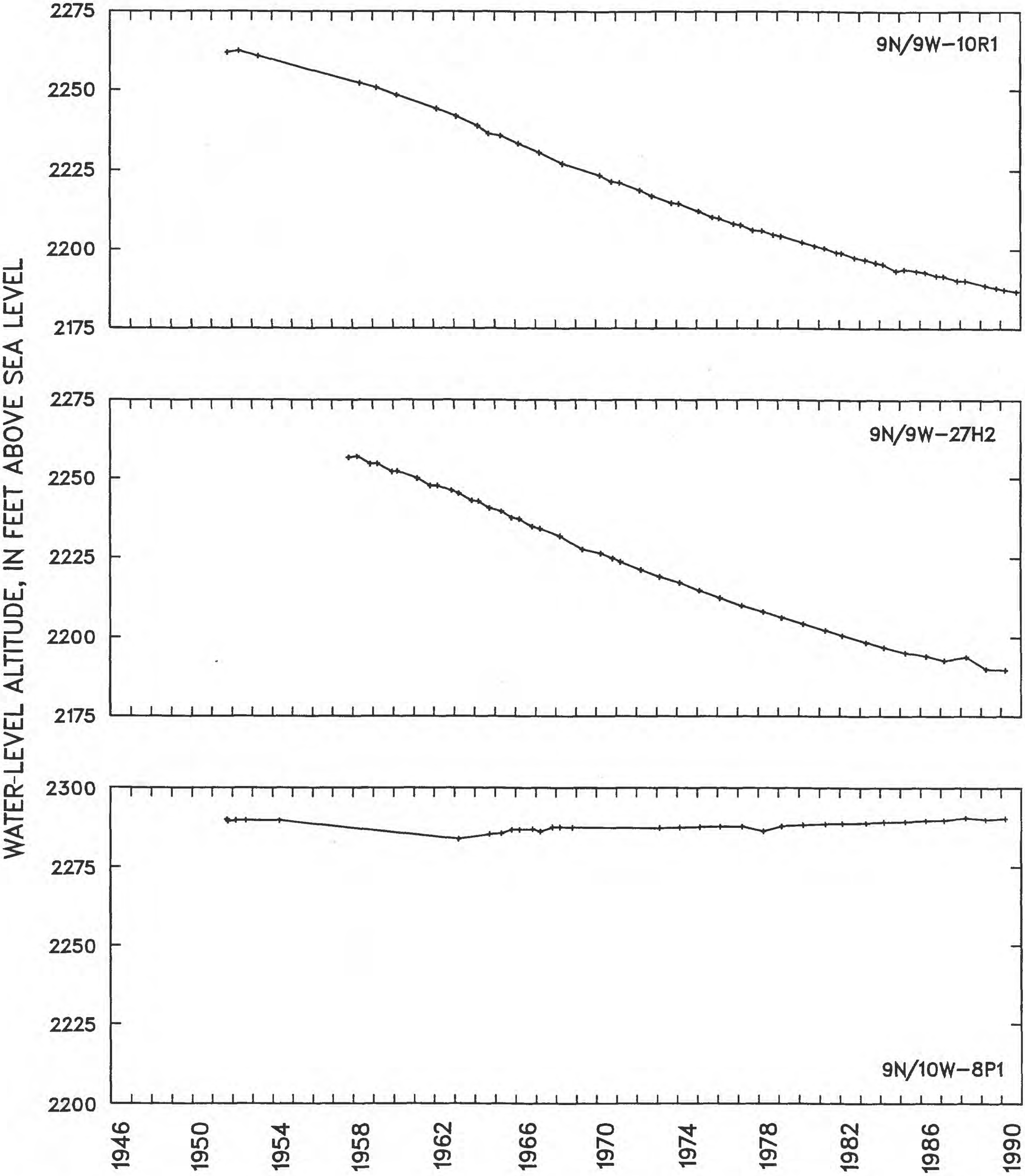

Figure 17. Water levels monitored by U.S. Geological Survey as part of the Antelope Valley-East Kern Water Agency (AVEK) monitoring program for wells on Edwards Air Force Base, 1947-90--*Continued.*

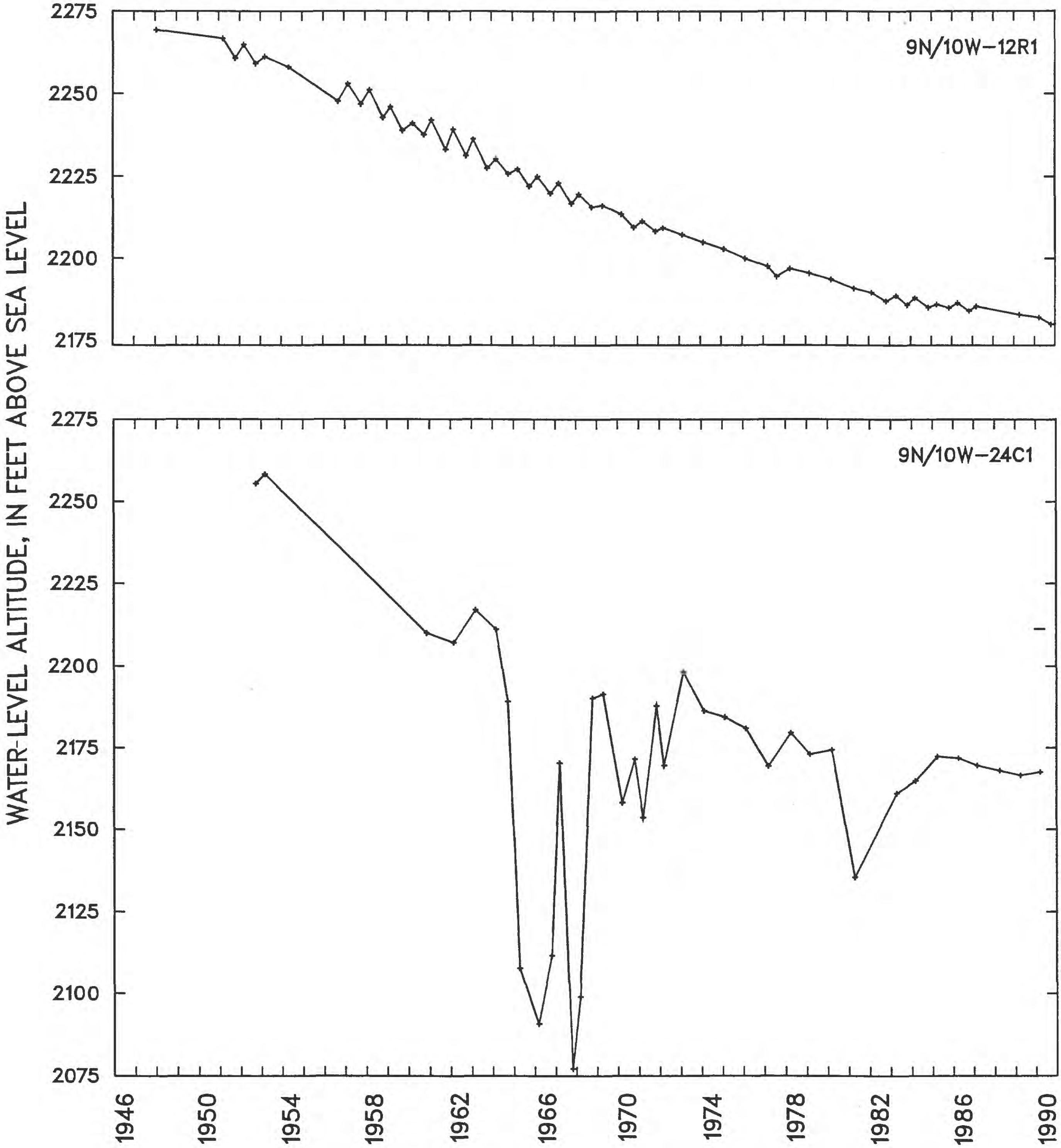

Figure 17. Water levels monitored by U.S. Geological Survey as part of the Antelope Valley-East Kern Water Agency (AVEK) monitoring program for wells on Edwards Air Force Base, 1947-90--*Continued.*

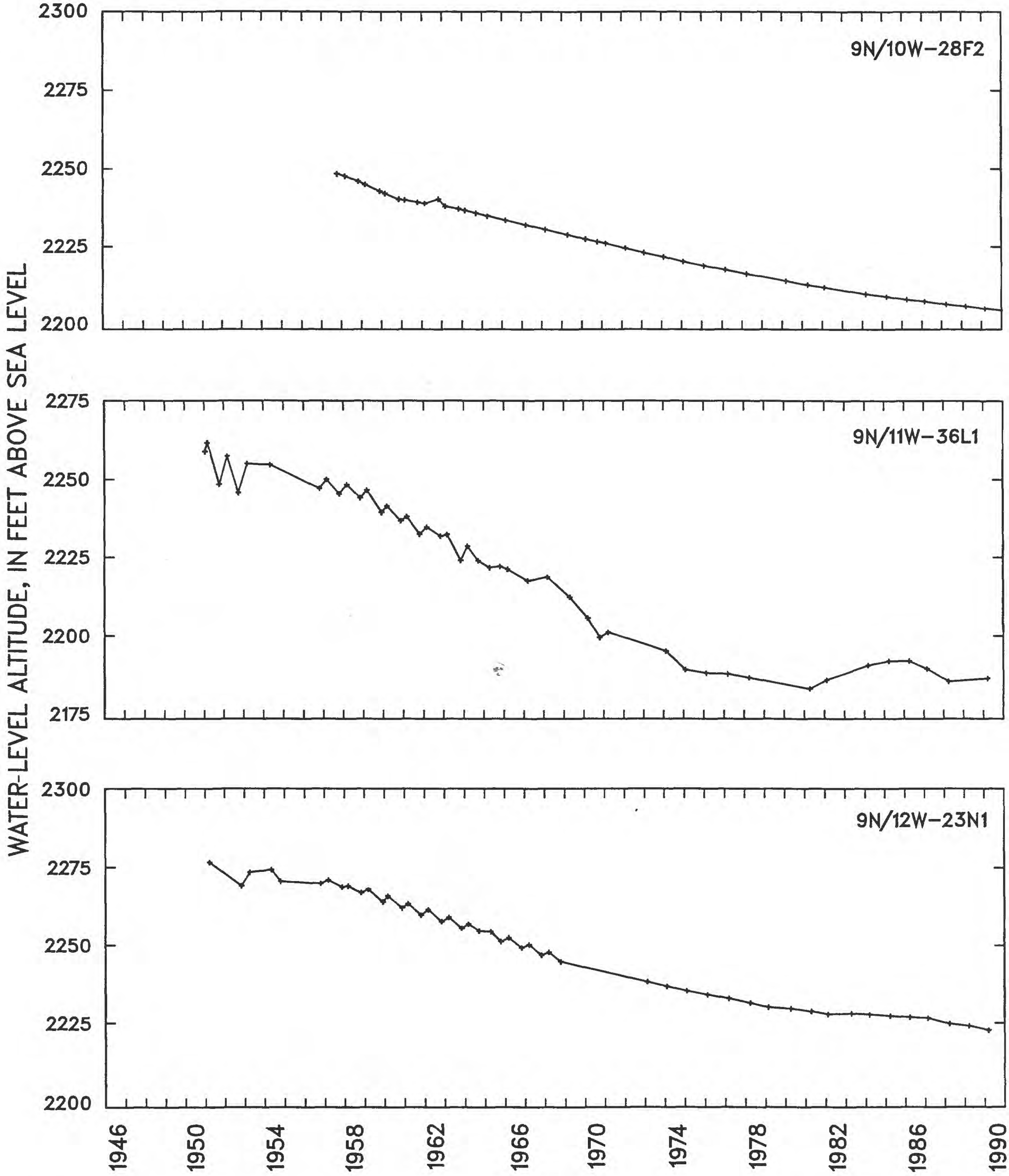

Figure 17. Water levels monitored by U.S. Geological Survey as part of the Antelope Valley-East Kern Water Agency (AVEK) monitoring program for wells on Edwards Air Force Base, 1947-90--*Continued.*

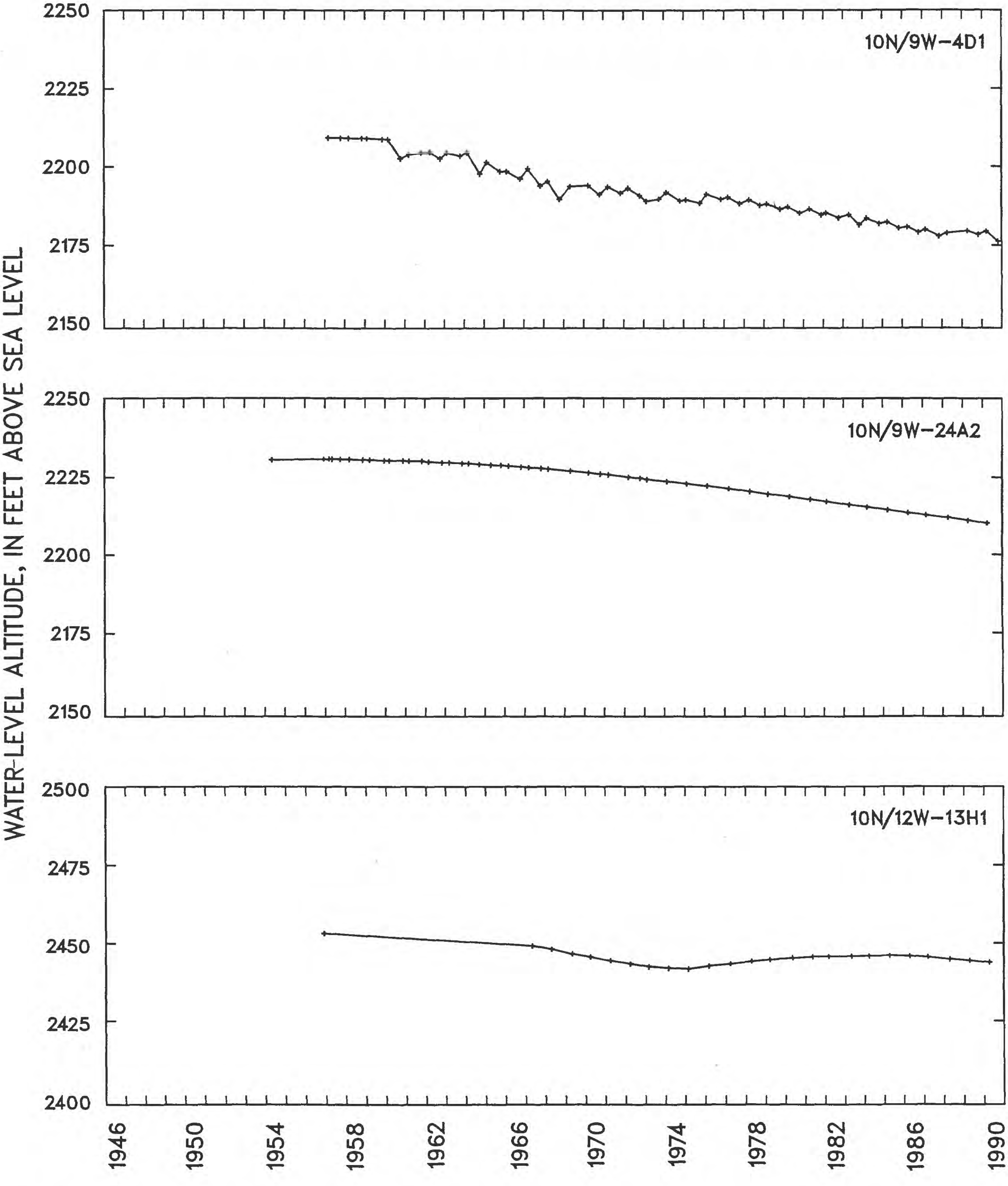

Figure 17. Water levels monitored by U.S. Geological Survey as part of the Antelope Valley-East Kern Water Agency (AVEK) monitoring program for wells on Edwards Air Force Base, 1947-90--*Continued.*

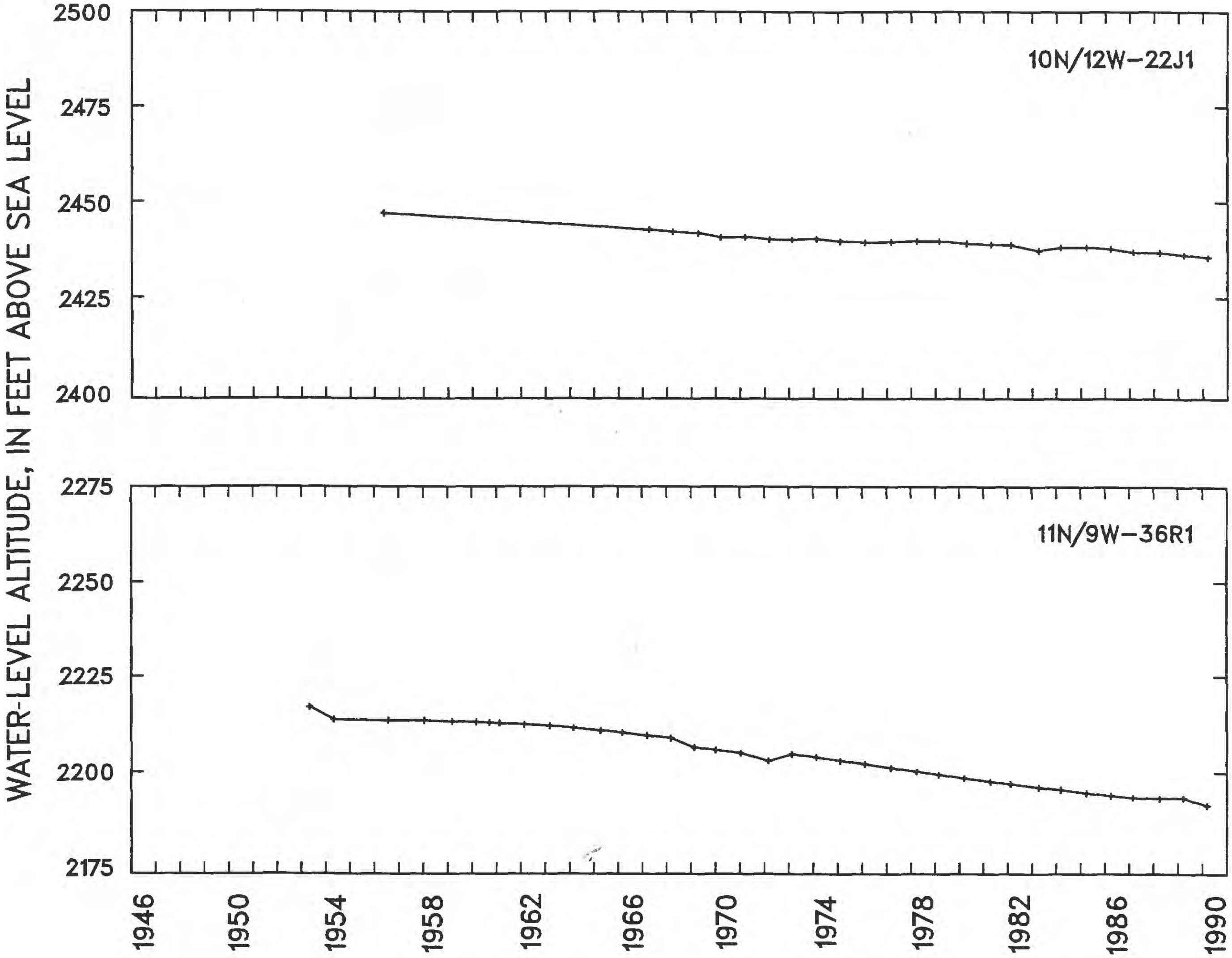

Figure 17. Water levels monitored by U.S. Geological Survey as part of the Antelope Valley-East Kern Water Agency (AVEK) monitoring program for wells on Edwards Air Force Base, 1947-90--*Continued.*

Water-level differences in the deeper wells (fig. 18*B*) show fluctuating responses to seasonal pumping stresses associated with production from the South Track well field (fig. 8). Monthly water-level changes in wells 8N/10W-1Q2 and 1Q3 are coincident, but 1Q3 has a slightly higher level, suggesting a hydraulic connection with high vertical connection within the 425- to 640-foot interval. Water-level changes in well 8N/10W-1Q1 generally are smaller than those of 8N/10W-1Q3. This may be due to the increased consolidation of the deeper alluvium and consequent decreased ground-water yield to the production wells with depth.

GROUND-WATER CHEMISTRY

During the spring of 1990, 14 ground-water samples were collected in the Rogers Lake area to determine concentrations of major ions and trace elements. These samples were collected from 10 of the new test wells drilled during 1989 and 1990 and from four base supply wells around the perimeter of the lake (fig. 19). The results of these analyses (table 6) indicate that the ground water near Rogers Lake ranges from soft to moderately hard (Hem, 1985, p. 159), and commonly has a high dissolved-solids concentration (greater than 500 mg/L). These

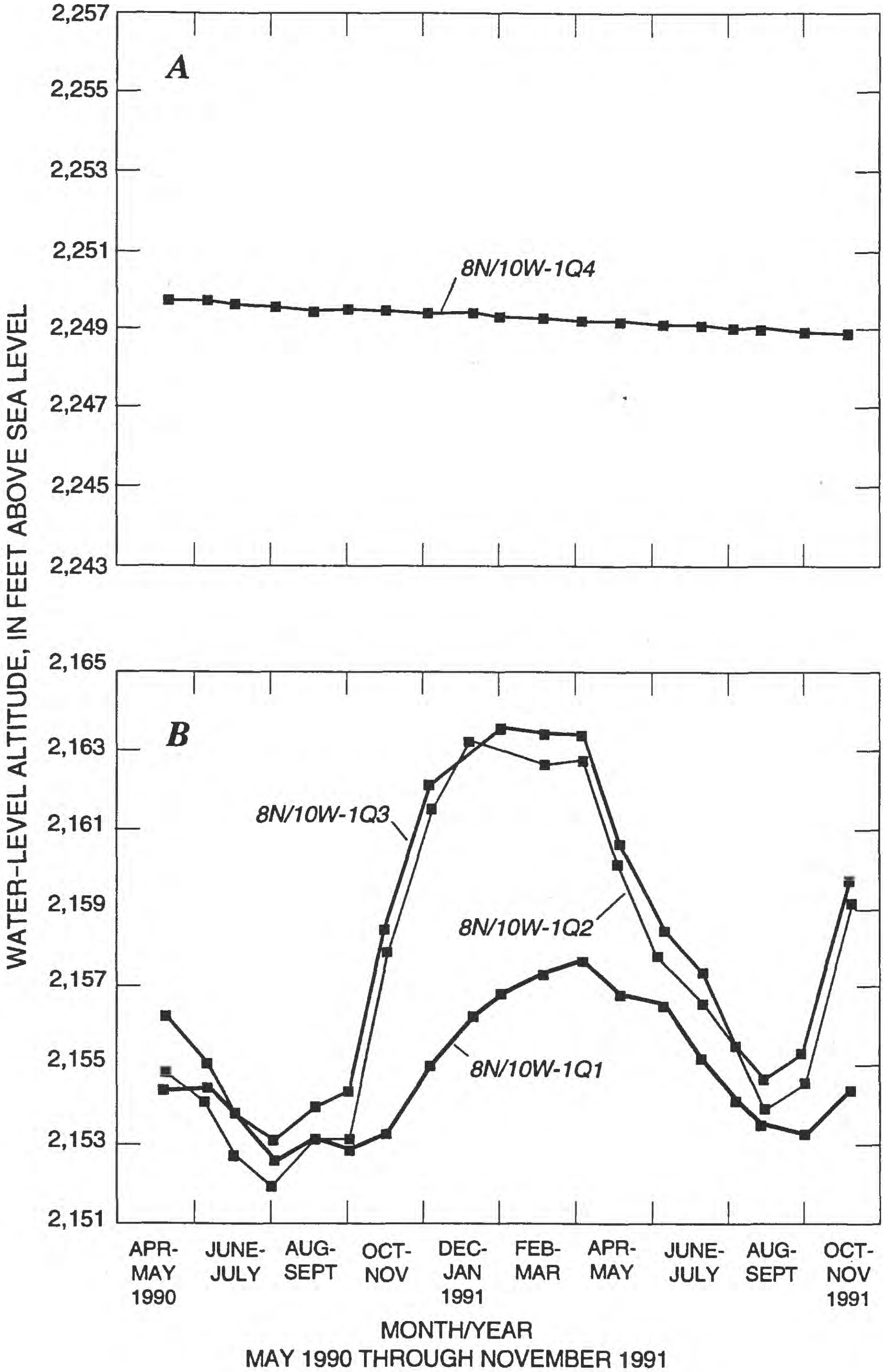

Figure 18. Water levels for wells at the Holly site on Edwards Air Force Base. *A*. Well 8N/10W-1Q4. *B*. Wells 8N/10W-1Q1-3.

analyses also indicate that, except for well 8N/10W-5A1 at the Buckhorn site (fig. 19), the concentrations of most determined constituents are less than the U.S. Environmental Protection Agency (EPA) primary and secondary drinking-water regulations for maximum contaminant levels (table 6). The only other exception was the high concentrations of fluoride in samples from the two deeper wells at the

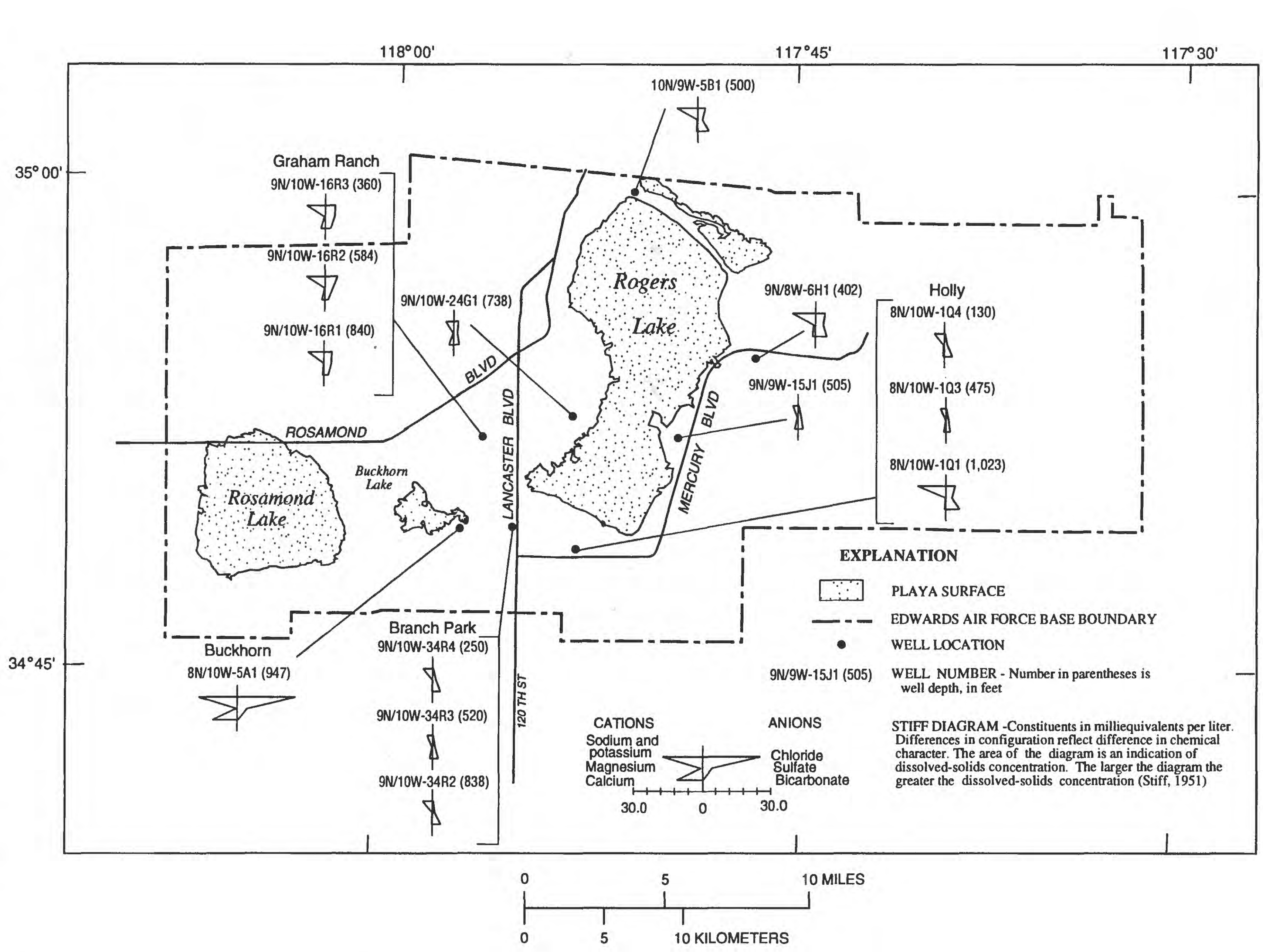

Figure 19. Ground-water quality for the Rogers Lake area on Edwards Air Force Base.

Table 6. Summary of water quality for selected wells on Edwards Air Force Base

[State well No.: See Well-Numbering System in text. USGS, U.S. Geological Survey. USGS site identification No.: Unique number for each site based on the latitude and longitude of the site. First six digits are latitude, next seven digits are longitude, and final two digits are a sequence number to uniquely identify each site. Depth of well: Depth is in feet below land surface. Altitude of land surface in feet above sea level, rounded to nearest foot. ft, foot; mg/L, milligram per liter; --, no data; µg/L, microgram per liter; µS/cm, microsiemen per centimeter (at 25 degrees Celsius); °C, degree Celsius; <, actual value is less than value shown]

State well No.		Local well name	USGS site identification No.	Date	Time	Depth of well	Altitude of land surface	Specific conductance (µS/cm)	pH (standard units)	Temperature, water (°C)
EPA drinking-water regulations								--	[1]6.5-8.5	--
8N/10W-	1Q1	HO1	344835117531301	5-14-90	0930	1,023	2,302	1,350	9.0	22.0
	1Q3	HO3	344835117531303	5-08-90	1630	475	2,302	324	8.0	24.5
	1Q4	HO4	344835117531304	5-08-90	1440	130	2,302	486	8.3	22.5
	5A1	BH1	344921117570601	5-12-90	1830	947	2,287	2,960	8.0	24.0
9N/8W-	6H1	EC2	345420117452901	5-10-90	1145	402	2,389	1,190	7.8	22.5
9N/9W-	15J1	PLA	345214117483701	5-10-90	1230	505	2,297	364	7.9	22.5
9N/10W-	16R1	GR1	345212117561801	5-13-90	1530	840	2,315	863	8.4	25.0
	16R2	GR2	345212117561802	5-13-90	1230	584	2,315	1,120	8.3	24.0
	16R3	GR3	345212117561803	5-13-90	1000	360	2,315	1,130	8.2	22.0
	24G1	S-2	345142117531201	5-10-90	0915	738	2,280	572	8.0	20.5
	34R2	BP1	344923117550301	5-08-90	1220	838	2,290	477	7.8	26.5
	34R3	BP2	344923117550302	5-12-90	1445	520	2,290	365	8.2	26.0
	34R4	BP3	344923117550303	5-11-90	1200	250	2,290	455	8.7	22.0
10N/9W-	5B1	NB5	345949117510501	5-10-90	1400	500	2,290	972	8.0	22.5

State well No.		Local well name	Hardness, total (mg/L as ($CaCO_3$)	Hardness, noncarbonate, dissolved (mg/L as $CaCO_3$	Calcium, dissolved (mg/L)	Magnesium, dissolved (mg/L)	Sodium, dissolved (mg/L)	Sodium (percent)	Potassium, dissolved (mg/L)	Alkalinity, water dissolved total field (mg/L as $CaCO_3$)
EPA drinking-water regulations			--	--	--	--	--	--	--	--
8N/10W-	1Q1	HO1	29	0	9.9	1.0	280	95	1.5	303
	1Q3	HO3	52	0	19	1.2	51	67	1.7	83
	1Q4	HO4	37	0	9.2	3.3	100	85	1.2	156
	5A1	BH1	570	540	220	3.8	390	60	4.0	20
9N/8W-	6H1	EC2	100	0	25	9.9	230	83	2.1	246
9N/9W-	15J1	PLA	86	0	29	3.3	48	54	2.1	106
9N/10W-	16R1	GR1	33	0	12	.77	160	91	1.7	72
	16R2	GR2	74	9	27	1.6	190	84	2.0	65
	16R3	GR3	120	12	40	5.3	190	77	2.3	110
	24G1	S-2	110	0	41	2.9	78	59	2.4	116
	34R2	BP1	20	0	6.9	.63	100	91	1.4	168
	34R3	BP2	75	0	24	3.6	52	59	2.4	106
	34R4	BP3	19	0	6.2	.75	97	91	1.2	140
10N/9W-	5B1	NB5	48	0	14	3.2	210	90	1.3	230

Table 6. Summary of water quality for selected wells on Edwards Air Force Base--*Continued*

State well No.		Local well name	Bicarbonate, water dissolved field (mg/L as HCO_3)	Sulfate, dissolved (mg/L)	Chloride, dissolved (mg/L)	Fluoride, dissolved (mg/L)	Silica, dissolved (mg/L)	Solids, residue at 180 °C, dissolved (mg/L)	Solids, sum of constituents, dissolved (mg/L)	Nitrogen, nitrite' dissolved (mg/L as N)
EPA drinking-water regulations			--	[1]250	[1]250	[1]2.0 [2]4.0	--	[1]500	--	--
8N/10W-	1Q1	HO1	289	130	140	3.3	31	813	783	<0.010
	1Q3	HO3	101	54	5.4	.30	28	192	212	<.010
	1Q4	HO4	190	63	7.8	1.5	15	289	295	<.010
	5A1	BH1	25	220	900	.30	19	1,830	1,770	<.010
9N/8W-	6H1	EC2	300	160	140	1.4	36	760	765	<.010
9N/9W-	15J1	PLA	129	62	11	.30	30	242	251	<.010
9N/10W-	16R1	GR1	88	150	100	9.7	22	510	500	<.010
	16R2	GR2	79	160	180	5.5	21	663	628	<.010
	16R3	GR3	134	190	150	.50	24	697	680	.020
	24G1	S-2	142	71	63	.30	27	362	357	<.010
	34R2	BP1	205	45	10	.60	51	309	317	<.010
	34R3	BP2	129	50	7.5	.20	25	239	230	<.010
	34R4	BP3	171	66	9.2	.70	30	311	298	<.010
10N/9W-	5B1	NB5	281	95	110	1.0	28	608	603	<.010

State well No.		Local well name	Nitrogen, NO_2+NO_3, dissolved (mg/L as N)	Aluminum, dissolved (µg/L)	Arsenic, dissolved (µg/L)	Boron, dissolved (µg/L)	Iron, dissolved, (µg/L)	Manganese, dissolved (µg/L)	Selenium, dissolved (µg/L)
EPA drinking-water regulations			--	--	[2]50	--	[1]300	[1]50	[2]10
8N/10W-	1Q1	HO1	0.600	40	11	1,300	18	3	1
	1Q3	HO3	.400	10	17	80	7	2	<1
	1Q4	HO4	<.100	50	18	390	47	8	<1
	5A1	BH1	<.100	<10	33	190	30	440	<1
9N/8W-	6H1	EC2	2.70	<10	20	990	7	<1	1
9N/9W-	15J1	PLA	.400	<10	7	70	7	10	<1
9N/10W-	16R1	GR1	<.100	80	12	300	38	33	<1
	16R2	GR2	.300	<10	39	210	<3	23	<1
	16R3	GR3	2.70	<10	2	270	<3	2	2
	24G1	S-2	.300	<10	9	130	7	<1	<1
	34R2	BP1	<.100	20	24	540	6	7	<1
	34R3	BP2	.300	<10	14	100	<3	<1	<1
	34R4	BP3	.500	250	17	190	180	6	<1
10N/9W-	5B1	NB5	.300	<10	39	800	24	<1	<1

[1]Secondary maximum contaminant level: Contaminants that affect the esthetic quality of drinking water. At high concentrations or values, health implications as well as esthetic degradation may also exist. Secondary levels are not Federally enforceable but are intended as guidelines.

[2]Maximum contaminant level: Enforceable health based regulations.

Graham Ranch site, 9N/10W-16R1 and 16R2, and from the deep well 8N/10W-1Q1 at the Holly site. The pH levels in samples from well 9N/10W-34R4 at Branch Park and well 8N/10W-1Q1 at Holly are slightly greater than EPA recommended secondary maximum contaminant levels (table 6).

Analysis of the sample from well 8N/10W-5A1 at the Buckhorn site (fig. 19), indicates that the water from this well exceeds EPA recommended maximum contaminant levels for chloride, dissolved solids, and manganese (table 6) and would be characterized as a very hard and slightly saline type of water (Hem, 1985, p. 157 and p. 159). The sample from this test well is from the 884- to 947-foot depth, and the poor quality of the water from this depth and location may not be representative of the water at shallower depths or of the surrounding area. At the Branch Park site, 2 mi east (fig. 19), the deepest well, 9N/10W-34R2, is open to the aquifer from 782 to 940 ft, and all determined constituents were within EPA recommended maximum contaminant levels.

The quality of the ground water in the Rogers Lake area, as characterized by major-ion concentrations, varies both areally and with depth (fig. 19). Water from the shallower wells, those wells less than 900 ft deep at the south end of Rogers Lake, generally is classified as a sodium bicarbonate type; however, the ground water at the north end of the lake and from the deep well at the Holly site (fig. 19), 8N/10W-1Q1 is classified as a sodium chloride bicarbonate type. At the Graham Ranch site (fig. 19), the ground water generally is a sodium chloride sulfate type and water from the deep test well at the Buckhorn site (fig. 19), 8N/10W-5A1 is classified as a sodium carbonate chloride type.

AQUIFER SYSTEM AT EDWARDS AIR FORCE BASE

HYDROGEOLOGIC BOUNDARIES

Two aquifers, termed "deep" and "principal", are present at EAFB. The deep aquifer underlies the entire base in the Lancaster subbasin and extends northward beneath Rogers Lake into the North Muroc subbasin. The principal aquifer underlies the southern part of EAFB as far north as the Rosamond Hills and the southern end of Rogers Lake (Durbin, 1978, pl. 1). The lateral and bottom boundaries of the deep aquifer in the area of EAFB are the contacts between the saturated alluvium and the bedrock. The upper boundary of the deep aquifer is the bottom of the lacustrine deposits, where present, and the water table elsewhere. The lateral boundaries of the principal aquifer are the contacts between the saturated alluvium and the bedrock, and between the saturated alluvium and top of the lacustrine deposits in areas where the lacustrine deposits extend above the water table. The bottom boundary is the top of the lacustrine deposits and the top boundary is the water table.

Dutcher and Worts (1963) included the Graham Ranch area as part of the main aquifer system in the Lancaster subbasin but do not indicate whether it is part of the deep or principal aquifer. Durbin (1978, pl. 1) does not include the Graham Ranch area as part of the aquifer system within the subbasin. The potentiometric surface (fig. 5) indicates that the Graham Ranch area may be weakly hydraulically connected to the deep aquifer. Lithologic and borehole geophysical logs of the wells drilled in the Graham Ranch area (figs. 9*D-F*) do not indicate the presence of any lacustrine deposits in this area. The aquifer material in this area is similar to that in the older alluvium in the lower part of the deep aquifer. The quality of the water in the Graham Ranch area is more similar to that of the water from wells on the north and east sides of Rogers Lake and deep well 8N/10W-1Q1 at the Holly site than to that of the water in the shallower wells at the Holly and Branch Park sites (fig. 19 and table 6). This similarity in water quality and lithologic data indicates that the Graham Ranch area may be part of the deep aquifer system.

Logs of boreholes drilled at the Buckhorn, Branch Park, and Holly sites indicate that the top of the lacustrine deposits is very shallow in these areas--40, 100, and 90 ft below land surface, respectively. At the Holly site, the depth to water in shallow well 8N/10W-1Q4 completed above the lacustrine deposits was about 50 ft below land surface. This shallow water level would indicate that the principal aquifer is only about 40 ft thick in this area. Land-surface altitudes at the Buckhorn and Branch Park sites are lower than at the Holly site and therefore, the principal aquifer may be even thinner at these locations. In the area of these wells and probably to the north, the principal aquifer is too thin to yield a significant volume of water. South of these sites, the principal aquifer becomes a major source of water as it thickens considerably because of the underlying southward dipping lacustrine beds (Durbin, 1978, pl. 1) and the increasing land-surface altitude.

Most of the ground water currently pumped at EAFB is presumed to come from the deep aquifer. Near EAFB well fields, the principal aquifer is either very thin or nonexistent and therefore is assumed to contribute very little water to the pumping wells. Ground water moving within the lacustrine deposits through sand stringers and interbeds also may contribute significantly to the ground-water supply at EAFB.

HYDRAULIC PROPERTIES

Aquifer hydraulic tests to determine the transmissive and storage properties of the ground-water flow system were not conducted as part of the initial phase of this study. However, several past investigations have provided estimates of aquifer properties based on pumping tests and specific capacity tests. These estimates are summarized in table 7 for the pumping tests and in table 8 for the specific capacity tests. Estimates of aquifer properties based on pumping tests range from 4,600 to 26,800 ft^2/d for transmissivity, 0.00036 to 0.13 for storage coefficient and 0.017 to 0.13 ft^2/d for vertical hydraulic conductivity of the confining unit between the principal and deep aquifers (table 7). Estimates of transmissivities based on specific capacity tests range from 600 to 32,000 ft^2/d (table 8).

Durbin (1978) estimated the aquifer properties for both the principal and deep aquifers within the area of EAFB for the purposes of modeling the ground-water flow of the entire Antelope Valley. The estimates of transmissivity were largely based on specific capacity measurements collected by McClelland (1963) and Bloyd (1967) and shown in table 8. These estimates range from 800 to 9,000 ft^2/d for the principal aquifer (Durbin, 1978, pl. 7) and from 1,700 to 14,000 ft^2/d for the deep aquifer (Durbin, 1978, pl. 8). Durbin (1978) also estimated the storage coefficient of the principal and deep aquifers based on values of the specific yield of deposits determined by Dutcher and Worts (1963). The estimates of the storage coefficient of the principal aquifer ranged from 0.05 to 0.10 (Durbin, 1978, pl. 11) and the estimate of the storage coefficient of the deep aquifer in the North Muroc ground-water subbasin and the area east of Rogers Lake was 0.15 (Durbin, 1978, pl. 12). Durbin (1978) estimated a constant storage coefficient value of 0.001 for the confined area of the deep aquifer and a constant vertical hydraulic conductivity of 0.01 ft/d for the confining bed between the two aquifers.

Table 7. Summary of pumping tests results for selected wells completed in the deep aquifer in vicinity of Edwards Air Force Base

[Well locations shown in figure 16. Type of test: MW, multiple well; SW, single well. ft/d, foot per day; ft^2/d, foot squared per day; h, hour. --, no data]

State well No.		Date	Duration (hours)	Transmissivity (ft^2/d)	Storage coefficient	Vertical hydraulic conductivity of confining unit (ft/d)	Type of test	Source
8N/10W-	1C1	8-17-61	12	[1]4,600	--	--	SW	McClelland (1963)
	1C2	5-27-85	30	[2,4]25,900/14,600	0.0023/0.00036	0.092/0.017	MW	Weston (1986)
9N/10W-	24G1	5-30-85	49	[2,4]8,300/7,200	0.0013/0.0028	0.078/0.13	MW	Do.
10N/9W-	5B1	5-24-85	55	[3]20,800	[5]0.0006	--	MW	Do.
11N/9W-	36C1	8-14-55	262	[1]12,000/26,800	[1]0.13	--	MW	McClelland (1963)

[1]Analyzed using the Theis nonequilibrium method (Theis, 1935).
[2]Analyzed using the Hantush-Jacob, Leaky Aquifer Method (Hantush and Jacob, 1955).
[3]Analyzed using the Boulton, Delayed Yield from Storage Method (Boulton, 1963).
[4]Values for transmissivity, storage coefficient, and vertical hydraulic conductivity of confining unit were computed for two monitoring wells.
[5]Storage coefficient computed from a match of the theoretical solution to the measured early-time response.

Table 8. Summary of estimated transmissivities based on specific capacity tests for selected wells in the vicinity of Edwards Air Force Base

[Well locations shown in figure 16; ft^2/d, foot squared per day]

State well No.		Transmissivity (ft^2/d)	Source
8N10W-	1C1	3,500	McClelland (1963)
	1C2	11,100	Weston (1986)
9N/8W-	6H1	25,700	McClelland (1963)
	6H2	32,000	Do.
9N/9W-	6A1	5,400	Do.
	6C1	3,800	Bloyd (1967)
	6E1	800	McClelland (1963)
	6L1	2,900	Do.
	6M1	600	Do.
	18C1	1,900/1,900	Do.
	24H1	600	Do.
9N/10W-	24C1	800	Weston (1986)
	24E2	1,000	Do.
	24F1	15,000	Do.
	24G1	2,500/3,100	McClelland (1963)
	36P1	12,000	Weston (1986)
10N/9W-	4D1	5,800	Bloyd (1967)
	5B1	7,900	Weston (1986)
	7A1	1,200	McClelland (1963)
	7A2	2,300	Do.
11N/9W-	32Q1	6,700	Weston (1986)
	36C1	6,300	McClelland (1963)

GROUND-WATER FLOW

The general direction of ground-water flow in the deep aquifer beneath EAFB is toward a pumping depression centered beneath the South Track well field (figs. 5 and 8). The direction of ground-water movement across the reported buried bedrock ridge under the north end of Rogers Lake (fig. 10) is uncertain at this time. Durbin (1978, p. 6) reported that prior to the extensive ground-water development in the Lancaster subbasin, the flow beneath Rogers Lake was toward the north into the North Muroc subbasin but that by 1961, as pumpage increased in the Lancaster subbasin, the flow direction had reversed and was from north to south. As a result of this reversal of flow direction, ground water may be flowing from the North Muroc subbasin into the Lancaster subbasin, depending on the location and depth to the buried bedrock ridge reportedly separating the two subbasins. If the buried ridge is near the surface and extends across the lake as suggested by Dutcher and Worts (1963), then it could be acting as a partial barrier to flow creating a ground-water divide between Lancaster and North Muroc subbasins. If the ridge is deeply buried beneath the lake bed as inferred by the gravity map of the area (fig. 10), then water could now be flowing from the North Muroc subbasin into the Lancaster subbasin. Additional geophysical surveys and exploratory drilling would provide more information about this buried ridge and its effect on ground water in the area.

The direction of ground-water movement in the principal aquifer beneath EAFB is uncertain at this time. Along the southern boundary of EAFB, it is probably flowing toward the large pumping depressions south of EAFB (fig. 5) and possibly toward the pumping depression at the South Track well field near the southern end of Rogers Lake.

Several faults are known to exist within the boundaries of EAFB (fig. 2). These faults have been mapped in the bedrock hills and in some instances they have been projected into the margins of the alluvial basins. Surface evidence provides no indication that these faults have disturbed the unconsolidated material nor does available water-level data indicate that faulting is affecting the flow of ground water within the unconsolidated material. The line of old dry springs that is in the Buckhorn Lake area corresponds very closely to the N. 50° to 60° E. striking faults inferred from the geophysical data. These old springs may be the result of the inferred faulting in the area or they may have occurred at this location because it is near the northern edge of the lacustrine deposits within the unconsolidated materials filling the basin. Additional deep observation wells, installed across this old spring line, would help to determine what effect, if any, the inferred fault has on the flow of ground water in the area.

CONCEPTUALIZATION OF AQUIFER SYSTEM AT HOLLY SITE

Hydraulic heads of the Holly site wells (fig. 8) were used to develop a conceptual model of the aquifer(s) for a localized part of the hydrologic basin (fig. 20). The large contrast in hydraulic heads between 8N/10W-1Q4 and the deeper wells (figs. 18*A* and 18*B*), combined with the lack of seasonal fluctuations in well 8N/10W-1Q4 (fig. 18*A*), due to

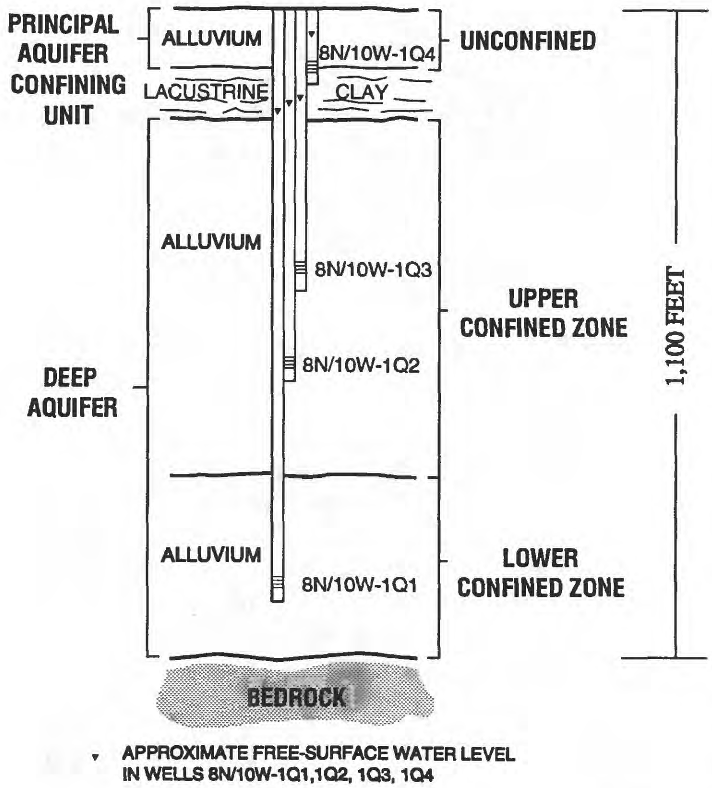

Figure 20. Conceptual model of the aquifer system at the Holly site on Edwards Air Force Base.

pumping stresses from the South Track well field (fig. 8) evident in the other Holly site wells, suggest at least two aquifers in the Holly area. The shallow aquifer monitored in well 8N/10W-1Q4 probably is an unconfined aquifer that is separated from the deeper zones by the fine-grained lacustrine sediments, evident on the resistivity logs and lithologic logs (fig. 9*C*), which act as a confining unit. The two aquifers are correlative to the previously defined principal and deep aquifers of the Lancaster ground-water subbasin.

Hydraulic heads measured in the deeper wells 8N/10W-1Q1, 1Q2, and 1Q3 indicate that formation fluid pressures are confined by the lacustrine sediments above. Seasonal fluctuations measured in wells 8N/10W-1Q2 and 1Q3 track each other closely and indicate that the aquifer thickness monitored by these wells is hydraulically well connected. However, the seasonal fluctuations measured in well 8N/10W-1Q1 are attenuated with respect to those in 1Q2 and 1Q3, indicating a poor hydraulic connection between the upper and lower zones of the deep aquifer.

Further evidence for a change in aquifer properties at the 970- to 1,075-foot depth in well 1Q1 is (1) the change in lithology from a fine- to coarse-grained material to a siltier, more indurated material and a shift to lower resistivity at about 837.5 ft; and (2) the change in water chemistry, reflected in the higher dissolved-solids concentration. On this basis, an upper and a lower zone may exist in the confined aquifer near the Holly site. The two zones may be poorly connected, with flow occurring from the upper to the lower zone, especially during the autumn and winter months of minimum pumping stress in the upper zone. The weathered bedrock in the core from the 1,097 to 1,107 ft interval (table 4) defines the lower limit of the lower zone in the confined aquifer.

The depth to water in well 8N/10W-1Q4 corresponds closely with the water level in well 8N/9W-6D1, about 1 mi to the northeast (fig. 16); however, the water levels in the deeper wells correspond closely to initial water levels measured in the newly constructed wells at Branch Park (9N/10W-34R2, 34R3, and 34R4) and Buckhorn (8N/10W-5A1) sites, about 2 and 4 mi to the west (table 3, fig. 8).

LAND SUBSIDENCE AND AQUIFER-SYSTEM COMPACTION

Subsidence of the land surface, related to ground-water withdrawal in the Antelope Valley, has been previously reported (Lofgren, 1965; Lewis and Miller, 1968; Poland, 1984). The subsidence is attributed to the compaction of fine-grained sediments in the aquifer system due to long-term pumping, lowering of aquifer hydraulic head, and increasing effective stress. In 1988, some of the effects of land subsidence were observed at EAFB with the occurrence of surface deformation features associated with land subsidence such as sinklike depressions and earth fissures. Other indications of land subsidence at EAFB include failure of production wells caused by collapsed well casings, and the protrusion above land surface of well casings, pump platforms, and survey benchmarks. In 1989-91, the USGS conducted vertical and horizontal control surveys to measure the extent and magnitude of land subsidence in the area and to establish a network of benchmarks to monitor future land subsidence (Blodgett and Williams, 1992).

Figure 21 shows measurements of land subsidence at selected benchmarks in the area. The measurements are based on a comparison of surveys made in 1961 and 1989-91. Land subsidence greater than 1 ft affects more than 100 mi^2 of EAFB (fig. 21). The largest amount of measured subsidence on EAFB is 3.3 ft, at benchmark P1155 near the intersection of Lancaster Boulevard and Avenue B, near the South Track well field. Subsidence near other base well fields is less than 1 ft. Subsidence in the areas of Main Base, North Base, and along the eastern side of Rogers Lake also is less than 1 ft. Four feet of subsidence was measured at benchmark J1147 (fig. 21) near Avenue I and Sierra Highway in the city of Lancaster. Lines of equal land subsidence magnitudes (fig. 21) show a large area between the southern edge of Rogers Lake and the city of Lancaster where 2 or more feet of subsidence has occurred. The shape of this area south of Rogers Lake is elongated along a northeast-southwest axis, consistent with the orientation of other structural and depositional trends of the East Antelope structural basin.

In May 1990, an extensometer was installed at the Holly site to measure vertical compaction of the aquifer system. The Holly site is near the South Track well field, and near benchmarks M1155 and P1155, where the maximum amount of land subsidence has been measured on EAFB. The extensometer is anchored at a depth of about 840 ft and provides a measure of the vertical compaction of the sediments between land surface and the 840-foot depth. Extensometer data and details of the extensometer design and construction are given by Blodgett and Williams (1992).

Figure 22 shows a graph of cumulative vertical compaction measured at the Holly extensometer from May 11, 1990 through November 6, 1991. Water-level altitudes measured in well 8N/10W-1Q3 also are shown for the same period. Two distinct slopes of the compaction curve are evident: one corresponding to the spring and summer declines in water level, and another corresponding to the autumn and winter water-level recoveries. During the spring and summer months, when ground-water production from the South Track well field and other production wells is largest, the rate of vertical compaction is about 1.93×10^{-4} ft/d. During the autumn and winter months, the aquifer system continues to compact, but the rate of vertical compaction decreases to about 1.12×10^{-4} ft/d. Because the two periods of compaction are each about 6 months in duration, an average annual rate of compaction, 5.57×10^{-2} ft/yr, can be estimated from the average of the two seasonal rates or one cycle of pumping and recovery. For the period of record, 544 days, 8.16×10^{-2} ft of vertical compaction has been measured at the Holly extensometer.

The measurements of aquifer-system compaction and water-level fluctuations at the Holly site (fig. 22) can be analyzed to gain insight to the vertical compaction occurring during successive cycles of ground-water level declines. Depending on the nature of the sediments, compaction may be elastic or inelastic. In general, coarse-grained deposits such as sand and gravel compact elastically, and the compaction is small and reversible, whereas fine-grained deposits such as clays compact largely inelastically, and the compaction is much greater and chiefly irreversible. For a saturated porous medium, the vertical deformation is controlled by the effective stress and the relation can be expressed in the equation given by Terzaghi (1943):

$$\sigma_z' = \sigma_z - p,$$

where the vertical effective stress, σ_z', represents the grain-to-grain load borne by the aquifer particles, and is the difference between the overburden stress of the saturated and unsaturated rocks and soil, σ_z, and the buoyant stress imparted by the aquifer fluid pressure, p. A decline in head (fluid pressure) causes a corresponding increase in the grain-to-grain load in the aquifer system, and the sediments compact. When the head decline is areally extensive relative to the location of interest in the aquifer, the horizontal components of stress can be neglected and the vertical effective stress represents the grain-to-grain load.

The vertical effective stresses were calculated for the Holly site for the stress periods shown in figure 22, and follow the technique summarized by Poland (1984). Ground-water levels measured in the four wells provide values of aquifer fluid pressure. All calculated stresses are expressed in terms of an equivalent height of water (hydraulic head) in feet. For the stress calculations, average values were assumed for the porosity, 0.40, specific retention of moisture contained above the water table, 0.20, and for the specific gravity of individual grains, 2.7 (Bear, 1979, and Todd, 1980). Stresses were

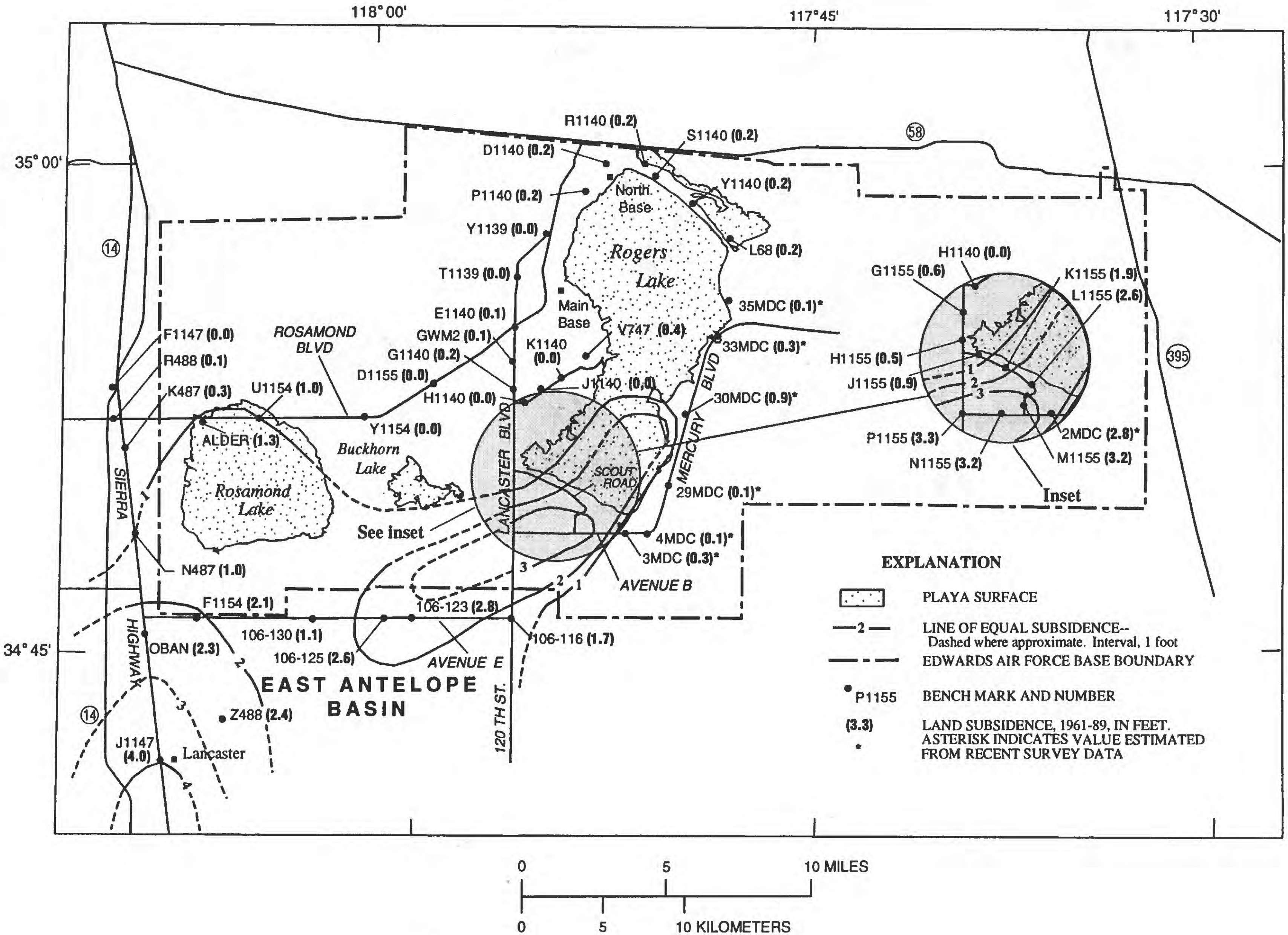

Figure 21. Magnitude of subsidence between 1961 and 1989 at selected benchmarks on Edwards Air Force Base and vicinity. Modified from Blodgett and Williams (1992).

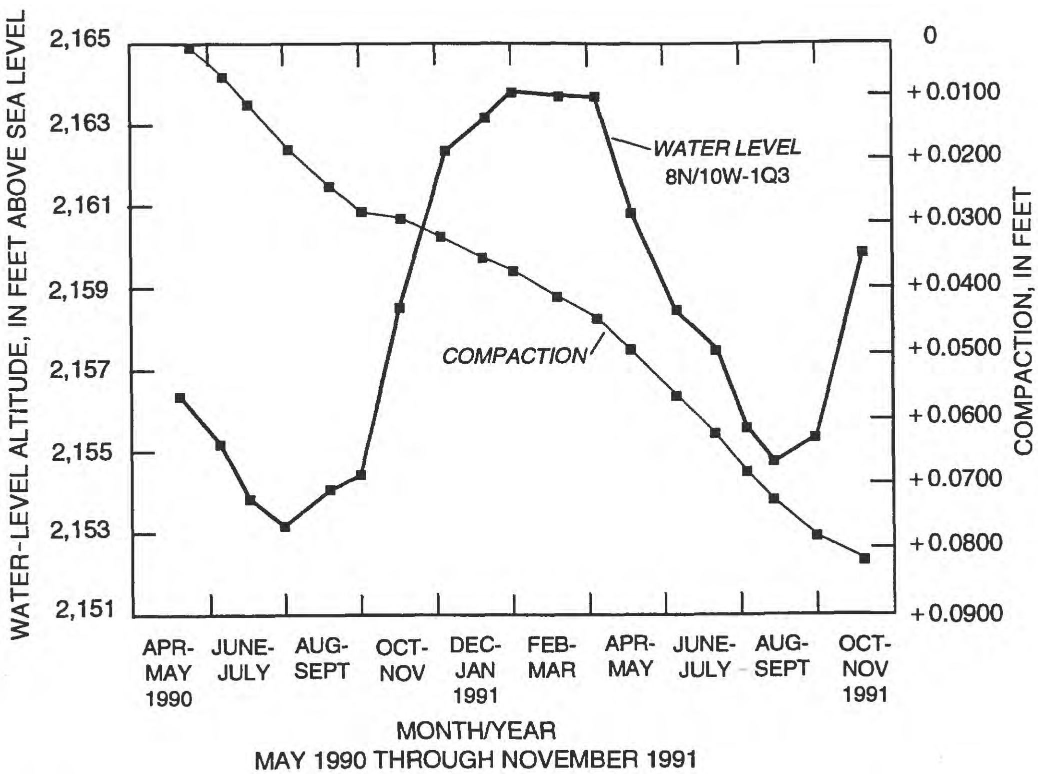

Figure 22. Water levels for well 8N/10W-1Q3 and cumulative vertical compaction at the Holly site on Edwards Air Force Base.

calculated at aquifer boundaries, according to the conceptual model of the local aquifer system (fig. 20) and at the midpoint of gravel-packed intervals. For the period of record, the maximum and minimum effective stresses in the upper zone of the confined aquifer correspond to the maximum and minimum water-level declines in 8N/10W-1Q2 and 1Q3. The change in effective stress is the difference between the effective stress, and the minimum value of effective stress computed for the selected depth in the aquifer profile. The change in effective stress represents the applied stress to the aquifer due to fluctuations of aquifer hydraulic head.

Figure 23 illustrates the change in effective stress at depth in the aquifer-system profile. The graph is based on water-level measurements made in wells 8N/10W-1Q1, 1Q2, 1Q3, and 1Q4, at the Holly site on August 3, 1990 (figs. 18*A* and 18*B*). This date corresponds to the minimum water level and maximum effective stress computed for well 8N/10W-1Q2 for the period of record. The graph shows that the upper zone of the confined aquifer, where the magnitude of hydraulic head fluctuations is greatest, experiences the greatest change in effective stress, about 10 to 11 ft expressed as an equivalent height of water. The unconfined aquifer shows little change and reflects the lack of seasonal water-level fluctuation evident in well 8N/10W-1Q4 (fig. 18*A*). The lower zone of the confined aquifer exhibits about a 5-foot change in effective stress, about one-half the amount computed for the upper zone, and also reflects the relative amplitude of the seasonal aquifer hydraulic heads measured in well 8N/10W-1Q1 (fig. 18*B*). The stress graph indicates that aquifer system compaction would be greatest in the upper zone of the confined aquifer, depending on the distribution and thickness of compressible, unconsolidated fine-grained clay units. Stresses in the lower zone also may cause compaction, but the small amounts of clay, and the degree of induration of the sediments logged in the lower zone may render the lower zone sediments less compressible than the nonindurated interbedded sediments in the upper zone.

The distribution and thickness of clay units in the upper zone of the confined aquifer (figs. 9*C* and 20) highlights the interbedded nature of the sediments

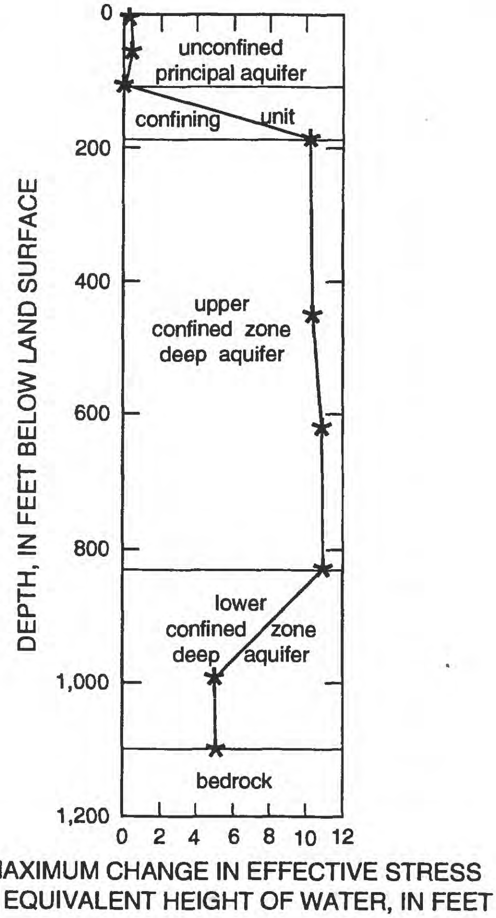

Figure 23. Maximum change in effective stress with depth at the Holly site on Edwards Air Base, for May 11, 1990 through November 6, 1991. Asterisks are the calculated change in effective stress; solid line connecting the asterisks is the inferred change in effective stress; horizontal lines are the aquifer boundaries.

that constitute the upper zone. Many 5- to 20-foot thick zones of low resistivity (fine-grained deposits) constitute the 400 to 600-foot depth interval. A thick, 90-foot interval of clayey material, constitutes the 300 to 400-foot section. Because of the large thickness, low hydraulic conductivity and relatively large compressibility of the interbedded clay layers, the compaction of the aquifer system, in response to an increased effective stress, is a time-dependent process. The lower hydraulic conductivity of the interbedded clay layers delay equilibration of hydraulic heads between the coarse-grained aquifer materials and the interbeds. Transient heads in the interbedded clays may result. These heads may be larger than the heads in the adjacent coarse-grained aquifer material, and the corresponding effective stress in the interbedded clays may be smaller due to the larger residual hydraulic heads in the clays. For a particular stress cycle, where aquifer hydraulic heads are equilibrated throughout the interbedded aquifer system, the aquifer will become 100 percent compacted for that level of stress. However, where the interbeds have not attained hydraulic-head equilibration, only a part of the ultimate compaction is realized for that stress cycle.

Figure 24 shows the relation between the change in effective stress in the upper zone of the confined aquifer to vertical compaction measured at the Holly site for the period May 11, 1990 through November 6, 1991. Most of the aquifer system compaction occurs during the two periods of largest change in effective stress. These periods are coincident with the two periods of increased rate of compaction evident in figure 22. When the change in effective stress decreases to 0 (fig. 24), the aquifer system continues to compact, albeit at a smaller rate. No expansion of the aquifer system is evident as a result of the cycling of effective stress to its smallest magnitude. A possible explanation is that any expansion of the compacted sediments is masked by the continuous compaction of clay horizons, where residual hydraulic heads are slowly equilibrating to the present day aquifer hydraulic heads. Johnson (1911) indicates that near the beginning of this century aquifer hydraulic heads in the upper zone were at altitudes higher than land surface near the Holly site and south Rogers Lake. Residual heads in some of the thicker and less permeable clay horizons in the upper zone and confining unit may not have yet equilibrated with the long-term decline in aquifer heads.

The rate of compaction, 5.57×10^{-2} ft/yr, computed for one cycle of aquifer hydraulic head decline and recovery during 1990-91 does not explain the approximately 3.2 ft of subsidence measured at nearby benchmark, M1155 since 1961 (fig. 21). At the 1990-91 rate, only 1.67 ft of subsidence would result, leaving about 1.5 ft of unaccounted land subsidence in this area. Two possible explanations are that the rate of compaction has decreased since 1961; or compaction is occurring in the sediments of the lower zone of the confined aquifer near the Holly site that are not being measured by the Holly extensometer. The latter explanation is least likely due to the reasons previously stated regarding the nature of the deposits in the lower zone. Hydrographs for two of the Antelope Valley-East Kern Water Agency wells (figs. 17*B* and 17*H*) monitored prior to 1961 show a fairly constant rate of water-level decline in

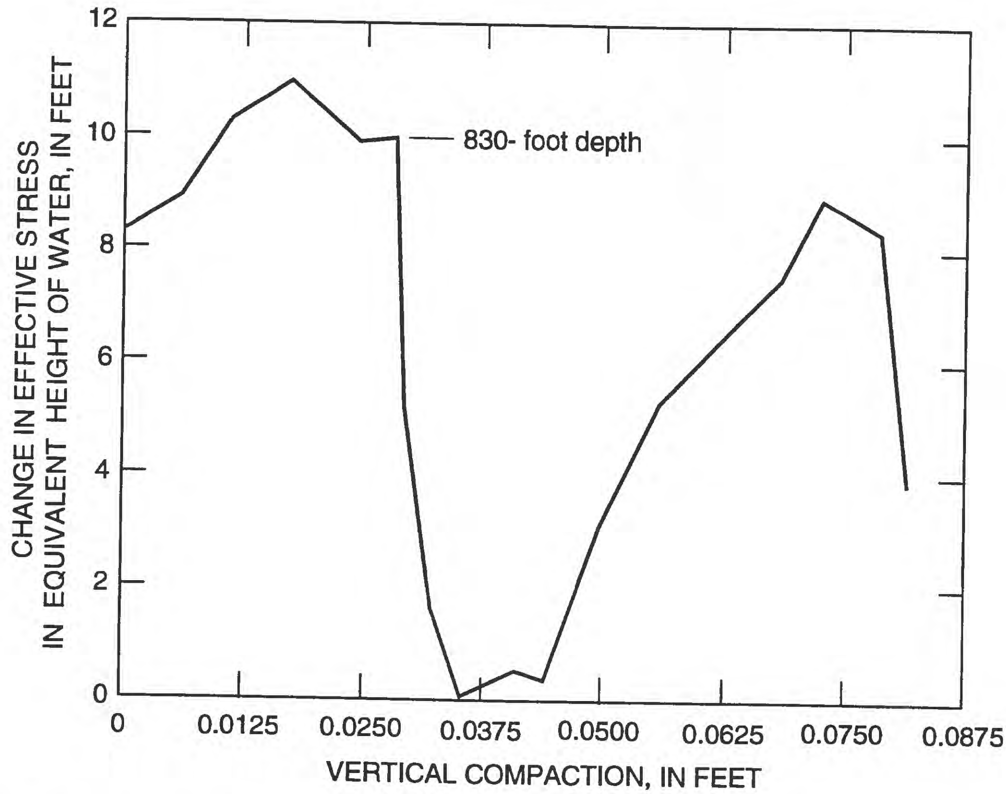

Figure 24. Relation between the change in effective stress to vertical compaction measured in the upper zone of the confined aquifer at the Holly site on Edwards Air Force Base.

early years, with a gradually decreasing rate of decline in the past 20 years. The two wells are about 4 mi west-southwest (fig. 17*B*) and 5 mi northeast (fig. 17*H*) of the Holly site on EAFB. If these trends in aquifer head declines are representative of the long-term trend at the Holly site, annual change in effective stress probably was greater at the Holly site during the decade of the 1960's, and the annual rate of compaction has been decreasing near south Rogers Lake since the early 1970's.

SUMMARY AND CONCLUSIONS

Edwards Air Force Base overlies two structural basins in the western Mojave desert; the East Antelope and the Kramer, which have been filled to depths of more than 5,000 and 2,000 ft, respectively, with Tertiary and Quaternary sediments. These sediments consist of a series of unconsolidated alluvial deposits interbedded with lacustrine deposits. Near the southern limit of the valley, the lacustrine deposits are buried beneath as much as 800 ft of alluvium, but are exposed at land surface near the northern limit.

The aquifer system in the Antelope Valley consists of two alluvial aquifers known as the principal aquifer and the deep aquifer. The principal aquifer is considered to be unconfined and overlies lacustrine deposits. This aquifer extends over most of the valley south and southwest of Rogers Lake and is the major source of ground water pumped in Antelope Valley. The deep alluvial aquifer underlies the lacustrine beds and extends to the north beneath Rogers Lake and beyond. This deep aquifer is the major source of ground water at EAFB.

Ground water in the Antelope Valley area originates primarily from precipitation in the San Gabriel and Tehachapi Mountains. Estimates of the average annual recharge to the aquifer system in the Antelope Valley range from 40,280 to 81,400 acre-ft.

Ground-water use in the Antelope Valley peaked in the early 1950's and estimates of annual pumpage for this period range from about 280,000 to 480,000 acre-ft. The estimated pumpage for 1988 was about 62,000 acre-ft. Since 1947, pumpage at EAFB has ranged from a minimum of about 1,000 acre-ft in 1947 to a maximum of about 6,700 acre-ft in 1965. EAFB pumpage in 1990 was about 6,150 acre-ft.

The data collected for this investigation includes lithologic, borehole geophysical, surface geophysical, ground-water level and quality, land subsidence, and aquifer-system compaction information. The lithologic and borehole geophysical data indicate a multiple-aquifer system south and west of Rogers Lake and a single-aquifer system in the Graham Ranch area.

Values for depth-to-bedrock differ among the three surface geophysical methods used in this study, but the shape and orientation of the basin's structural configuration generally are coincident. Gravity and seismic refraction data define the East Antelope structural basin as a relatively narrow N. 50° - 60° E. trending trough extending to the southwest from beneath the southern part of Rogers Lake. Seismic refraction survey data are concordant with the gravity and surface-resistivity data, and delineate the Graham Ranch area as a partly isolated sediment-filled basin.

Long-term water-level declines of as much as 90 ft have been recorded on EAFB. Ground-water levels, lithologic, and geophysical evidence at the Holly site indicate two separate aquifers, correlative with the principal and deep aquifers of the Lancaster ground-water subbasin. The very slight, nonseasonal, yet steady water-level decline in the shallow zone suggests that the principal aquifer is not hydraulically connected to the deep aquifer, where water levels have fluctuated seasonally as much as 8 to 10 ft.

The quality of ground water near Rogers Lake and in the Graham Ranch areas ranges from soft to moderately hard, and the water commonly has a high dissolved-solids concentration. The concentrations of most constituents are generally less than the U.S. Environmental Protection Agency primary and secondary drinking-water regulations for maximum contaminant levels. The quality of the water from the well at the Buckhorn site is characterized as a very hard and slightly saline type, and exceeds recommended Environmental Protection Agency limits for dissolved solids, chloride, and manganese.

On the basis of comparison differential surveys, more than 1 ft of land subsidence has occurred since 1961 over the southwestern part of EAFB. An extensometer installed at the Holly site, near the South Track well field, showed an average annual rate of compaction of 5.57×10^{-2} ft/yr from May 1990 to November 1991. This current annual rate would account for only 1.67 ft of the total 3.2 ft of subsidence measured from 1961 to 1990, indicating that compaction rates at the Holly site probably were higher in years prior to 1990.

REFERENCES CITED

Backman, A.E., 1928, Supplemental report on Antelope Valley, California: Federal Land Bank of Berkeley, March 21, 1928, 29 p.

Bartley, J.M., Glazner, A.F., and Schermer, E.R., 1990, North-south contraction of the Mojave Block and strike-slip tectonics in southern California: Science, v. 248, no. 4961, p. 1398-1401.

Bear, Jacob, 1979, Hydraulics of groundwater: New York, McGraw-Hill, 569 p.

Benda, W.K., Erd, R.C., and Smith, W.C., 1960, Core logs from five test holes near Kramer, California: U.S. Geological Survey Bulletin 1045-F, p. 319-393.

Blodgett, J.C., and Williams, J.S., 1992, Land subsidence and problems affecting land use at Edwards Air Force Base and vicinity, California, 1990: U.S. Geological Survey Water-Resource Investigations Report 92-4035, 25 p.

Bloyd, R.M., Jr., 1967, Water resources of the Antelope Valley-East Kern Water Agency area, California: U.S. Geological Survey Open-File Report, 69 p.

Bortugno, E.J., and Spittler, T.E., 1986, Geologic map of the San Bernardino quadrangle: California Department of Mines and Geology, Map No. 3A, scale 1:250,000.

Boulton, N.S., 1963, Analysis of data from nonequilibrium pumping tests allowing for delayed yield from storage: Institute of Civil Engineers, London, England, Proceedings, v. 26, p. 469-482.

Burchfiel, B.C., and Davis, G.A., 1981, Mojave Desert and Environs, *in* Ernst, W.G., ed., The Geotectonic Development of California, v. 1: Englewood Cliffs, New Jersey, Prentice-Hall, p. 218-252.

California Department of Water Resources, 1947, Report to the Assembly of the State Legislature on water supply of Antelope Valley in Los Angeles and Kern Counties pursuant to House Resolution Number 101 of February 16, 1946: California Department of Water Resources, 21 p.

California Department of Public Works, 1955, Memorandum report on water conditions in Antelope Valley in Kern, Los Angeles, and San Bernardino Counties: California Department of Public Works, 27 p.

California State Water Resources Control Board, 1974, Water quality control plan report, South Lahontan basin: California State Water Resources Control Board, 300 p.

Cheadle, M.J., Czuchra, B.L., Byrne, T., Ando, C.J., Oliver, J.E., Brown, L.D., and Kaufman, S., 1986, The deep crustal structure of the Mojave Desert, California, from COCORP Seismic reflection data: Tectonics, v. 5, no. 2, p. 293-320.

Dibblee, T.W., Jr., 1952, Geology of the Saltdale quadrangle, California: California Division of Mines Bulletin 160, 66 p., scale 1:62,500.

_____1957, Simplified geologic map of the western Mojave Desert: U.S. Geological Survey Open-File Report, scale 1:250,000.

Dibblee, T.W., Jr., 1958a, Geologic map of the Boron quadrangle, Kern and San Bernardino Counties, California: U.S. Geological Survey Mineral Investigations Field Studies Map MF-204, scale 1:62,500.

_____1958b, Geologic map of the Castle Butte quadrangle, Kern County, California: U.S. Geological Survey Mineral Investigations Field Studies Map MF-170, scale 1:62,500.

_____1959a, Geologic map of the Rosamond quadrangle, California: U.S. Geological Survey Open-File Report, scale 1:62,500.

_____1959b, Geologic map of the Rogers Lake quadrangle, California: U.S. Geological Survey Open-File Map, scale 1:48,000.

_____1959c, Geologic map of the Alpine Butte quadrangle, California: U.S. Geological Survey Mineral Investigations Field Studies Map MF-222, scale 1:62,500.

_____1959d, Preliminary geologic map of the Mojave quadrangle, California: U.S. Geological Survey Mineral Investigations Field Studies Map MF-219, scale 1:62,500.

_____1960a [1961], Geologic map of the Lancaster quadrangle, Los Angeles County, California: U.S. Geological Survey Mineral Investigations Field Studies Map MF-76, scale 1:62,500.

_____1960b [1961], Geology of the Rogers Lake and Kramer quadrangles, California: U.S. Geological Survey Bulletin 1089-B, p. 73-139.

_____1963, Geology of the Willow Springs and Rosamond quadrangles, California: U.S. Geological Survey Bulletin 1089-C, p. 141-253.

_____1967, Areal geology of the western Mojave Desert, California: U.S. Geological Survey Professional Paper 522, 153 p.

_____1981, Regional structure of the Mojave Desert, *in* Howard, K.A., and others, eds., Tectonic framework of the Mojave and Sonoran Deserts, California and Arizona: U.S. Geological Survey Open-File Report 81-0503, p. 26-28.

Dokka, R. K., 1986, Patterns and modes of early Miocene crustal extension, central Mojave Desert, California, *in* Mayer, L., ed., Extensional tectonics of the Southwestern United States: A perspective on processes and kinematics: Geological Society of America, Special Paper 208, p. 75-95.

_____1989, The Mohave extensional belt of southern California: Tectonics, v. 8, no. 2, p. 363-390.

Droste, J.B., 1961, Clay minerals in the playa sediments of the Mojave Desert, California: San Francisco, California Division of Mines, Special Report 69, 19 p.

Duell, L.F.W., Jr., 1987, Geohydrology of the Antelope Valley area, California, and design for a ground-water-quality monitoring network: U.S. Geological Survey Water-Resources Investigations Report 84-4081, 72 p.

Durbin, T.J., 1978, Calibration of a mathematical model of the Antelope Valley ground-water basin, California: U.S. Geological Survey Water-Supply Paper 2046, 51 p.

Dutcher, L.C., Bader, J.S., Hiltgen, W.J., and others, 1962, Data on wells on Edwards Air Force Base, California: California Department of Water Resources Bulletin 91-6, 208 p.

Dutcher, L.C., and Worts, G.F., Jr., 1963, Geology, hydrology, and water supply of Edwards Air Force Base, Kern County, California: U.S. Geological Survey Open-File Report, 225 p.

Giessner, F.W., and Robson, S.G., 1965, Ground-water inventory for 1964, Edwards Air Force Base, California: U.S. Geological Survey Open-File Report, 28 p.

Giessner, F.W., and Westphal, J.A., 1966, Ground-water inventory for 1965, Edwards Air Force Base, California: U.S. Geological Survey Open-File Report, 24 p.

Glazner, A.F., Bartley,J.M., and Walker, J.D., 1989, Magnitude and significance of Miocene crustal extension in the central Mojave Desert, California: Geology, v. 17, p. 50-53.

Hantush, M.S., and Jacob, C.E., 1955, Nonsteady radial flow in an infinite leaky aquifer: Transactions of the American Geophysical Union, v. 36, no. 1, p. 95-100.

Hem, J.D., 1985, Study and interpretation of the chemical characteristics of natural water: U.S. Geological Survey Water-Supply Paper 2254, 264 p.

Hewett, D.F., 1954, General geology of the Mojave Desert region California, *in* Jahns, R.H., ed., Geology of Southern California: California Department of Mines and Geology, Bulletin 170, Chapter 2, p. 5-20.

Holzer, T.L., ed., 1984, Man-induced land subsidence: Reviews in engineering geology, v. 6, 221 p.

Hughes, J.L., 1975, Hydrologic evaluation of the Haystack Butte area with emphasis on possible discharge of class-I wastes, Edwards Air Force Base, California: U.S. Geological Survey Water-Resources Investigations Report 7-75, 34 p.

Johnson, H.R., 1911, Water resources of Antelope Valley, California: U.S. Geological Survey Water-Supply Paper 278, 92 p.

Koehler, J.H., 1969, Ground-water inventory for 1967, Edwards Air Force Base, California: U.S. Geological Survey Open-File Report, 15 p.

Lewis, R.E., and Miller, R.E., 1968, Geologic and hydrologic maps of the southern part of Antelope Valley, California, supplement to U.S. Soil Conservation Service Report on the cooperative soil survey of Antelope Valley area, California: U.S. Department of Agriculture Report, 13 p.

Lofgren, B.E., 1965, Subsidence related to ground-water withdrawal, *in* Landslides and subsidence: California Resources Agency, Geologic Hazards Conference, 2d, Los Angeles, California, 1965, Proceedings, p. 105-110.

Mabey, D.R., 1960, Gravity survey of the western Mojave Desert, California: U.S. Geological Survey Professional Paper 316-D, p. 51-73.

McClelland, E.J., 1963, Aquifer-test compilation for the Mojave Desert region, California: U.S. Geological Survey Open-File Report, 47 p.

McMillan, J.F., 1973, Land subsidence--Antelope Valley area of Los Angeles County: Department of County Engineer, Survey Division, Los Angeles, California, 11 p.

Meinzer, O.E., 1927, Plants as indicators of ground water: U.S. Geological Survey Water-Supply Paper 577, 95 p.

Morin, R.L., Mariano, John, and Jachens, R.C., 1990, Isostatic residual gravity map of Edwards Air Force Base and vicinity, Kern, Los Angeles, and San Bernardino Counties, California: U.S. Geological Survey Open-File Report 90-664, scale 1:62,500, 1 sheet.

Motts, W.S., 1970, Introduction to playa studies, *in* Motts, W.S., ed., Geology and hydrology of selected playas in Western United States: Amherst, Massachusetts, University of Massachusetts, Final Scientific Report Contract No. AFL 19(628)-2486, Air force Cambridge Laboratories, p. 9.

Motts, W.S., and Carpenter, David, 1970, Geology and hydrology of Rogers Playa and Rosamond Playa, California, *in* Motts, W.S., ed., Geology and hydrology of selected playas in western United States: Amherst, University of Massachusetts, Final Scientific Report Contract No. AFL 19(628)-2486, Air force Cambridge Laboratories, p. 23-65.

Moyle, W.R., Jr., 1960, Ground-water inventory for 1959, Edwards Air Force Base, California: U.S. Geological Survey Open-File Report, 35 p.

National Oceanic and Atmospheric Administration, 1989, Climatological data annual summary, California, 1989: National Oceanic and Atmospheric Administration, v. 93, no. 13.

_____1990, Climatological data annual summary, California, 1990: v. 94, no. 13.

Neal, J.T., Langer, A.M., and Kerr, P.F., 1968, Giant desiccation polygons of great basin playas: Geological Society of America Bulletin, v. 79, p. 69-90.

Noble, L.F., 1953, Geology of the Pearland quadrangle, California: U.S. Geological Survey Geologic Quadrangle Map GQ-24, scale 1:24,000.

Poland, J.F., ed., 1984, Guidebook to studies of land subsidence due to ground-water withdrawal, no. 40 of UNESCO Studies and Reports in Hydrology: Paris, France, United Nations Educational, Scientific and Cultural Organization, 305 p., 5 appendixes.

Press, F., 1966, Seismic velocities, *in* Clark, S.P., Jr., ed., Handbook of Physical Constants: Geological Society of America, Memoir 97, p. 197-218.

Rimrock Geophysics, Inc., 1987-89, SIPIN and SIPEDT, PC programs for creating and editing seismic refraction data for input to USGS seismic refraction modeling program SIPT1 and Rimrock Geophysics enhanced version SIPT2: Lakewood, Colorado, 37 p.

Snyder, J.H., 1955, Ground water in California--The experience of Antelope Valley: Berkeley, California, University of California, Division of Agriculture Science, Giannini Foundation Ground-Water Studies No. 2, 171 p.

Snyder, D.B., Roberts, C.W., Saltus, R.W., and Sikora, R.F., 1982, Description of magnetic tape containing principal facts of 64,026 gravity stations in the State of California: U.S. Geological Survey Report, 34 p.

Stiff, H.A., Jr. 1951, The interpretation of chemical water analysis by means of patterns: J. Petrol. Tech., Pt.15.

Terzaghi, K., 1943, Theoretical soil mechanics: New York, John Wiley, 510 p.

Thayer, W.N., 1946, Geologic features of Antelope Valley, California: Los Angeles County Flood Control District Report, 20 p.

Theis, C.V., 1935, The relation between the lowering of the piezometric surface and the rate and duration of discharge of a well using ground-water storage: Transactions of the American Geophysical Union, v. 16, p. 579-534.

Thomas, H.E., and Phoenix, D.A., 1976, Summary appraisals of the Nation's ground-water resources--California Region: U.S. Geological Survey Professional Paper 813-E, 51 p.

Thompson, D.G., 1929, The Mohave Desert region, California, a geographic, geologic, and hydrologic reconnaissance: U.S. Geological Survey Water-Supply Paper 578, 759 p.

Todd, D.K., 1980, Groundwater hydrology, second edition: New York, John Wiley, 535 p.

Tyley, S.J., 1967, Ground-water inventory for 1966, Edwards Air Force Base, California: U.S. Geological Survey Open-File Report, 10 p.

U.S. Department of Commerce, Bureau of the Census, 1990.

Weir, J.E., Jr., 1962, Ground-water inventory for 1961, Edwards Air Force Base, California: U.S. Geological Survey Open-File Report, 54 p.

_____1963, Ground-water inventory for 1962, Edwards Air Force Base, California: U.S. Geological Survey Open-File Report, 30 p.

_____1965, Ground-water inventory for 1963, Edwards Air Force Base, California: U.S. Geological Survey Open-File Report, 28 p.

Weston, Roy F., Inc., 1986, Water supply availability and distribution system evaluation, Edwards Air Force Base, California: Prepared for Edwards Air Force Base, Air Force Systems Command, Andrews Air Force Base, DC.

_____1988, Work Plan--Water supply availability and distribution system evaluation, rocket site, Edwards Air Force Base, California: Prepared for Edwards Air Force Base, Air Force Systems Command, Andrews Air Force Base, DC.

Wright, R.V., 1924, Report on agriculture, economic, and ground-water situation, Antelope Valley, California: Federal Land Bank of Berkeley, November 6, 1924, 115 p.

Zettlemoyer, B., 1990, 1988 annual water use-water supply balances: California Department of Water Resources Memorandum Report, 59 p.

Zohdy, A.A., and Bisdorf, R.J., 1990, Ground-water exploration using deep Schlumberger soundings at Edwards AFB-California, Part 1: Graham Ranch and Rogers Lake: U.S. Geological Open-File Report 90-536, 95 p.

Zohdy, A.A., Eaton, G.P., and Mabey, D.R., 1974, Application of surface geophysics to ground-water investigations: U.S. Geological Survey Techniques of Water-Resources Investigations, Book 2, Chapter D1, 116 p.